EVAPOTRANSPIRATION IN GREENHOUSES

by

© RICHARD L. BELLO, B.A.

A Thesis
Submitted to the School of Graduate Studies
in Partial Fulfilment of the Requirements
for the degree
Doctor of Philosophy

McMaster University

January 1982

EVAPOTRANSPIRATION IN GREENHOUSES

DOCTOR OF PHILOSOPHY (1982)
(Geography)

McMASTER UNIVERSITY
Hamilton, Ontario

TITLE: Evapotranspiration in Greenhouses

AUTHOR: Richard L. Bello, B.A. (McMaster University)

SUPERVISOR: Professor W.R. Rouse

NUMBER OF PAGES: viii, 111

Abstract

A physically based evapotranspiration model has been developed and tested in an experimental greenhouse. Good agreement was found between hourly model estimates and mass balance measurements of the latent heat flux. The model recognizes the advective nature of the greenhouse microclimate and thus represents an improvement over empirical model estimates of evaporation based on the measurement of radiation alone. Although radiant heating is the dominant mechanism responsible for evapotranspiration it does not represent a constant proportion on an hourly or daily basis. As a result, the Bowen ratio varies over time. Most of the variation was attributable to advection, and to a lesser extent, the sensible and latent heat fluxes at the glazing. During the daytime, the evapotranspiration process utilized in excess of 70% of the net available energy at the surface. However, model estimates and empirical evidence indicate this proportion can equal or exceed 100%. Variations in the latent heat flux are shown to depend on greenhouse design and the ambient microclimate. Simulation of the greenhouse humidity environment using 10 year hourly climatic means for Woodbridge, Ontario demonstrates the effect of modifying ventilation rates, glazing transmission and intake humidity on potential evapotranspiration. A relation is presented which permits the real-time adjustment of ventilation resistance from meteorological measurements of solar radiation and dry and wet-bulb air temperature. The maintenance of potential evapotranspiration for optimal crop productivity is shown to be incompatible with the collection and storage of sensible heat of the exhaust air as a means of defraying greenhouse heating costs.

ACKNOWLEDGEMENTS

I wish to express my sincere gratitude to my supervisor Dr. W.R. Rouse for his assistance and financial support throughout the course of this investigation. Also I would like to acknowledge the helpful guidance and advice of Dr. J.A. Davies and Dr. R. Judd. I am most grateful to Mr. J.R. Worthington for his hospitality in permitting his home to be transformed into a research center and to Mr. E. Bello for materials and design contributions during greenhouse construction. I would also like to thank Mrs. C. Moulder for typing the manuscript and Dr. J. Drake for GRAFF. My gratitude also extends to Dr. T. Uboegbulam, Mr. J. Howard, Mr. B. McArthur and Mr. A.M. Sawchuck for many meaningful discussions and assistance which occurred during the data analysis period. Special thanks are due to Ms. S.J. Margo and to my parents for providing me with the opportunity to pursue my education. Thanks Drew, Terry and the kids for the adrenaline.

TABLE OF CONTENTS

LIST OF ILLUSTRATIONS

CHAPTER ONE

INTRODUCTION

1.1 THE ROLE OF EVAPOTRANSPIRATION

Evapotranspiration is important in two major areas of greenhouse research. The first pertains to soil water uptake by plants and the optimum irrigation required to produce a profitable crop. Also, the incidence of plant pathogens and physiological disorders is related to the soil and air moisture environments. The second pertains to solar heating and the ability of the greenhouse structure to provide an adequate growing environment with a reduced dependence on supplemental heating.

Since plants and the soil are the principle sources of moisture for the air in the greenhouse, determination of evapotranspiration is an important task. Greenhouse crops do not receive precipitation therefore irrigation takes its place. The optimum growth of crops requires optimum moisture supply. Measurement of crop water usage is a direct means of evaluating irrigation requirements.

The relationship between evapotranspiration and solar heating is less well understood as it has only recently been brought to focus by the rapid escalation in fuel prices. The solar energy entering a greenhouse is generally stored in two ways. Mainly, it is absorbed by the ground or other objects of large thermal mass and warms them conductively. As the greenhouse air cools in the evening, the stored heat is released thereby moderating the greenhouse environment. The second method involves

extracting warm air which has been heated convectively by the surface and transferring the heat to an isolated storage mass. The stored energy is then mechanically transferred back to the greenhouse in the evening.

The former method of passive solar energy collection and storage is well understood and has been extensively modelled by Mazria (1979), Balcomb, Hedstrom and McFarland (1977), Wray and Balcomb (1979) and Besant (1979).

Passive solar heating has been demonstrated to be the most cost effective means of providing heat for buildings. Nevertheless, increasing research is devoted to the second type of solar collection as an exclusive means of heating buildings or as a passive/active hybrid system. This is because in some instances, passive heating alone cannct supply one hundred per cent of the structure's heating requirements.

However, the environments that have been studied have been devoid of vegetation. The primary function of the simulation models of the above authors has been to assess the potential for solar heating in integral or attached solariums or "sun-rooms". Unlike sun-rooms, the microclimate of plant environments is very different. Conductive ground heating and convective air heating are relatively minor terms in comparison to the latent heating comprizing evapotranspiration. Outdoors, ground heating typically constitutes 6-10% of the energy available at the surface and evapotranspiration is three to ten times greater than sensible heating. Hence, in a greenhouse containing vegetation, evapotranspiration is a major term and it is likely that current models would greatly overestimate potential solar heating.

Since the accurate prediction of evapotranspiration is central to the estimation of irrigation requirements and potential for solar heating

in domestic and commercial greenhouses, it is appropriate to review the progress that has been made in this regard.

1.2 ESTIMATING EVAPOTRANSPIRATION

1.2.1 Simulation Models

The purpose of greenhouse simulation models has been to predict the behaviour of air temperature and humidity and soil temperature over time as a function of outside temperature, humidity and solar radiation. Although these models do not provide a direct assessment of the sensible and latent heat fluxes per se, the results are amenable to these calculations. Very few authors, (Takakura et al., 1971) however, have chosen to present their results in this manner.

This type of model has the advantage that the impact of design changes on the microclimate can be assessed. Unfortunately, several models have been presented which have not been validated with field measurements (Kimball, 1973), and others that have report only modest success in replicating actual conditions (Froelich et al., 1979). What distinguishes these models from those for solariums is the parameterization of evapotranspiration. Unfortunately, the simulation of the latent heat flux not only requires the parameterization of the radiation and temperature environment but the parameterization of moisture supply as well. Clearly, the availability of water has as dominant a role in the latent heat flux as the energy available to evaporate water. The movement of soil water to the root zone is likely the least well understood component of the greenhouse environment. Nakayama et el. (1980) found that approximately 70% of moisture supply came from irrigation, 11.5% from horizontal subsurface moisture flow and 18.5% from vertical subsurface

moisture flow. However, these proportions are dependent on location within the greenhouse and would be expected to vary with soil type, outside precipitation and greenhouse management. Even if soil moisture supply were ample the availability of the moisture to the air is controlled by the plant stomata. As Takami and Uchijima (1977) point out, moisture not only has to traverse the aerodynamic resistance offered by the ventilation "wind" regime, but the canopy resistance offered by the composite effect of all of the stomata of the crop. An 'a priori' knowledge of stomatal closure requires considerable further research. Being unable to account for moisture availability, current greenhouse simulation models have provided minimal insight into the role of evapotranspiration in greenhouses to date.

1.2.2 Empirical Models

The most common approach to evaluating evapotranspiration is to use regression relationships between evapotranspiration and radiant energy supply. This approach assumes that the sun's energy is the driving force behind the evapotranspiration process. Although this assumption will be examined in more detail in Chapter Two, it nevertheless provides an attractive methodology due to the abundance of meteorological stations measuring incident solar radiation and the common use of pyranometers in most greenhouse microclimate studies. Relationships of this type could also be useful to horticulturalists. As Mastalerz (1977) states, "It would be interesting to know if the amount of water per unit of solar radiation remains constant. (sic) If this were so, would plants be subjected to the same degree of moisture stress between applications?" Unfortunately, this is not known since empirical findings differ considerably.

For example, Hanan (1967) reported correlation coefficients of 0.57 and 0.92 between evapotranspiration and solar radiation for separate experiments in one location. Similarly, Morris et al. (1957) reported correlation coefficients between 0.41 and 0.97.

Also, regression coefficients are highly variable. Morris et al. reported values from 0.229 to 1.38. Stanhill et al. (1973) reported values of 1.54 between evapotranspiration and net radiation. Nakayama and Yamanaka (1975) found values ranging from 1.37 to 0.79. Linacre et al. (1964) found evaporation to exceed net available energy by 27%.

It is clear that this empirical approach is not well suited to estimating evapotranspiration. It does emphasize the variability in the evaporative flux however. It also demonstrates that it is not uncommon for the latent heat flux to exceed net radiation or incident solar radiation. This latter observation is particularly important because it is responsible for the general belief that these findings were physically impossible and inconsistent with observed greenhouse performance. Consequently, most of the results have been attributed to measurement error and ignored.

A second empirical approach employed in Japan, involves the regression of measured evapotranspiration and evaporation from a 20 cm diameter pan located within the greenhouse. Nakayama and Yamanaka reported high correlation coefficients (0.85, 0.99) but regression coefficients varied from 2.28 to 0.68. Also, the regression of pan evaporation and net radiation indicated pan evaporation exceeded net radiation. Although this empirical approach demonstrates no marked advantage over the previous method it also supports the contention that evaporation can exceed the radiant energy supply.

1.3 RESEARCH OUTLINE

This thesis will investigate whether evapotranspiration can exceed received net radiation and remain consistent with observed greenhouse performance using the energy budget framework. A physically based model is developed which accounts for four major influences on evapotranspiration. The construction and instrumentation of a small greenhouse are outlined. Model estimations of evapotranspiration are compared with measured values. Model sensitivity to various assumptions and measurement errors is analysed. The suitability of the greenhouse combination model as a design tool is investigated.

CHAPTER TWO

THEORETICAL FRAMEWORK

2.1 THE ENERGY BUDGET APPROACH

Greenhouse environments fall within the broader categorization of "man modified climates". However, the extent of this control is so great that the term "controlled environment agriculture" is used to distinguish their unique attributes. The energy budget approach formalizes the environmental control that greenhouse design and management exerts on the microclimate.

2.1.1 Radiation Budget

Figure 2.1 shows how the component fluxes of shortwave K and longwave L radiation are modified in the greenhouse environment. The radiation balance at the crop surface is defined as

$$Q^* = K^* + L^* \quad , \qquad (Wm^{-2}) \qquad (2.1)$$

where Q* is the net radiation, K* is the net solar radiation and L* the net longwave radiation. ($K^* = K\downarrow - K\uparrow$; $L^* = L\downarrow - L\uparrow$)

The net solar radiation is a function of the outside incident solar radiation, the reflectivity α_g and absorptivity of the glazing a_g and the albedo of the surface α_s. Figure 2.1 is necessarily simplified as the total net solar flux at the surface is a composite of glazing reflectivity and absorptivity of all facets of the greenhouse. Structural members will have different characteristics from those of the glazing and both the type of glazing and proportion of glazing to

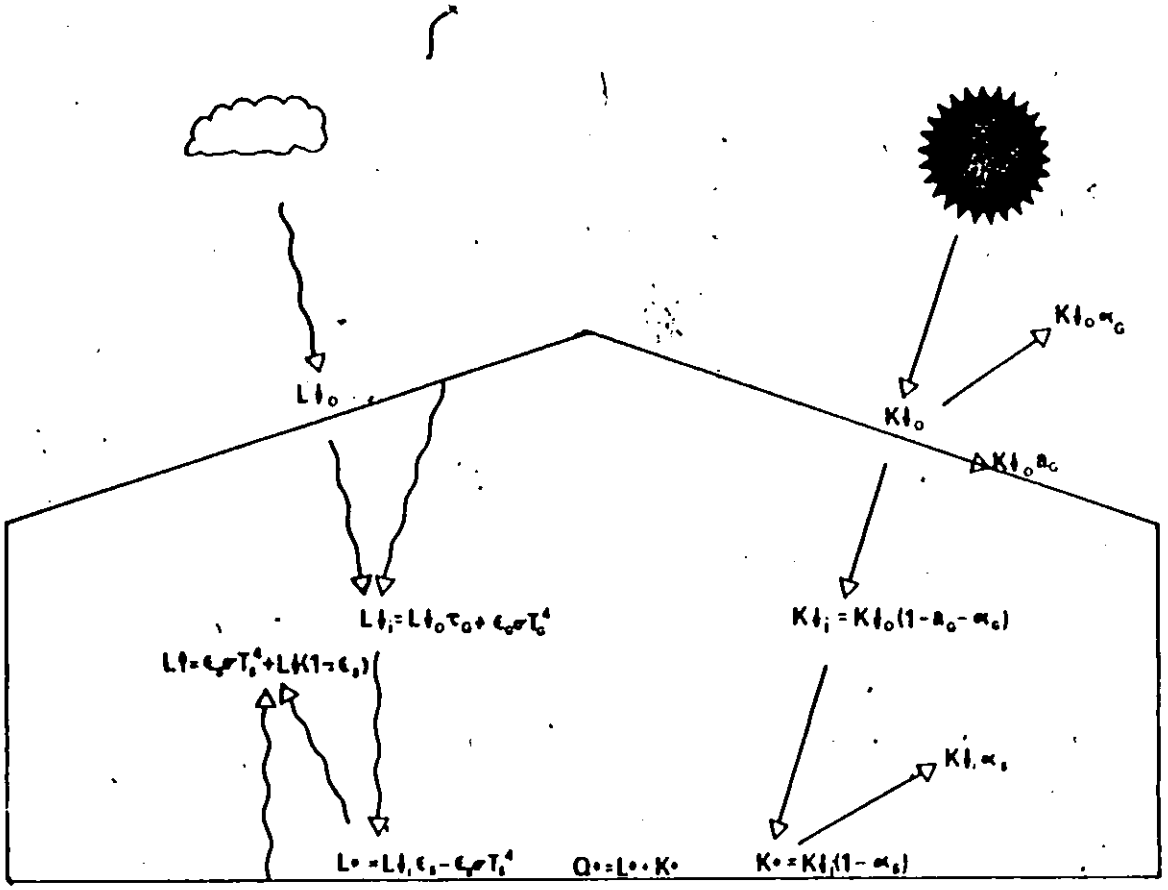

Figure 2.1. Component fluxes of radiation.

structural members will differ with greenhouse design. The angle of incidence of the solar beam, the ratio of direct to diffuse solar radiation, and the occurrence of condensation and dirt on the glazing causes the incident solar flux to vary with time. The albedo of the crop surface is also dependent on the direct/diffuse ratio and spectral nature of incident solar radiation. Crop characteristics including crop type, percentage cover, moisture content and row orientation also affect albedo.

The net longwave radiation at the crop surface is also affected by the outside longwave radiation. The extent of this dependence is a function of the longwave transmission of the glazing τ_g. Glass exhibits a longwave transmission close to zero but polyethylene exhibits transmissions as large as 80%. Dirt and condensation also affect longwave transmission of polyethylene. A decrease of polyethylene transmission resulting from the presence of water or dirt also increases polyethylene emissivity ($\varepsilon = 1 - \tau - \rho$), where ρ is longwave reflectivity. The emissivity of the glazing affects the emitted longwave flux from the glazing through the Stefan-Boltzman Law ($L\downarrow = \varepsilon\sigma T_g^4$, where σ is the Stefan-Boltzman constant 5.67×10^{-8} Wm^{-2} K^{-4}). The incident longwave flux at the crop surface is reflected ($L\downarrow_i = [L\downarrow_o \tau_g + \varepsilon_g \sigma T_g^4](1 - \varepsilon_s)$, where $\varepsilon_s = 0.95$). The surface emits longwave radiation as a function of the fourth power of the absolute surface temperature. An understanding of the interaction of the component radiative fluxes of energy with the structure and crop surface permits the greenhouse designer to optimize the net radiation at the surface. Unfortunately, an 'a priori' knowledge of the net radiation of the crop surface has been difficult to estimate. In general, the greenhouse structure reduces light transmission

to 40 to 80% of that outside, thereby reducing net radiation during the day. Because the glazing always has a higher temperature than the sky, the downward longwave radiation and hence net longwave radiation is always larger inside. This effect is not large enough to counteract the decrease in solar radiation. However, nocturnally it results in the net radiation being greater inside than outside.

However, the specific flux of net radiation at any moment in time is more difficult to assess, primarily, due to the variability in radiative transfer caused by condensation and dirt accumulation on the glazing. These can further reduce solar transmission by 30 and 40% respectively. In the case of longwave transmission in polyethylene, values as low as 20% have been reported when condensation is heavy.

Considering the importance of net radiation as the driving force behind all environmental energy processes, it is unfortunate that models do not exist which enable its prediction with any degree of accuracy. Of greater concern is the absence of net radiation measurements in all but a very few experimental programs.

2.1.2 The Energy Budget

Figure 2.2 summarizes the components of the energy budget. The energy budget equation for the crop surface is given by

$$Q^* = Q_H + Q_E + Q_G + Q_p \quad , \qquad (Wm^{-2}) \qquad (2.2)$$

where Q_H is the sensible heat flux, Q_E is the latent heat flux, Q_G is the soil heat flux and Q_p is the photosynthetic heat flux. The energy utilized in net photosynthesis is generally only 1-3% of net radiation

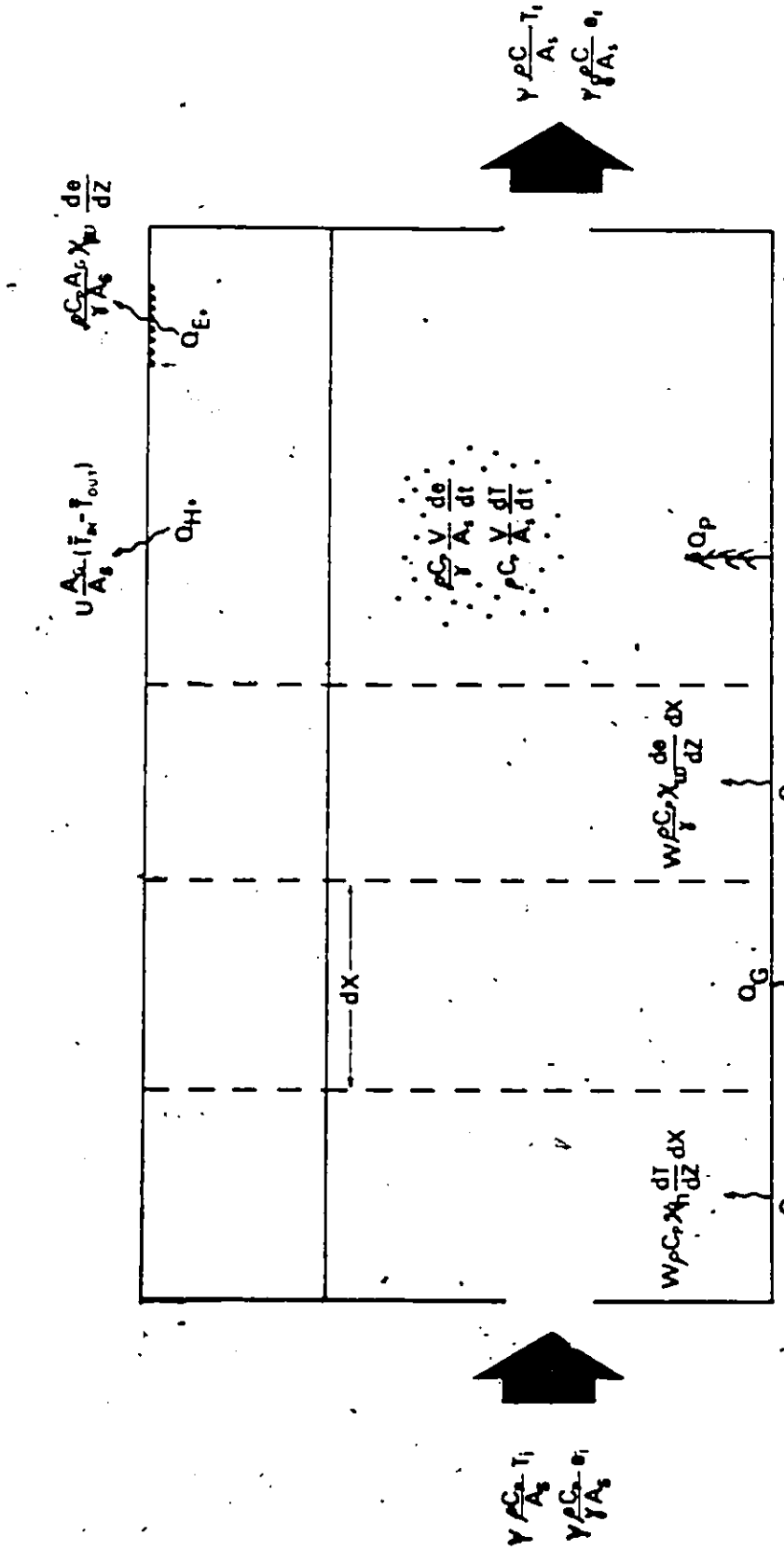

Figure 2.2. Energy budget components.

(Oke, 1978) and is commonly ignored in energy budget analysis.

The sensible heat flux is determined from

$$Q_H = \frac{\rho C_p}{A_s} \psi(T_e - T_i) + \rho C_p \frac{V}{A_s}\frac{dT}{dt} + U\frac{A_G}{A_s}(\bar{T}_{in} - \bar{T}_{out}) \quad (Wm^{-2}) \qquad (2.3)$$

The first term of (2.3) is the component of the sensible heat flux determined by measuring exhaust T_e and intake T_i temperatures, where ρ is air density (kgm^{-3}), C_p is air specific heat ($J\ kg^{-1}C^{-1}$), ψ is the ventilation rate (m^3s^{-1}) and A_s is surface area (m^2). The second term represents the storage of sensible heat in the air, where V is greenhouse air volume (m^3) and dT/dt is replaced by the finite difference form $\Delta T/\Delta t$ and represents the change in average inside temperature over time interval Δt. The third term represents the sensible heat lost through the greenhouse glazing of area A_g, where U is the glazing heat loss factor (glazing "U-factor", $Wm^{-2}C^{-1}$) and $\bar{T}$ is the time average of inside (in) and outside (out) temperatures (C). In general, when the greenhouse ventilators are on the first term dominates Q_H, the third term is secondary and the second term is negligible and can be safely ignored. When the ventilators are turned off the first term is zero and only the final two terms are operative (Appendix One).

Similarly, the latent heat flux Q_E is determined from

$$Q_E = \frac{\rho C_p}{\gamma}\frac{\psi}{A_s}(e_e - e_i) + \frac{\rho C_p}{\gamma}\frac{V}{A_s}\frac{de}{dt} + \frac{A_g}{A_s}\frac{\rho C_p}{\gamma} K_w \frac{(e_{in} - e_g)}{\Delta z} \quad (Wm^{-2}) \qquad (2.4)$$

The first term represents the change in water vapour content between exhaust and intake air, where γ is the psychrometric constant ($kPaC^{-1}$) and e is vapour pressure (kPa). The second term represents

the change in the vapour pressure of the air volume over time. The third term is the condensation latent heat flux of the glazing (positive outwards), where K_w is the eddy diffusivity for water vapour, e_{in} is the vapour pressure of the inside air at distance Δz from the glazing and e_g is the vapour pressure of the glazing surface. The third term is particularly difficult to parameterize as e_g is dependent on moisture availability. When condensation is absent the third term equals zero. Once condensation has commenced, the surface vapour pressure will be dependent on the extent and size of water droplets which are difficult to measure. Also, it is not known how beadflow and dripping affect condensation extent and what effects, if any, these have on surface vapour pressure. The use of (2.4) is therefore simplified when condensation is known not to be occuring. Again, the ventilation term dominates Q_E when the fans are on and is zero when the greenhouse is closed.

The latent heat flux can also be measured gravimetrically or lysimetrically from

$$Q_E = \lambda E \quad , \qquad (Wm^{-2}) \qquad (2.5)$$

where E is the evaporation rate (kg m^{-2} s^{-1}) and λ is the latent heat of vapourization of water (J kg^{-1}). A discussion of the relative merits of (2.4) and (2.5) for measuring evapotranspiration will be reserved for Chapter Five.

The ground heat flux can be measured directly by implanting soil heat flux transducers immediately below the soil surface. Several of these transducers are commonly employed and located at several positions

in the greenhouse to eliminate spatial bias resulting from a single measurement location.

Equations (2.3) to (2.5) demonstrate the means of assessing the various surface energy budget components from a greenhouse air volume. However, because the surface contributes the energy required for the various environmental processes it is illustrative to re-express Q_H and Q_E in terms of surface parameters. Thus

$$A_s Q_H = C_p \int_0^W \int_0^L K_H \rho \frac{dT}{dz} \, dx \, dy \quad , \tag{2.6}$$

$$A_s Q_E = C_p \int_0^W \int_0^L K_W \rho \frac{de}{dz} \, dx \, dy \quad , \tag{2.7}$$

where the fluxes are assumed to be uniform across greenhouse width W and K_H and K_W are the eddy diffusivities for sensible and latent heat respectively. In practice (2.6) and (2.7) are approximated by

$$A_s Q_H = WC_p \sum_{x=0}^{L} K_H \rho \frac{\Delta T}{\Delta z} \Delta x \quad , \tag{2.8}$$

$$A_s Q_E = WC_p \sum_{x=0}^{L} K_W \rho \frac{\Delta e}{\Delta z} \Delta x \quad , \tag{2.9}$$

where T and e are measured Δz apart in close proximity to the surface. Equations (2.8) and (2.9) are inappropriate for the measurement of Q_H and Q_E since many measurements are required along the greenhouse length, separated at intervals Δx. Also, eddy diffusivities vary with time and location and require detailed wind measurements for their assessment. Furthermore, it is unlikely that a fully adjusted boundary layer of sufficient depth would be established to enable flux measurements from

vertical profile analyses (see Appendix One). First, the nominal 100:1 fetch-height ratio would not be satisfied in all but the longest commercial greenhouses. Second, vertical flux gradient techniques require some uniformity in the horizontal wind regime to ensure the data collected is representative of the underlying surface. Since there is no universal standard for the location of intake and exhaust fans it would appear that three dimensional variability in the wind regime would preclude this type of analysis. Nevertheless with (2.8) and (2.9) it is possible to describe how property gradients near the crop surface are responsible for the observed microclimate in greenhouses.

Equation (2.2) can be rearranged to yield the latent heat flux

$$Q_E = (Q^* - Q_G)/(1 + \beta) \quad , \tag{2.10}$$

where $Q^* - Q_G$ is referred to as the net available energy as it is the energy available for atmospheric processes, and β $(= Q_H/Q_E)$ is the Bowen ratio. If an 'a priori' knowledge of the Bowen ratio were possible then Q_E could be evaluated without the calculation of Q_H. If the Bowen ratio were constant over time then the prediction of Q_E would be simplified considerably. This is the basis of the hypothesis forwarded by Mastalerz (1977) and is implicit in the energy balance calculations of Walker (1965).

The Bowen ratio can be evaluated from

$$\beta = 1 + \gamma \frac{K_H}{K_W} \frac{\Delta T}{\Delta e} \quad . \qquad (2.11)$$

Swinbank and Dyer (1967) and Dyer (1967) demonstrated that the ability of eddies to transport both sensible and latent heat was equal hence (2.10) reduces to

$$Q_E = (Q^* - Q_G)/(1 + \gamma \frac{\Delta T}{\Delta e}) \quad . \qquad (2.12)$$

Excellent agreement between results from this type of analysis and direct lysimeter measurements has been demonstrated consistently to support the method and its assumptions. However, the Bowen ratio varies over time and surface. Bowen ratios of 10.0 for dry desert surfaces, and 0.1-0.3 for freely transpiring vegetation and water bodies are commonly reported. Negative Bowen ratios are also reported. These are generally found in proximity to coastlines and over irrigated fields surrounded by non-irrigated land. Clearly, the greenhouse microclimate falls into this latter category. In microclimates where the Bowen ratio is negative the term "advective environments" is used to typify the energetics of these surfaces.

2.1.3 The Greenhouse as an Advective Environment

The nature of advection can be demonstrated with the example of an open irrigated field surrounded by non-irrigated land. Consider for the moment, the energetics of these two surfaces in the absence of wind. Under these conditions each surface will promote its own distinctive environment. As water is freely available over the irrigated plot during

the daytime, the net available energy at the surface raises the vapour pressure at the surface causing a large surface to air vapour pressure gradient. From (2.7), this results in a large latent heat flux. With little energy remaining to sensibly heat the surface the vertical temperature gradient remains small and consequently from (2.6), Q_H is small. A small Bowen ratio results.

Over the non-irrigated land, in the absence of freely available water, the vapour pressure gradient remains small as does Q_E. Intense heating of the surface ensues which promotes a large vertical temperature gradient, thereby causing a large sensible heat flux. The Bowen ratio is large. The air over the irrigated plot is more moist and cool than that over the surrounding land.

When a wind regime is introduced the energetics of the irrigated surface are disrupted. The dry air from the surrounding land overflows the irrigated plot. The vapour pressure gradient is now larger than normal and the surface responds by evapotranspiring more water. This leaves less energy for sensible heating and the Bowen ratio approaches zero. Typically, the evaporative flux is enhanced to such a large extent that it exceeds the net available energy at the surface. Conservation of energy principles require that this excess be matched by a supplemental energy source. In this case, the source is the downward directed (negative) sensible heat flux. This is possible because the advected upwind air is warmer than the irrigated surface. Hence, dT is negative and inversion conditions exist. Bowen ratios are negative. This is consistent with (2.10) wherein negative values of β are necessary for Q_E to exceed $Q^* - Q_G$.

Constructing a glass or polyethylene enclosure over the irrigated

plot has interesting implications for the surface, in terms of the energy budget. Businger (1963) indicated the nature of the control that the greenhouse exerts on the outside environment. Because the net radiation is generally smaller inside the greenhouse, its higher temperature can not be attributed to the radiative considerations of the "greenhouse effect". Only at night does the enhancement of the net longwave flux have any appreciable effect on greenhouse warming. The principal cause of greenhouse warming is the suppression of natural convection. Because greenhouse ventilaters do not promote the same degree of air exchange with the crop as the natural wind regime the greenhouse structure acts to trap the sensible and latent heat departing the surface. Being unable to disperse as readily within a larger volume, the temperature and humidity of greenhouse air increases. This trapping of energy is shown in (2.6) and (2.7) wherein the sensible and latent heat flux is seen to be proportional to the eddy diffusivity. Since eddy diffusivity increases with increasing wind speed the impact of greenhouse and ventilation design becomes apparent. If the greenhouse structure severely restricts the natural wind regime and/or the ventilation rates are small, the eddy diffusivities are small. The surface responds by increasing surface temperature and vapour pressure thereby providing gradients large enough to sustain sensible and latent heat fluxes that balance the net available energy at the surface. If the ambient wind regime were unrestricted by the greenhouse structure or ventilators maintained an equivalent air exchange with the crop, then the greenhouse would resemble the microclimate of the open field irrigated crop except that the net radiation may differ. Thus the ventilation rate has a large impact on the microclimate.

If the ventilators are turned off, the air would rapidly become saturated because the greenhouse air has been completely isolated from the larger atmospheric sink. This would restrict evapotranspiration. The sensible heat flux on the other hand, is not completely isolated from the atmospheric sink because sensible heat transfer proceeds through the glazing. This resistance is, nevertheless, larger than the convective resistance when the ventilators are open. Latent heating does not cease completely because the greenhouse air will increase in temperature thereby reducing the relative humidity of the air. Hence, evapotranspiration still remains coupled to air temperature increase even when the greenhouse is closed. Air temperature will continue to increase until glazing sensible heat loss equals or exceeds surface sensible heat flux (2.3).

Most greenhouses would lie between the extremes of a totally isolated air volume and an unrestricted ambient wind regime during the course of normal operation. The findings of Stanhill et al. (1973) are illustrative in this regard. In an open-sided greenhouse in Israel, evapotranspiration exceeded net radiation by 37%. The authors noted the large evaporation totals but offered no explanation. However, they also indicated that air temperature was 2 C warmer than the crop surface below. Interestingly, the authors precluded advection from having any influence as there was no pronounced spatial assymetry in evapotranspiration (measured gravimetrically) within the greenhouse. This is not surprising considering the nature of wind flow through an open-sided greenhouse. Clearly, in such advective environments the Bowen ratio can be negative and evapotranspiration can exceed net available energy. Furthermore, it is not incongruent with observed greenhouse performance that evapotranspiration equal or exceed net available energy and that greenhouse air,

particularly in the upper levels of the greenhouse be warmer than outside. As (2.11) indicates, inverted temperature profiles lead to negative Bowen ratios. Also, it is not necessary for the Bowen ratio to be negative for an advective environment to exist. Even in more restrictive ventilation regimes, the introduction of drier outside air will increase Q_E above that which would normally be experienced, though not necessarily in excess of $Q^* - Q_G$.

The abundance of experimental findings showing latent heating in excess of radiation receipts would indicate that negative Bowen ratios are not isolated occurrences in greenhouse microclimates. However, it remains difficult to assess what characteristics of greenhouse design and what types of ambient environments are conducive to the evapotranspiration totals reported.

2.2 THE GREENHOUSE COMBINATION MODEL

2.2.1 Purpose

This model provides a framework for delineating and assessing mechanisms responsible for evapotranspiration. The framework for the first combination model was proposed by Penman (1948). It recognizes that the flux of latent energy is a function of radiant energy, the ability of the atmosphere to withdraw this energy and the ability of the surface to supply moisture. Variants of the combination model have been developed for water bodies (Priestley and Taylor, 1972), arid environments (Rouse and Stewart, 1972), outdoor agricultural crops (Davies and Allen, 1973) and for forests (Tan and Black, 1976). Other researchers have dissected the model to enable a better understanding of surface control on evapotranspiration (Monteith, 1965; Tanner and Fuchs, 1968; Sziecz

and Long, 1969; Thom, 1972). However, none of these models is appropriate for advective environments because they require measurements within the fully adjusted boundary layer.

2.2.2 Derivation

In an idealized greenhouse where neither sensible nor latent heat flow takes place at the glazing the latent heat flux of the crop is defined by

$$Q_{E1} = \frac{\rho C_p}{\gamma} \frac{\psi}{A_s} (e_e - e_i) \quad . \tag{2.13}$$

The ratio A_s/ψ has the dimensions of a resistance (sm^{-1}) and will be called the ventilation resistance r_v. Strictly speaking $r_v = A_s/\psi$ is valid only when the evaporating surface is equal to the ground surface area. Furthermore, A_s will increase as the crop matures as will the ventilation resistance. Thus

$$Q_{E1} = \frac{\rho C_p}{\gamma r_v} (e_e - e_i) \quad . \tag{2.14}$$

Similarly, the surface sensible heat flux is defined as

$$Q_{H1} = \frac{\rho C_p}{r_v} (T_e - T_i) \quad . \tag{2.15}$$

Using the slope of the saturation vapour pressure-temperature curve S

$$S = \frac{d\, e_s(T)}{dT} \approx \frac{e_s(T) - e_s(T_w)}{T - T_w} \tag{2.16}$$

and the psychrometric equation

$$e = e_s(T_w) - \gamma(T - T_w) \quad , \tag{2.17}$$

(2.16) and (2.17) yield

$$e_s(T) - e = (S + \gamma) D \quad , \tag{2.18}$$

where e_s is the saturation vapour pressure at temperature T, and $D = T - T_w$ and is referred to as the wet-bulb depression where T and T_w are the dry and wet bulb temperatures of the air respectively. Hence,

$$e_i = e_s(T_{wi}) - \gamma D_i$$

$$e_e = e_s(T_{we}) - \gamma D_e$$

$$e_e - e_i = S(T_{we} - T_{wi}) - \gamma (D_e - D_i) \quad . \tag{2.19}$$

The energy budget now becomes

$$Q^* - Q_G = Q_{E1} + Q_{H1} = \frac{\rho C_p}{\gamma} \frac{\Delta e}{r_v} + \rho C_p \frac{\Delta T}{r_v} \tag{2.20}$$

$$= \frac{\rho C_p}{r_v}\left[\frac{S}{\gamma}(T_{we}-T_{wi}) - (D_e-D_i) + (T_e-T_i)\right] , \tag{2.21}$$

where $\Delta e = e_e - e_i$ and $\Delta T = T_e - T_i$. Since $D = T - T_w$,

$$Q^* - Q_G = Q_{E1} + Q_{H1} = \frac{\rho C_p}{r_v}\left[\frac{S}{\gamma}(T_{we} - T_{wi}) + (T_{we} - T_{wi})\right] \quad (2.22)$$

$$= \frac{\rho C_p}{r_v}\left(\frac{S+\gamma}{\gamma}\right)\Delta T_w \quad (2.23)$$

and $$\left(\frac{\gamma}{S+\gamma}\right)(Q^* - Q_G) = \frac{\rho C_p}{r_v}\Delta T_w \ . \quad (2.24)$$

From (2.14) and (2.19)

$$Q_{E1} = \frac{\rho C_p}{r_v}\left[\frac{S}{\gamma}\Delta T_w - \Delta D\right] \quad (2.25)$$

and $$\frac{\gamma}{S} Q_{E1} = \frac{\rho C_p}{r_v}\Delta T_w - \frac{\gamma}{S}\frac{\rho C_p}{r_v}\Delta D \ , \quad (2.26)$$

where $\Delta D = D_e - D_i$. Using (2.25)

$$\frac{\gamma}{S} Q_{E1} = \frac{\gamma}{\gamma + S}(Q^* - Q_G) - \frac{\gamma}{S}\frac{\rho C_p}{r_v}\Delta D \quad (2.27)$$

and $$Q_{E1} = \frac{S}{S+\gamma}(Q^* - Q_G) + \frac{\rho C_p}{r_v}(D_i - D_e) \ . \quad (2.28)$$

The latent heat flux has been separated into a radiation dependent and a ventilation dependent term. The second term describes the coupling between evapotranspiration and the outside temperature and humidity. If the incoming air is very dry then D_i is large and so is the advective influence on evapotranspiration. In a mid-latitude environment this would occur during an extended period without precipitation. Shortly after a rainfall D_i may be very small and the advection term could become negative. This would be the case if the greenhouse surface

dried out or stomatal closure occurred. In this case advection is still occurring but acts to retard rather than enhance the latent heat flux.

When $D_i = D_e$ there is no advection, the second term equals zero and evapotranspiration is controlled solely by the radiative term. It should be noted that when $D_e = D_i$ the exhaust and intake vapour pressures are not equal. Due to the nature of D (see 2.18) the exhaust vapour pressure is higher owing to its higher temperature. The condition $D_i = D_e$ indicates that the interior and exterior water vapour environments are in equilibrium. The first term of (2.28) is therefore referred to as the "equilibrium" term.

Equilibrium evapotranspiration would similarly occur when the ventilators were turned off. In this case $r_v \to \infty$ and the advection term approaches zero. Evapotranspiration continues as a function of the net available energy, as long as it is positive. The term $S/(S + Y)$ describes the coupling between an increase in air temperature as a result of sensible heating and the ability of the air to accept more moisture.

Equation (2.28) does not account (1) for the part of the latent heat flux emanating from the surface in response to condensation on the glazing (2) for sensible heat loss through the glazing. The reason for including these two terms is apparent from (2.3) and (2.4). If condensation is occurring on the glazing then the vapour pressure of the exhaust air is lower than it would normally be. The converse is true if condensate is evaporating from the glazing. Similarly, if sensible heat is being lost through the glazing, the exhaust air temperature would be lower than normal.

Let Q_{H*} be the glazing sensible heat flux (positive outwards). Let Q_{E*} be the glazing latent heat flux (positive for condensation,

negative for condensate evaporation). The energy balance is now defined as

$$A_s(Q^*-Q_G) = A_s(Q_H+Q_E) = A_s(Q_{H1}+Q_{E1}) + A_g(Q_{H*}+Q_{E*}) \quad , \tag{2.29}$$

where A_g is glazing area (m^2). Making appropriate substitutions for Q_{H1} and Q_{E1}

$$A_s(Q^*-Q_G) = \frac{S+\gamma}{\gamma} A_s \frac{\rho C_p}{r_v} \Delta T_w + A_g Q_{H*} + A_g Q_{E*} \tag{2.30}$$

$$\frac{\gamma}{S+\gamma}(Q^*-Q_G) = \frac{\rho C_p}{r_v} \Delta T_w + \frac{\gamma}{S+\gamma}\left[\frac{A_g}{A_s} Q_{H*} + \frac{A_g}{A_s} Q_{E*}\right] \quad . \tag{2.31}$$

The latent heat flux is given by

$$Q_E = Q_{E1} + \frac{A_g}{A_s} Q_{E*} \tag{2.32}$$

$$= \frac{\rho C_p}{r_v}\left[\frac{S}{\gamma}\Delta T_w - \Delta D\right] + \frac{A_g}{A_s} Q_{E*} \tag{2.33}$$

$$\frac{\gamma}{S} Q_E = \frac{\rho C_p}{r_v} \Delta T_w - \frac{\gamma}{S}\frac{\rho C_p}{r_v} \Delta D + \frac{\gamma}{S}\frac{A_g}{A_s} Q_{E*} \quad . \tag{2.34}$$

Using (2.31)

$$\frac{\gamma}{S} Q_E = \frac{\gamma}{S+\gamma}(Q^* - Q_G) - \frac{\gamma}{S+\gamma}\frac{A_g}{A_s}\left[Q_{H*} + Q_{E*}\right]$$

$$- \frac{\gamma}{S}\frac{\rho C_p}{r_v} \Delta D + \frac{\gamma}{S}\frac{A_g}{A_s} Q_{E*} \quad , \tag{2.35}$$

the latent heat flux then becomes

$$Q_E = \frac{S}{S+\gamma}(Q^*-Q_G) + \frac{\rho C_p}{r_v}(D_i-D_e) - \frac{S}{S+\gamma}\frac{A_g}{A_s}Q_{H^*} + \frac{\gamma}{S+\gamma}\frac{A_g}{A_s}Q_{E^*} \quad . \quad (2.36)$$

Equation (2.36) is referred to as the Greenhouse Combination Model. The first two terms (equilibrium and advection) remain unchanged. Since the glazing sensible heat transfer is usually directed outwards, the third term acts to depress evapotranspiration as this energy is unavailable to the evapotranspiration process. Increasing condensation increases the surface latent heat flux. Evaporation of condensate depresses the surface latent heat flux.

2.2.3 Application

Net radiation, soil heat flux, intake and exhaust dry and wet bulb temperatures are needed to evaluate the model. With these six measurements the equilibrium term can be estimated. The saturation vapour pressure e_s at wet bulb temperature is given by Dilley (1968) as

$$e_s(T_w) = a \exp\left[bT_w/(T_w + c)\right] \quad , \qquad (kPa) \qquad (2.37)$$

where $a = 0.61078$, $b = 17.2693882$, $c = 237.3$.

Hence, the slope of the saturation vapour pressure-temperature curve can be evaluated from

$$S = \frac{de_s}{dT_w} = \left[f/(T_w + c)^2\right] \exp\left[\frac{bT_w}{T_w + c}\right] \quad , \quad (kPaC^{-1}) \qquad (2.38)$$

where $f = 2502.99221$ and T_w is evaluated at the mean of the intake and exhaust wet bulb temperatures.

The glazing sensible heat transfer is given in (2.3) as

$$Q_{H*} = U(\bar{T}_{in} - \bar{T}_{out}) \quad . \tag{2.39}$$

The assumption that U is a constant is a simplification. Being a composite of conductive, convective and radiative terms it can vary considerably over time. A more detailed examination of the U-factor is reserved for Chapter Four. The U-factor can be evaluated if initially periods are selected when condensation is not occurring.

When the ventilators are closed, combining (2.3) and (2.4) gives the sensible and latent heat fluxes as

$$Q^*-Q_G = Q_H + Q_E = \rho C_p \frac{V}{A_s}\frac{dT}{dt} + \frac{A_g}{A_s} U(\bar{T}_{in}-\bar{T}_{out}) + \frac{\rho C_p}{\gamma}\frac{V}{A_s}\frac{de}{dt} \quad , \tag{2.40}$$

and

$$U = A_s(Q^*-Q_G) - V\rho C_p[dT/dt + de/\gamma dt][A_g(\bar{T}_{in}-\bar{T}_{out})]^{-1} \quad . \tag{2.41}$$

Sampling errors in T_{in} are minimized if the greenhouse air is well mixed.

The ventilation resistance must be evaluated when the ventilators are operating and again this is simplified if periods are selected when condensation is not occurring ($Q_{E*} = 0$). The ventilation resistance is calculated by residual by comparing measured evapotranspiration with combination model estimations. Q_E can be measured lysimetrically, gravimetrically or by use of (2.4).

$$r_v = [\rho C_p(D_i-D_e)][Q_{Emeas.} - \frac{S}{S+\gamma}((Q^*-Q_G) + \frac{A_g}{A_s} Q_{H*})]^{-1} \tag{2.42}$$

In mechanically ventilated greenhouses the ventilation resistance should vary little over time periods as short as two or three days. This is partly because turbulent exchange is constant and controlled. In the outside environment, r_v is affected by both wind speed and buoyancy effects. Buoyancy effects become more pronounced when the surface is warm. Even though the greenhouse ground surface is warmer than outside, the glazing acts to retard buoyant convection. Also, the buoyant convection that does occur does not interact with the atmospheric sink. Therefore, drier air is not brought down to replace the moist eddies leaving the surface.

As the crop matures, surface roughness increases as would the ventilation resistance. Hence, a comparison of r_v from (2.42) with $r_v = A_s/\psi$ where A_s is ground surface area should indicate any crop growth effects as the plants reach maturity.

It is instructive to note that the greenhouse combination model in its present form differs from previously published evapotranspiration models because it requires the measurement of T and T_w between inlet and outlet of the greenhouse air volume. Therefore, it is sensing the response of the air temperature and humidity regimes resulting from latent and sensible heating at the surface. Because of this, parameterization of water availability and stomatal response is not required because these influences are embodied in the difference between inlet and outlet wet bulb depressions. As such, the ventilation resistance is a purely aerodynamic term and should not be influenced by stomatal response.

With a parameterization of U and r_v the evaluation of the combination model is made possible. The sole exception is that the solution for the glazing condensation flux Q_{E*} has not been treated

explicitly. Further discussion of glazing condensation will be presented in Chapter Four.

CHAPTER THREE

EXPERIMENTAL PROCEDURE

3.1 EXPERIMENTAL SITE AND OBSERVATION PERIOD

The research site was located at Greensville, Ontario, about 6 km from Hamilton (LAT. 43°21' N; LONG. 80°00' W). A greenhouse was constructed on flat land in the centre of a 0.6 hectare garden which was bounded on all sides by farmland in vegetable production. A barn was situated due west, 70 m away from the greenhouse. During the summer solstice it had no effect on solar radiation reaching the greenhouse. Approximately 50 m due east of the greenhouse, a farm house and row of mature maples would shade the greenhouse between 0630 and 0830 for intermittent periods during the summer solstice. The south and north horizons were unobstructed.

Energy budget data were collected from May 25 to June 24th, 1978. Radiation data was collected from May 2 to December 18, 1978 and during July 1979. The measurement program was disrupted during the major measurement period as a result of severe thunderstorm activity. This necessitated repairs of the greenhouse and replacement of instruments and data loggers. The farmhouse basement was used as a laboratory. It housed the data logger (Solatron, 2.5 μV resolution). Values were recorded every ten minutes and stored on hardcopy and punched paper tape.

3.1.1 Greenhouse Construction

The greenhouse had a square floor plan and was designed after the Brace greenhouse (Brace Research Institute, Lawand et al., 1975).

It was a wooden lean-to style greenhouse of 40 m^2 ground area. The north roof/wall was oriented due east-west and insulated with R-10 fiberglass batts and covered inside and out with 9 mm construction grade plywood. Three coats of exterior grade white latex paint were applied to all wooden surfaces. The roof was angled towards the south at 25° from the vertical. This angle is approximately equal to the zenith angle of the sun at solar noon at the summer solstice. Thus, no part of the growing surface was shaded. The south roof and wall and the east and west gable ends were covered in a double layer of 0.15 mm ultraviolet resistant polyethylene (C.I.L.). The two polyethylene layers were attached to the outside of the frame at their margins by an aluminum extrusion (Polylok) and separated by pressurized air supplied by an inflation fan. The separation between the layers ranged from 0 m at the margins to 0.3 m near the centres of roof and walls. (Figure 3.1) The entrance was a small door on the east gable end adjacent to the north wall. The total surface area of glazing and wall was 2.76 times that of the floor area (110 m^2). The ratio of glazing-area, including gable ends, to floor area was 2.0 (80 m^2). The ratio of insulated wall to floor area was 0.76. The floor of the greenhouse comprised the indigenous garden soil.

The greenhouse was ventilated with two thermostatically controlled blowers. The blower near ground level operated continuously. When the greenhouse air temperature exceeded the thermostat setting, a mechanical damper system admitted outside air through this blower via an air inlet located 0.5 m above ground level midway through the north wall. This coincided with the operation of the exhaust blower which was suspended from the north wall, near the ridge of the greenhouse.

When greenhouse air temperature fell below the thermostat setting,

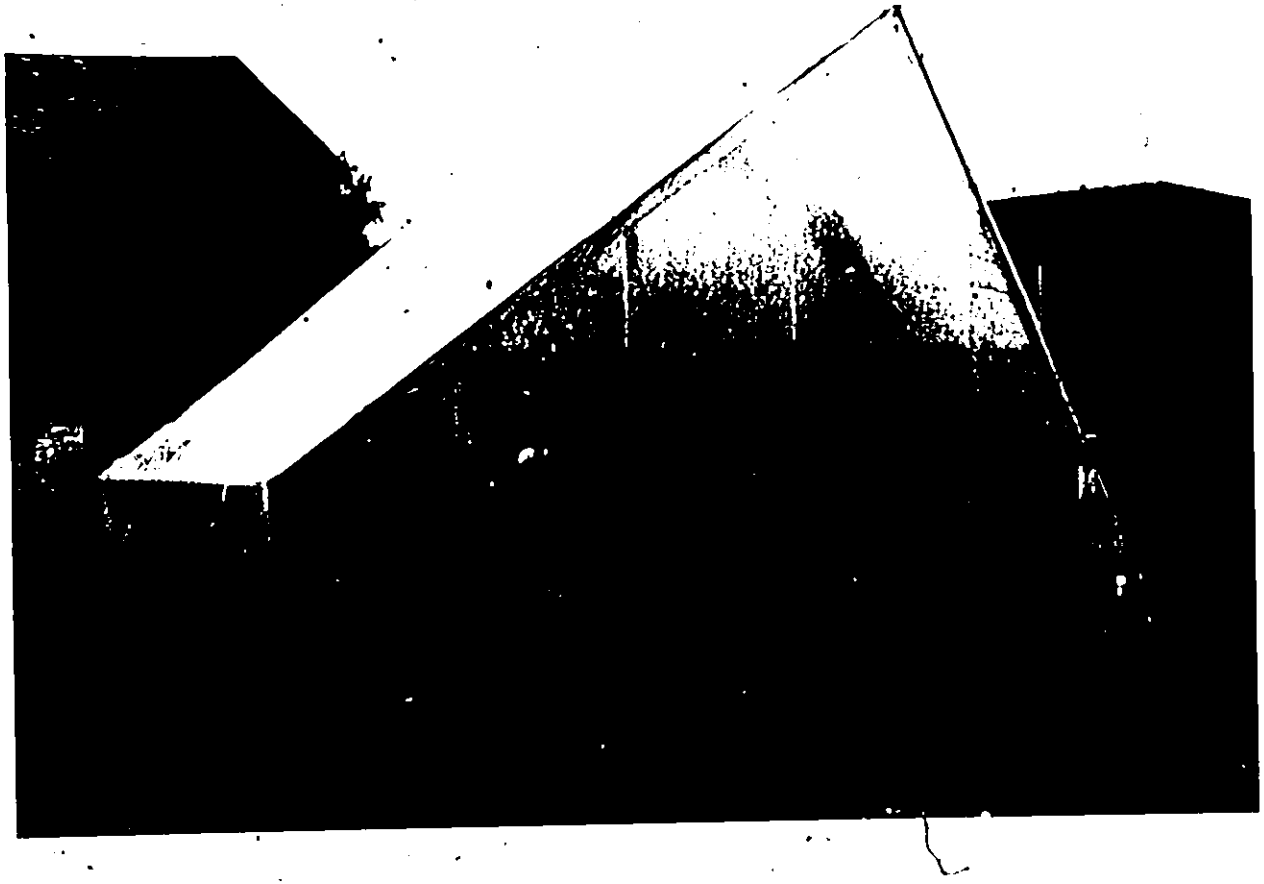

Figure 3.1. Experimental Brace greenhouse, Greenville, Ontario.

the exhaust blower was turned off and the damper system prevented outside air entry and diverted air flow through a vertical duct, which extracted air from the ridge of the greenhouse, thoroughly mixing the greenhouse air.

Blower capacity was determined by periodically measuring blower cage rotation. Ventilation rates were then determined from data supplied by the manufacturer. These tests indicated an average ventilation rate of 0.75512 m^3 s^{-1} ($\pm$ 5%) during the measurement period. This is somewhat less than ventilation rates provided in commercial greenhouses as 4.5 minutes were required for one air volume change. The implications of this ventilation rate for the energy budget will be discussed in Chapter Four.

Board insulation 5 cm thick was buried around the perimeter of the greenhouse to a depth of 30 cm. The purpose of the insulation is to minimize sub-surface horizontal heat loss from the soil block. The material used was neither as thick nor as deep as commonly recommended (Mazria, 1979) but was limited by the resources available at the time.

3.2 INSTRUMENTATION AND FIELD PROGRAM

3.2.1 Radiation Measurements

The instrument locations and greenhouse dimensions are shown in Figure 3.2. Five radiometers were located centrally at a height of 2 m above the ground. One Eppley (black and white) pyranometer measured incoming solar radiation. A second inverted Eppley pyranometer measured reflected solar radiation. The third and fourth radiometers were Funk-type, Swissteco (S-1) pyrradiometers. One had both upper and lower thermopile surfaces covered with thin polyethylene domes. As this

Figure 3.2. Dimensions and instrument locations in experimental greenhouse.

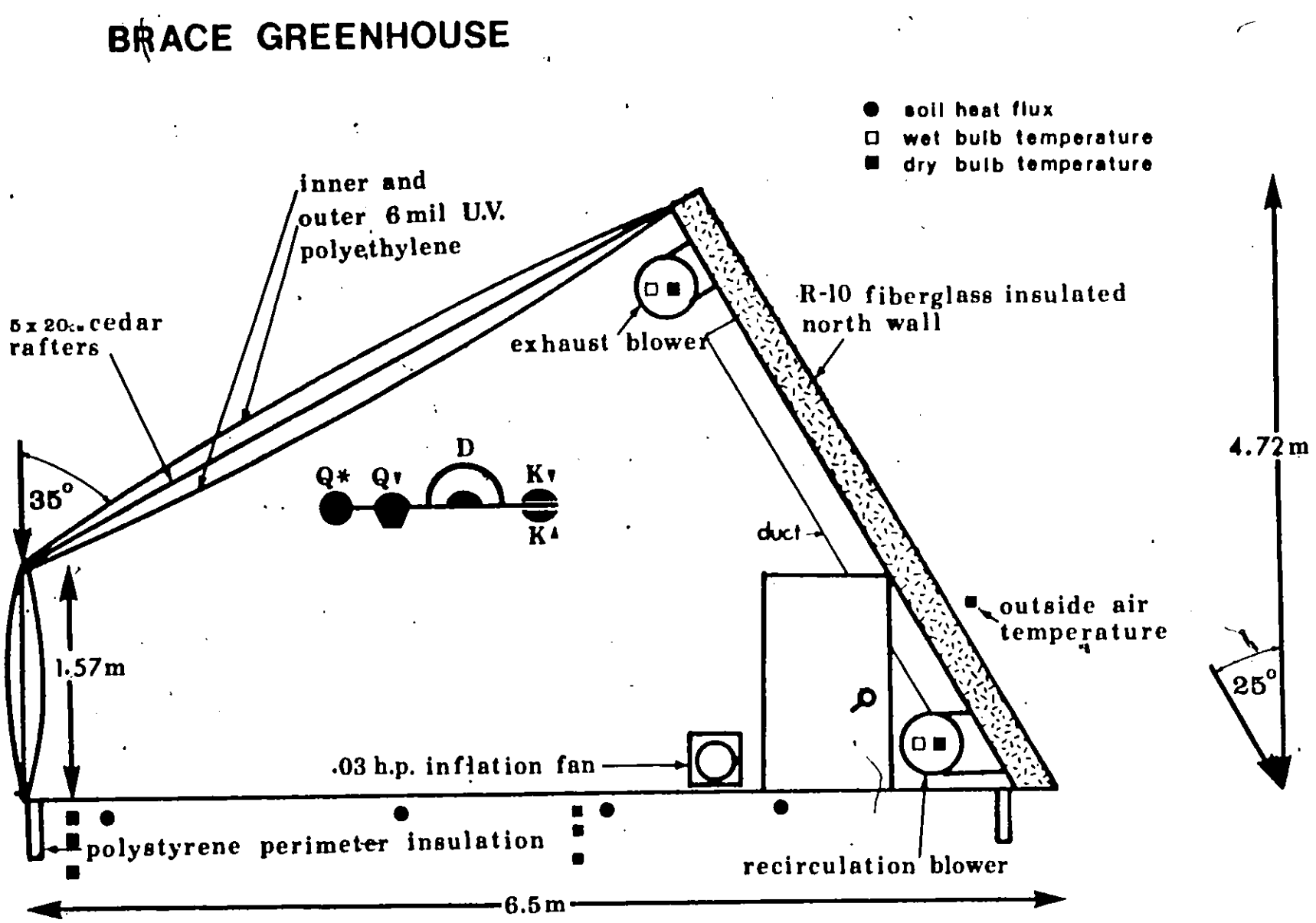

polyethylene transmits both short and longwave radiation this sensor measured net radiation Q*. At night it provided a measure of the net longwave radiation directly. During the day, the net longwave radiation was determined by subtracting the net solar flux from the net radiation. The second pyrradiometer was fitted with a lower cast aluminum shield (black body cavity). The temperature of the cavity was monitored with a copper-constantan thermocouple embedded in the aluminum. This sensor measured incoming allwave radiation ($K\downarrow + L\downarrow$). Thus, the upward and downward longwave fluxes could be determined by residual from the $K\downarrow$ and Q* measurements. The Swissteco instruments were continuously aspirated with dried air. The air flow was necessary to inflate the domes and reduce variations in convective regimes about the upper and lower thermopile surfaces. The fifth radiometer measured diffuse solar radiation but does not constitute part of the present analysis.

The view factors for the downfacing sensors were determined from

$$VF = r^2 / (h^2 + r^2) \quad , \tag{3.1}$$

where r is the average radius of the crop surface underlying the sensor and h is the height of the sensor above the crop surface. For bare soil VF = 0.68 and for a mature canopy VF = 0.83.

Post experimental calibration comparing all pyranometers with a precision Eppley pyranometer showed that pre-experimental calibration, by the Atmospheric Environment Service radiation laboratories in Toronto, agreed within 3%. The calibration of the downfacing Eppley pyranometer was increased 1.4% following the recommendations of Latimer (1970) for inverted sensors. After the experiment the Swissteco pyradiometers were

found to agree within 5% of each other.

3.2.2 Temperature and Humidity Measurements

Dry and wet bulb air temperatures were measured at two locations in the greenhouse with five-junction copper-constantan thermopiles. Companion sensors were housed in aspirated psychrometer shields (Lourence and Pruitt, 1969). One was located in the centre of the airstream from the intake blower, approximately 0.5 m above ground level. The second was located at the ridge of the greenhouse, midway (0.5 m) between the exhaust blower outlet and the recirculation duct inlet. When the exhaust ventilator was on, the lower psychrometer measured inlet temperature and vapour pressure. The upper psychrometer measured exhaust temperature and vapour pressure. When the exhaust ventilator was closed and air was being recirculated within the greenhouse, the psychrometers measured temperature and vapour pressure at their respective locations. A comparison of temperatures and vapour pressures between them provided a measure of the thoroughness of air mixing.

The upper psychrometer was within 0.5 m of the glazing and was used to determine inside temperature in the calculation of the glazing U-factor. When in the recirculation mode, the evaluation of dT/dt and de/dt was provided by the lower psychrometer.

A fifth thermopile was located outside at screen height in a similar aspirated psychrometer shield. It provided a measure of the outside air temperature.

Wet bulb feeds consisted of muslin wick extending approximately 5 cm from the tip of the thermopile. The other end of the wick was immersed in a small, shielded water reservoir. Wicking was inspected and

replaced periodically when the surface accumulated dirt.

All thermopiles were referenced to an ice-point oil bath. Some difficulties were encountered, early in the measurement program, in maintaining the oil bath at 0 C due to the very hot greenhouse temperatures. This problem was circumvented by locating the oil bath in the incoming ventilator air stream and by adding a shading device to reduce radiant heating. All data presented were collected after this adjustment.

Five-junction copper-constantan thermopiles produce a nominal emf of 0.2 mV C^{-1}. Pre and post season laboratory calibrations against precise platinum resistance thermopiles indicated that the thermopiles are accurate to between 3 and 8 one-hundreths of a degree between 0 and 40 C.

3.3.3 Soil Heat Flux Measurements

Soil heat flux was measured directly with soil heat flow transducers (Middleton). Four transducers were wired in series and buried approximately 5 cm below the soil surface before the greenhouse was planted. The four sensors were spaced equidistant across the north-south midline of the greenhouse to provide a spatially representative value for Q_G. Planting, transplanting and irrigation were performed irrespective of sensor location.

Soil thermistors were buried at depths of 5, 10 and 25 cm at two locations adjacent to the most southerly and most central soil heat flux plates. The resistance of the six sensors was measured periodically with a portable digital multimeter (Kiethly). Because these signals were collected manually, the frequency of data collection differed from that of the data logger and the signals were incompatible for the calibration

of soil heat flux divergence in the upper 5 cm. The soil heat flux values reported are therefore, the raw values collected from the soil heat flow transducers. A post season calibration of these sensors against a comparison set of heat flux plates show that the manufacturer's calibrations were valid to within 2-3%. This is better than the manufacturer's claimed accuracies of 5-10%.

3.3.4 Supplemental Measurements

Cumulative wind kilometers were recorded with a cup anemometer (Casella) located at screen height 5 m south-east of the greenhouse. A record was kept of the presence and absence of condensation on the glazing. Idiosyncracies in radiation receipt (shading by trees, rafters, etc.) were noted as was radiometer and psychrometer maintenance.

3.3 GREENHOUSE MANAGEMENT

The greenhouse was managed as a typical hobby greenhouse. It was planted with an assortment of vegetable and flower seedlings. As a particular plant reached maturity it was harvested and replaced with a new seedling, also raised in the greenhouse. After May 22, when the last of the original seedlings was transplanted, there were no large expanses of soil unoccupied by plants. However, with seedling spacing of approximately 0.25 m, bare soil did dominate the surface at this time. The latest data presented here, represent 33 days of plant growth, at which time the surface, except for walkways, was dominated by vegetation.

Irrigation was performed manually when it was observed that the soil surface had undergone significant drying and later when any plant

wilting became apparent. Pest and disease problems were also dealt with.

Because greenhouse management departs considerably from conventional commercial practice and was not aimed at optimal crop productivity, a horticultural assessment of the crop was not performed. In retrospect, an independent assessment of plant mass (dry matter production or leaf area index) would have been desirable in the parameterization of the ventilation resistance. However, it was felt that periodically removing plants for such analysis would unduly influence the character of the growing surface because of its small size.

All aspects of the research program with the exception of greenhouse construction were performed solely by the author.

CHAPTER FOUR

RESULTS

4.1 RELATIONSHIP BETWEEN INCIDENT SOLAR RADIATION AND NET RADIATION

Although incident solar radiation is not required for the greenhouse combination model it is quite often the only radiative flux measured in greenhouse research programs. Hence, the model has greater applicability if the requirement for measured Q* is relaxed. The assessment of radiation in greenhouses however, is complicated by shading by components of the greenhouse structure. In the Brace greenhouse, the opaque north wall affects radiation receipt, particularly in early morning and late evening. However, this poses minimal problems because the shading of the radiometer generally coincides with shading of the crop surface. The greatest difficulty is posed by framing members and, in this respect, sampling errors are similar between the Brace greenhouse and more conventional greenhouses. Measured radiation is not representative of surface radiation when rafters shade the pyranometer. Also, sensor location further obscures the true surface flux because the pyranometer receives direct radiation through a single facet of the greenhouse, whereas, the crop is receiving radiation through the integrated effect of all facets.

During the measurement program, a small experiment was conducted to assess what bias may exist from measuring solar radiation at a single, centrally located position. A pyranometer was alternately moved every 10 minutes throughout the day from a purlin 2 m to the north, then 2 m to the south of the central pyranometer. Signals from both pyranometers were recorded every 10 minutes. Thus, a comparison of incident solar

radiation between the central sensor and either north or south was possible every 20 minutes. Figure 4.1 indicates the measured values of $K\downarrow$ at the three locations on June 10, which was a relatively cloudless day. In general, the south sensor receives approximately 3-5 Wm^{-2} more, and the north sensor 3-5 Wm^{-2} less than the central sensor around midday. In early morning and late afternoon, the north receives less $K\downarrow$ due to wall shading. Because during this time of the year the sun views very little of the north wall, the reflecting capabilities of the white surface play a negligible role in the spatial variation of solar radiation. The higher and lower values for the south and north locations respectively result from the occlusion of north sky diffuse radiation by the wall. These effects would be more pronounced for overcast skies but there are no direct measurements to confirm this. The results indicate that for cloudless skies at this time of year, the central sensor does provide a representative value for incident solar radiation.

Nevertheless, the rafter effects are pronounced and similar effects for measured net radiation also occur but not at the same times due to slightly different sensor locations. Thus, when comparing incident solar and net radiation, the instantaneous values show a large amount of scatter. Hence, the relationship between the hourly values of these two fluxes was examined by numerically integrating values using Simpson's rule. Daytime net and solar radiation were highly correlated during the measurement period ($0.91 < r < 0.96$) however, regression coefficients ranged from 0.56 to 0.76 with the values generally decreasing from spring to summer. Since an error in the estimation of Q* of 35% is probably too large (Chapter Five) for the successful use of the combination

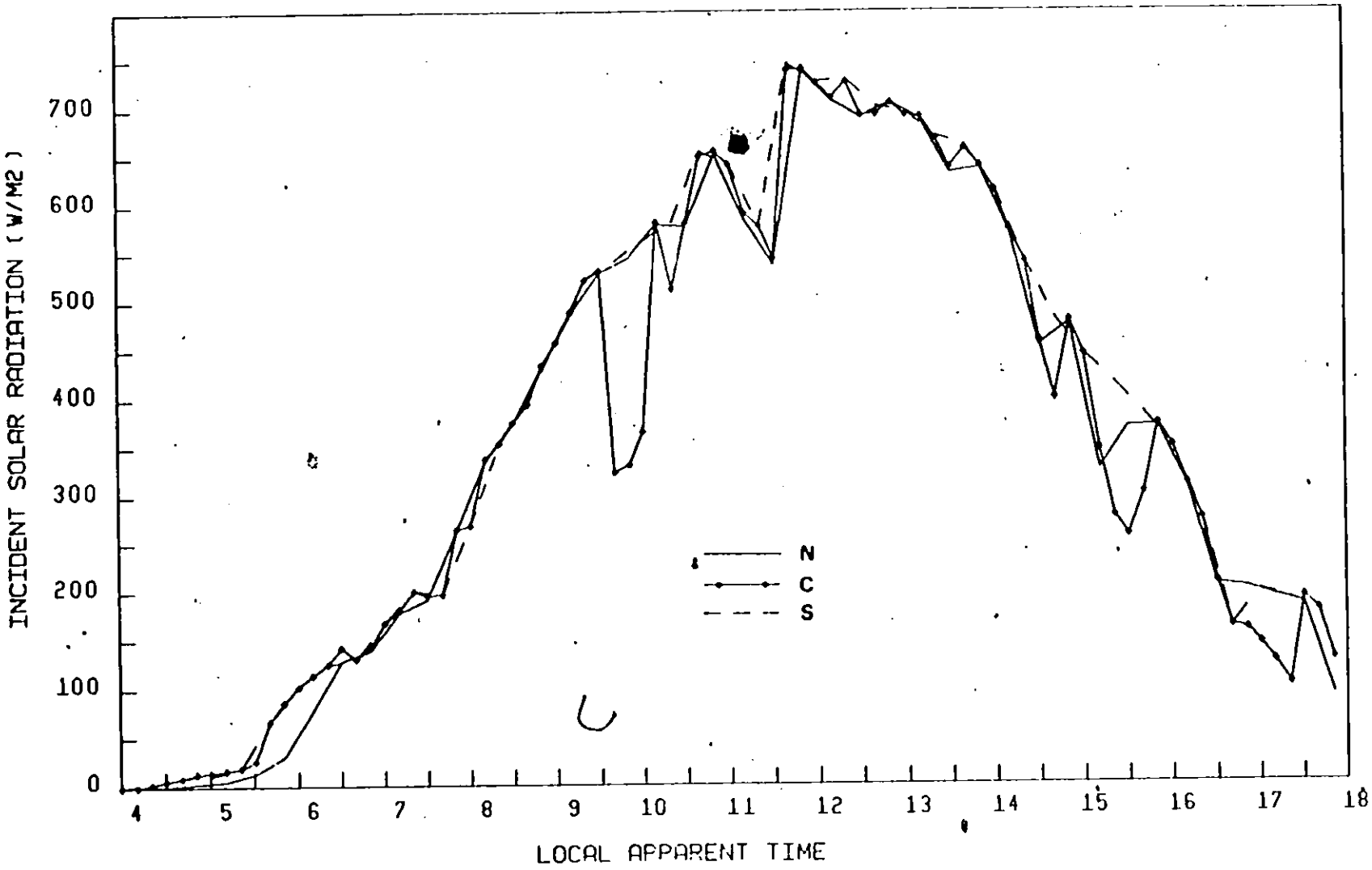

Figure 4.1. Comparison of incident solar radiation at north, south and central sensor locations.

model, it would appear inappropriate to use $K\downarrow$ as a surrogate for Q* within the regression framework. There is no basis, nocturnally, to estimating Q* from $K\downarrow$. Direct measurement of net radiation is the best alternative at this time.

It should be noted that although scanning radiation signals every 10 minutes over this measurement period produced voluminous amounts of data, this is clearly too long an interval to get accurate hourly radiation totals. It is suggested that scanning data loggers should use a one or two minute interval such that anomalous values caused by shading, would receive lesser numerical weighting in quadrature formulations. The use of integrating data loggers demonstrates a marked superiority in this regard.

4.2 RELATIONSHIP BETWEEN NET RADIATION AND SOIL HEAT FLUX

The measurement of soil heat flux with transducers, although straightforward, requires the additional investment of time and resources. This measurement program indicates that the soil heat flux may be estimated with a purely empirical approach. For the period May 25 to July 12, regression of hourly soil heat flux and net radiation indicates regression coefficients between 0.09 and 0.12 ($0.91 < r < 0.95$). Integrated daily totals also indicate the soil heating component of net radiation falling between 9 and 12%. Figure 4.2 a, b shows the regression of Q_G and Q* for 24 hourly values on two days. The hysteresis effect is apparent. Even though few of the data points actually fall on the regression line the correlation coefficients are sufficiently large and the magnitude of Q_G sufficiently small that minimal error would result from estimating Q_G in this manner. It is valid to point out however,

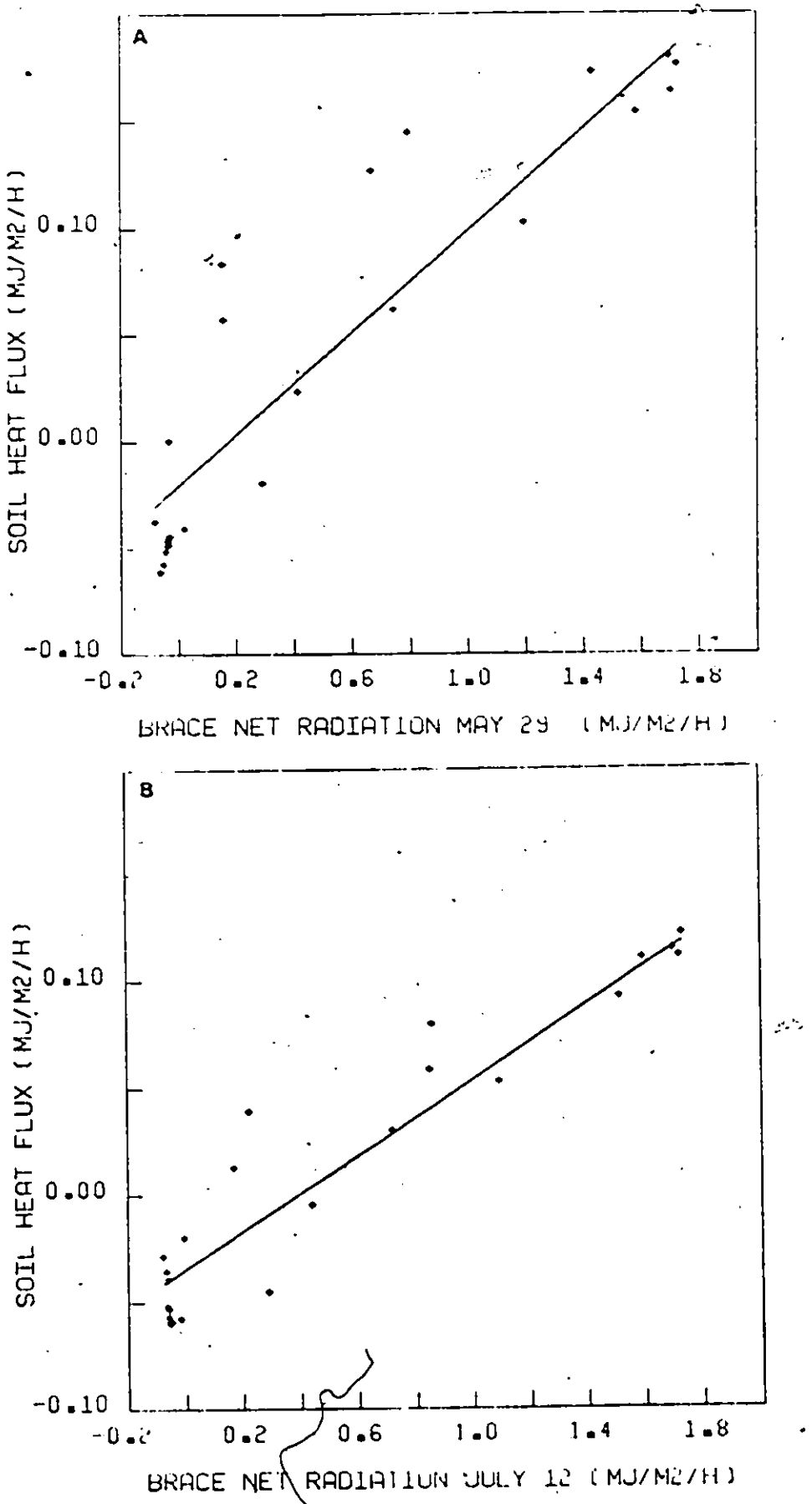

Figure 4.2. Relationship between net radiation and soil heat flux.

that the limited data set reported here would prohibit any sweeping generalizations being drawn in this regard. Also, instantaneous values of Q_G approach 20% of Q^* and ignoring soil heat flux altogether would lead to systematic errors of at least 10% in the estimation of net available energy.

4.3 MODEL ESTIMATIONS OF EVAPOTRANSPIRATION

The latent and sensible heat fluxes were initially calculated using instantaneous values in (2.3) and (2.4). A channel of the data logger was reserved to monitor fan operation. A shorted signal signified that the exhaust fan was on. When the greenhouse was being ventilated the storage terms in (2.3) and (2.4) were found to represent 1.1% and 0.8% of the net radiation of the crop surface respectively during the midday period. Hence, their omission in energy budget calculations is justified when the ventilators are on.

Generally, the dry and wet bulb temperatures show a predictable trend over the day with air temperatures reaching 39 C as a result of the low ventilation rates. Figure 4.3 a, b shows the course of dry and wet bulb temperatures for two diurnal periods. Relative humidities as low as 35-40% are reached during the day and as high as 95-98% at night. Upper and lower dry bulb temperatures departed as much as 0.5 C during the evening when greenhouse air was being recirculated but were quite often less than 0.1 C indicating thorough air mixing. One benefit of the high inside temperatures was that they permitted a more reliable estimation of the glazing U-factor, although they are too high for optimal crop growth. Cool weather crops in particular lettuce and chard,

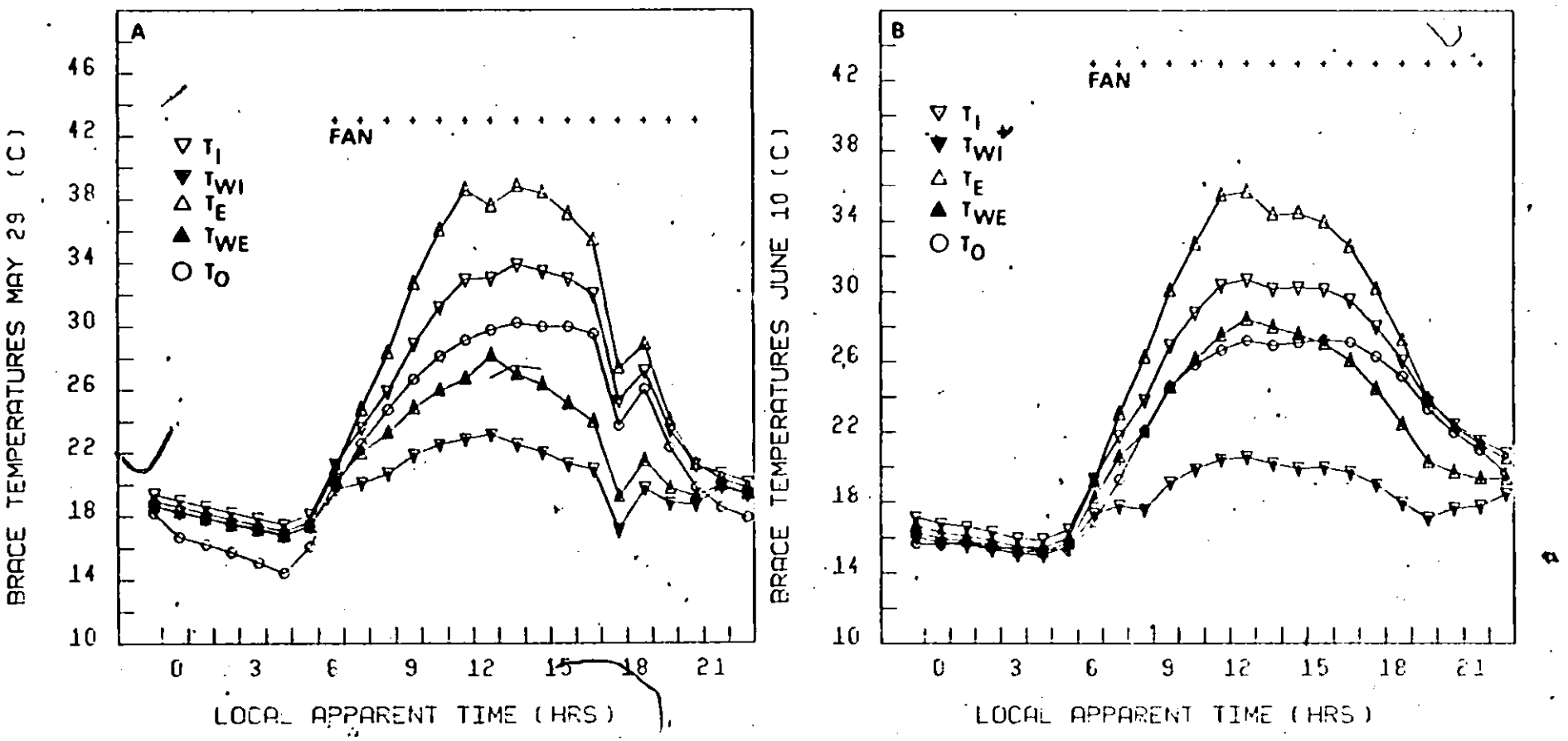

Figure 4.3. Variations in intake and exhaust dry and wet-bulb temperatures and outside temperature.

demonstrated a strong tendency to bolt.

Two problems were encountered in the calculation of Q_{E1} and Q_{H1}. The first occurred in early morning and late evening when air temperatures inside were close to the thermostat setting. During these periods, the exhaust fan would typically cycle on and off a few times. This made it difficult to determine the mode of fan operation from the single scanned value once every ten minutes. The ventilation terms (first term) of (2.3) and (2.4) are highly dependent on the mode of fan operation. Second, when the fan switched from ventilation to recirculation, the storage terms of (2.3) and (2.4) were difficult to assess because they require the evaluation of de/dt and dT/dt respectively. However, at the previous scan T and T_w were representative of the incoming air because the fan was still in the ventilation mode. An attempt was made to avoid applying the model on days where this cycling effect was persistent, nevertheless at least one value each day will contain this error. Instantaneous values of Q_{E1} and Q_{H1} were integrated numerically to determine hourly totals for the sensible and latent heat fluxes ($MJ\ m^{-2}\ h^{-1}$).

The equilibrium and advection terms of the combination model were then calculated. The shading effects of rafters were reduced somewhat when hourly values of Q^* were determined. The systematic underestimation of true net radiation, however, cannot be removed by this process. Rafter shading was particularly acute, for the 17th and 19th hourly values for net radiation, each day. An inspection of the other radiation signals indicated that the sun was tracking along a rafter which shaded the net radiometer for extended periods (30-40 minutes). These values were replaced with interpolations from adjacent values of

net radiation.

Hourly averages were used for T and T_w and in the subsequent calculation of S from (2.38). The evaluation of r_v was accomplished using (2.42) for the data from May 27 initially. The derived value of r_v was then applied to the May 26 data with the assumption that plant effects on r_v would be negligible over such a short time interval. Equation (2.42) requires an 'a priori' knowledge of Q_{H*} the glazing sensible heat flux. Again, May 27 data was used to derive the U-factor needed for Q_{H*}. The use of (2.41) for this purpose was not satisfactory for early morning values because condensation was present on the glazing at this time. The absence of condensation is a condition required for (2.41). Late afternoon and early evening values were more appropriate because condensation had not yet occurred and because the inside-outside temperature difference was still large enough to provide reasonable accuracy in the determination of U.

May 26 results are illustrated in Figure 4.4 a, b. The abscissa is local apparent time (solar time) for the calendar day. Figure 4a shows how the estimated evapotranspiration is made up of the equilibrium component and the advection component. This day is particularly interesting because it represents the microclimate of the greenhouse only four days after transplanting was completed. The advective term was, of course, zero until fan operation commenced just before 0800. The advective influence was large as air initially entered the greenhouse because of the damp and high humidity conditions prevailing through the previous evening. Soil moisture was freely available at the surface. However, after a short period of time the soil surface dried and with a relatively sparse plant covering, water could not be supplied on demand.

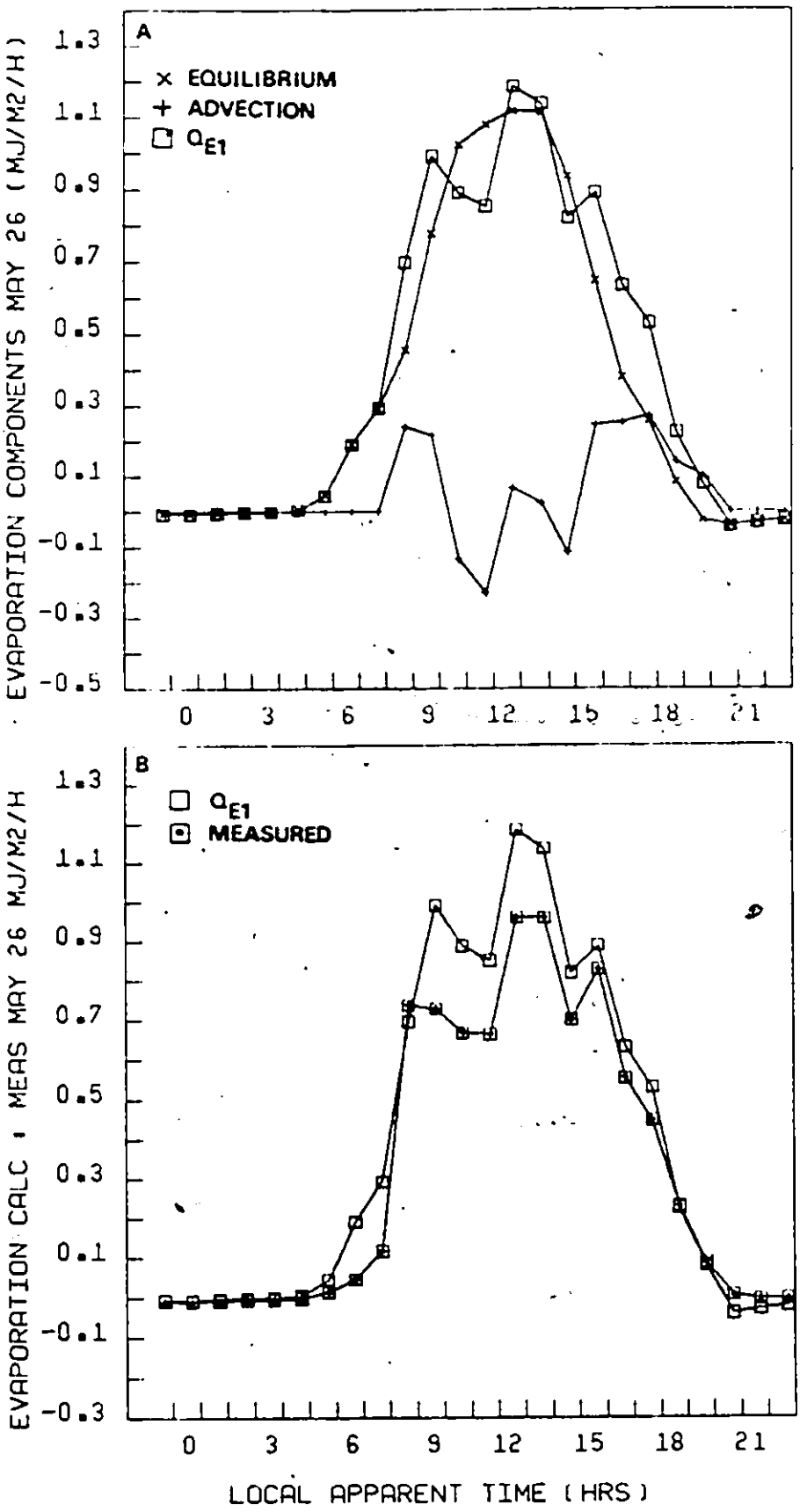

Figure 4.4. a. Variation in the equilibrium, advection and combined terms of the combination model for May 26.
Figure 4.4. b. Comparison of combined term and measured evapotranspiration for May 26.

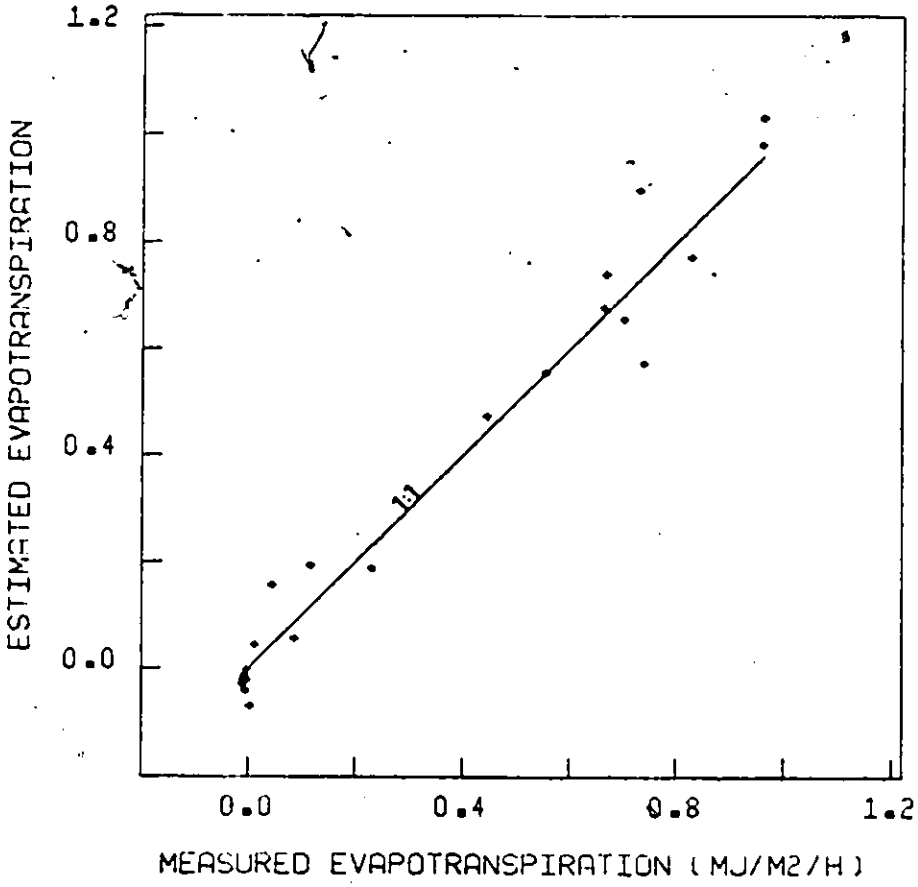

Figure 4.5. Comparison of estimated and measured evapotranspiration for May 26.

The advective influence in fact rapidly became negative. Thus D_e exceeded D_i and the greenhouse surface depressed evaporation while enhancing sensible heating. A major application of water just before 1200, rapidly forced the advection term positive again. However the advective influence did not return to its early morning magnitude because radiant demands were at their peak by then, as was the evaporative flux. The desication of the soil surface is represented by another decrease in the advection term to negative values. Another irrigation prior to 1600 again caused an enhancement of the latent heat flux resulting from positive advection. Because radiant energy supply diminished rapidly, the surface was able to maintain an adequate moisture supply until the cessation of fan operation around 2000.

Figure 4.4 b compares the measured evapotranspiration using (2.3) (lower curve) with that estimated by the first two terms of the combination model (upper curve). The diurnal variations in measured Q_E are well represented by the equilibrium and advection terms of the combination model. To test the accuracy of the combination model, the third term (glazing sensible heat flux) was subtracted from the first two terms (2.38) and the model estimate was regressed with measured Q_E. As Figure 4.5 suggests, agreement is quite good with $r = 0.95$ and slope of 0.98. For comparison purposes a regression of measured Q_E and net radiation yields, $Q_E = 0.458\ Q^* - 0.06$ ($r = 0.89$).

Twenty days after transplanting, transpiration by the crop had begun to dominate Q_E. As Figure 4.6 a illustrates, advection always enhanced evapotranspiration and only a minor decrease in advection occurred prior to irrigation before 1200. After irrigation, the advective influence increased but in a more controlled manner. Again, model

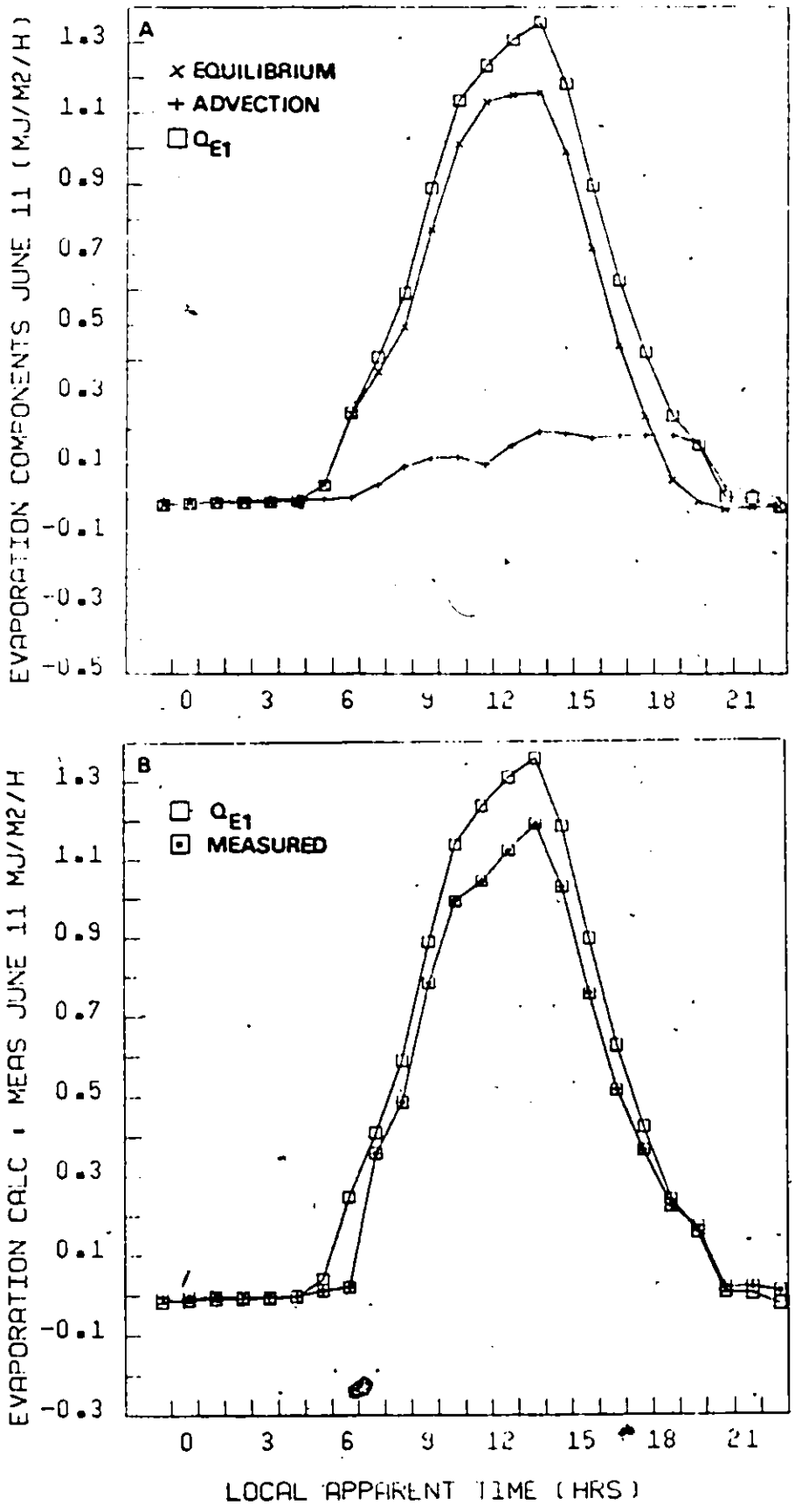

Figure 4.6. a. Variability in the equilibrium, advection and combined terms of the combination model for June 11.
Figure 4.6. b. Comparison of combined terms and measured evapotranspiration for June 11.

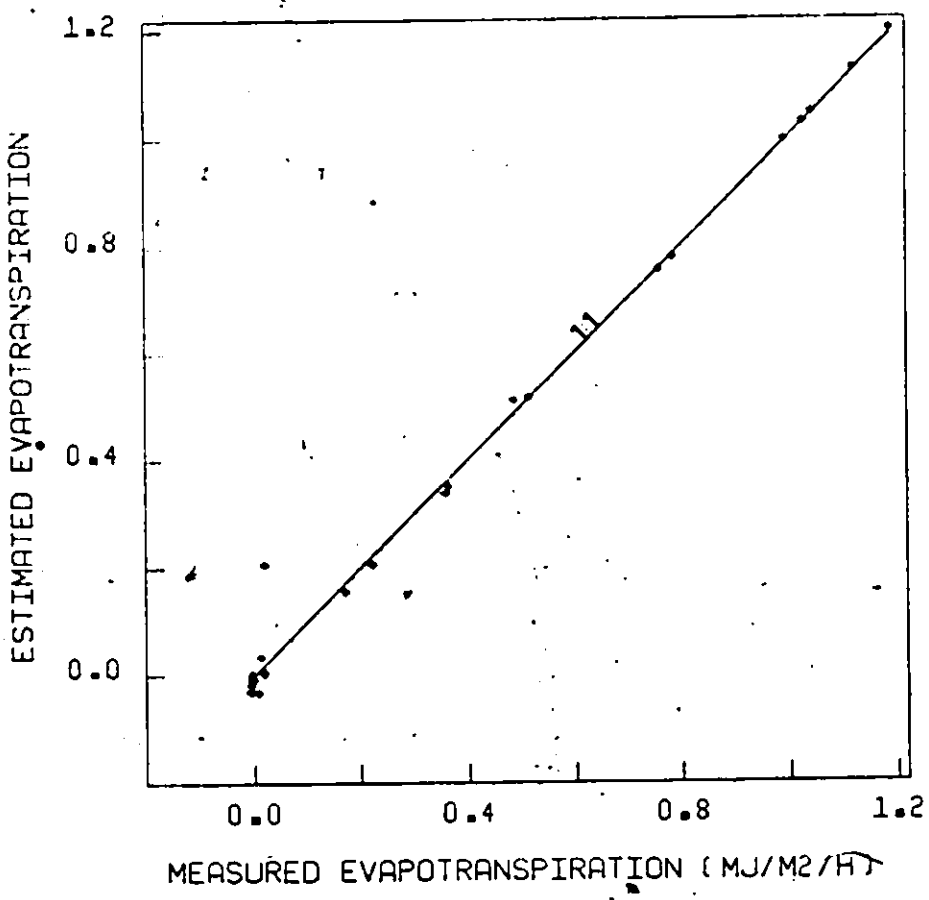

Figure 4.7. Comparison of estimated and measured evapotranspiration for June 11.

estimations prior to the inclusion of the glazing term demonstrate overestimation (Figure 4.6 b) and the regression results (Figure 4.7) show very good agreement (r = 0.98, slope = 0.96). For comparison purposes, the regression of Q_E measured and Q* yields Q_E = 0.60 Q* - 0.05 (r = 0.94).

By June 24, thirty-one days had elapsed since transplanting. Irrigation water was applied just after noon on the previous day. Advection was positive during early morning but then began to decrease towards a noon-hour minimum (Figure 4.8 a). After 1200 advection again increased. However, irrigation water was not applied until just before 1600. The role of the plant stomata are clearly evident. Under intense demand around noon, the plants could no longer extract soil moisture at a rate sufficient to prevent wilting and the stomata closed in response. As net radiation rapidly declined, root extraction could keep up with demand and the stomata re-opened, thereby humidifying the air and increasing advection. With the application of water around 1600, moisture supply was ample and the advective influence more pronounced. Again, Figure 4.8 b compares estimated (equilibrium + advection) evapotranspiration with measured values and Figure 4.9 shows the regression relationship (r = 0.94, slope = 0.96). Regression of Q_E measured and Q* yields Q_E = 0.560 Q* - 0.083 (r = 0.90). Figure 4.10 summarizes the relationship between measured and predicted Q_E for the six complete 24 hour periods of the data collection period (r = 0.95).

4.4 ANALYSIS OF RESIDUALS

In general, the greenhouse combination model has provided a fairly good representation of measured evapotranspiration. Approximately 90% of

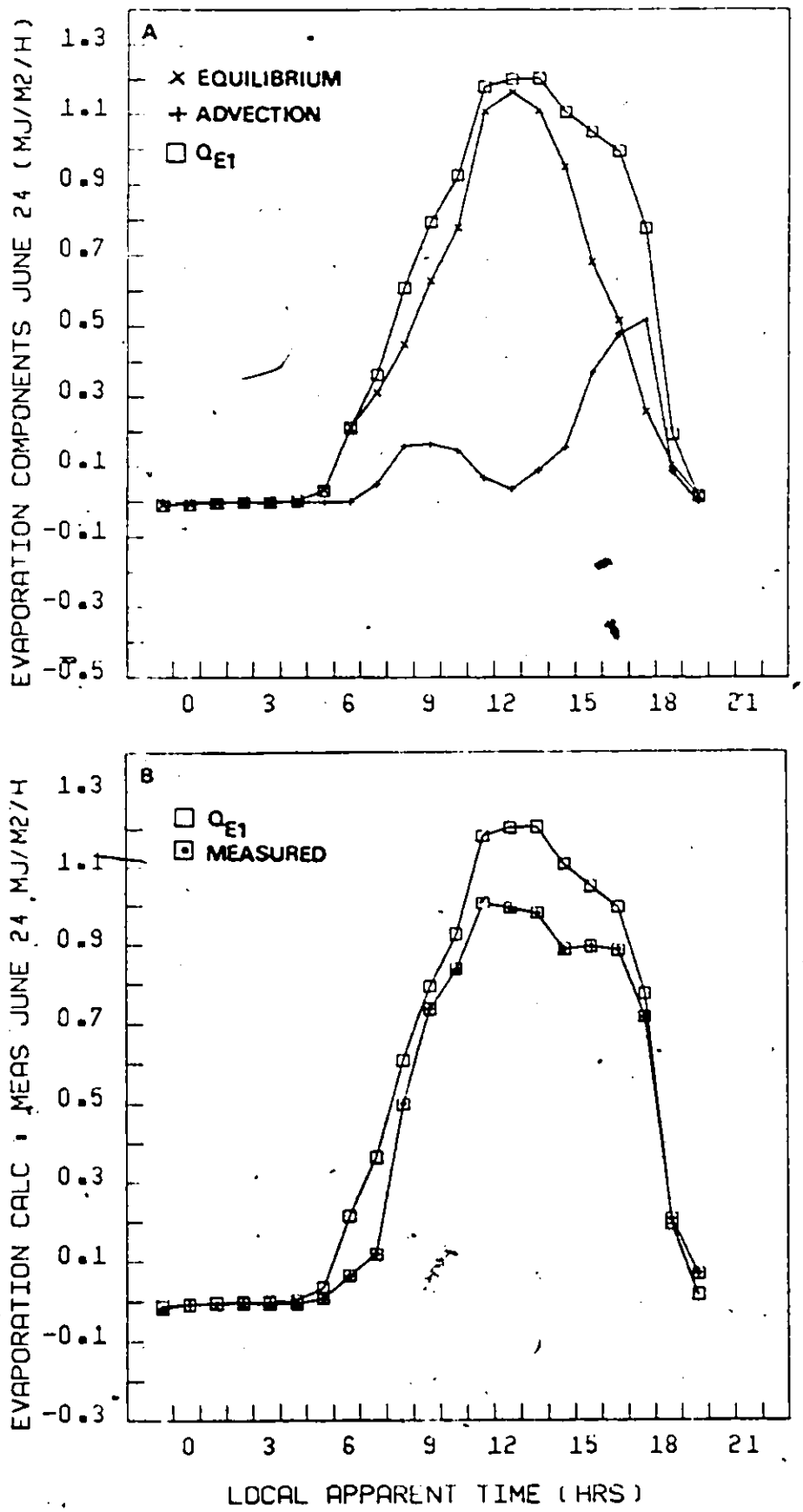

Figure 4.8. a. Variation of the equilibrium, advection and combined terms of the combination model for June 24.
Figure 4.8. b. Comparison of the combined term and measured evapotranspiration for June 24.

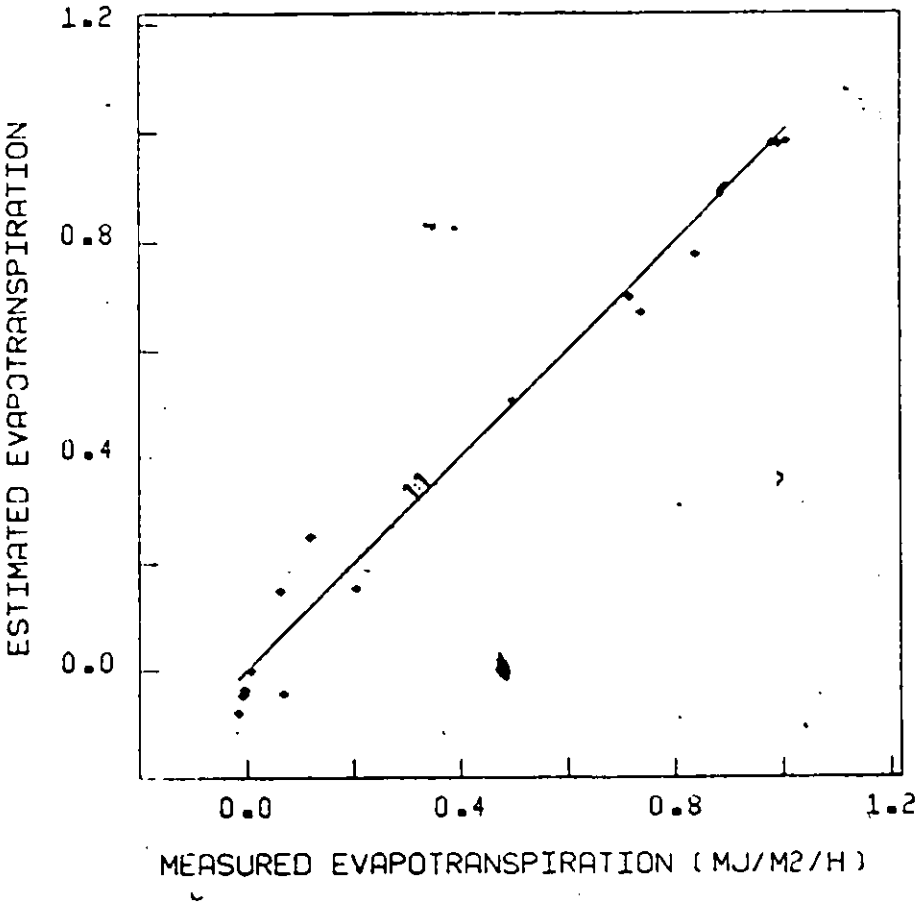

Figure 4.9. Comparison of estimated and measured evapotranspiration for June 24.

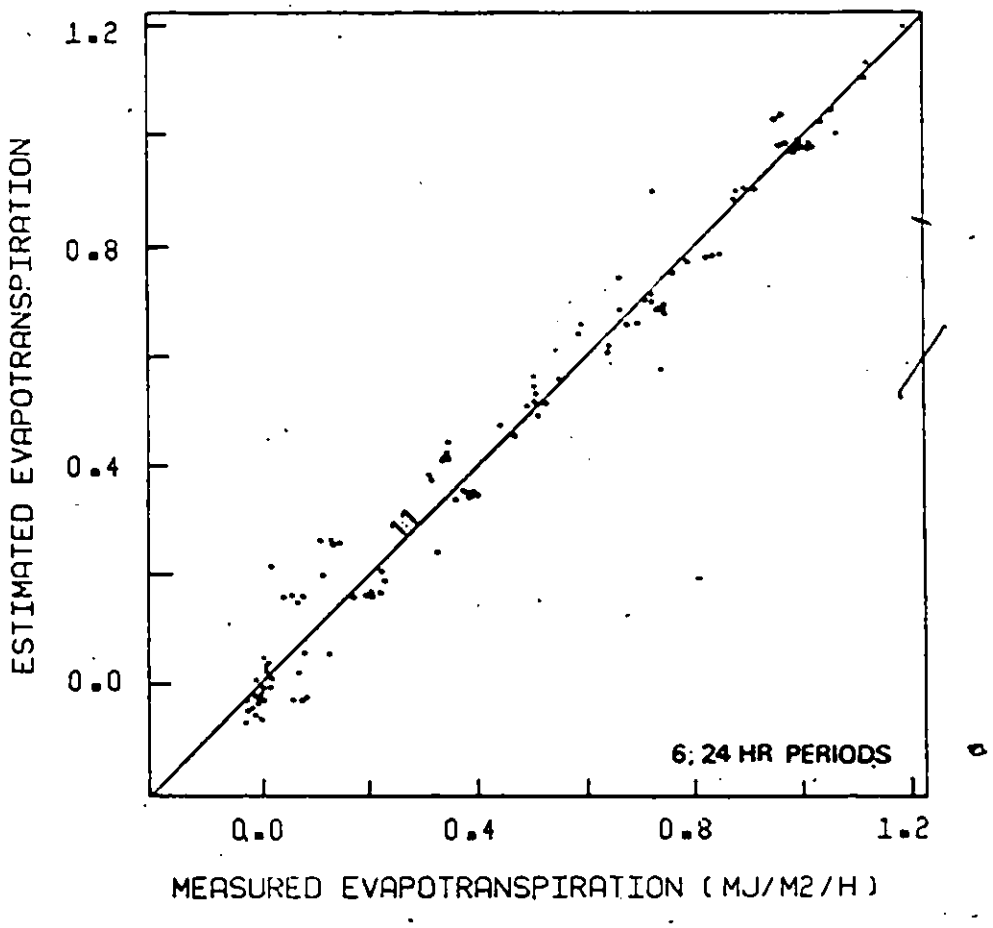

Figure 4.10. Comparison of estimated and measured evapotranspiration for six complete day periods.

the variability in actual evapotranspiration can be predicted by model estimations. This is approximately 10% more explanation than provided by a simple regression of Q_E measured and net radiation. The regression equations of course have different slopes to account for the advective affects on Q_E.

The derived model, however, contained a fourth condensation term which was not treated explicitly. In the absence of instrumental or sampling errors, the difference between measurements and model values could be attributed to condensation. Figures 4.11a , 4.11b and 4.11c are the daily plots of differences for the three previously discussed days.

The results indicate that the data and/or the analysis is too crude to provide an analysis of condensation. The results indicate that glazing condensation and condensate evaporation (negative condensation) occurred at various times throughout the day when it was observed that no condensation existed. Furthermore, the magnitude of the values is probably incorrect. The calculation of the residual was based on per meter squared of glazing area. This was felt to be the most physically satisfying means of presenting the data as observation indicated that most condensate accumulated on the glazing. However, the wall of the Brace greenhouse did not remain dry. Correct parameterization lies somewhere between the present assumption and one where condensation occurs uniformly on glazing and wall.

Nevertheless, the trend in residuals is interesting. All days indicate a peak in condensation in early morning with a subsequent decline to negative values shortly thereafter. This is consistent with the more rapid rise in greenhouse air temperature and vapour pressure than

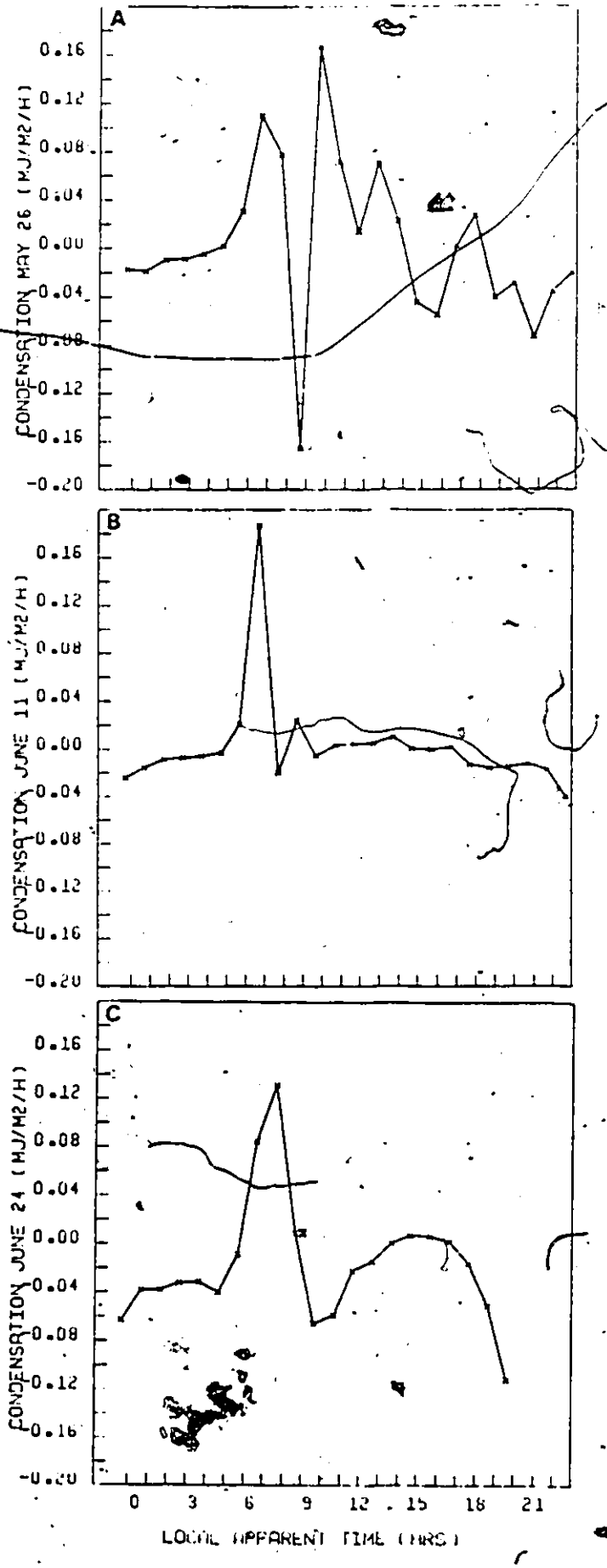

Figure 4.11. Plot of residuals for a. May 26, b. June 11, c. June 24.

outside before the fan comes on. As ventilation commences measured Q_E exceeds that predicted by the model. The source of this moisture is the glazing condensate.

Interestingly, the June 11 values are minor compared with those for the other two days. June 11 was a day when particular note was made of the absence of appreciable condensation. However, the closeness of fit between measured and model results on this day is almost certainly fortuitous and may be attributed as much to the small variability in advection as anything else.

This data set does not provide a particularly good assessment of glazing condensation in greenhouses because outside air temperature was typically only 1-2 C below dew point temperature and therefore not conducive to large latent heat exchange at the glazing surface. The inability to explicitly treat condensation is disappointing in view of the findings of Mihara and Hayashi (1979) which showed that condensation increased greenhouse heat loss by 17%. This data set does not permit such analysis.

4.5 THE GREENHOUSE ENERGY BUDGET.

The present measurement program would preclude any conclusions being drawn regarding a "typical" greenhouse energy budget. Figures 4.12 a, b and 4.13 a, b indicate the energy budget and Bowen ratios for May 26 and June 11. The Bowen ratio was lower and much less variable on June 11 when the crop canopy was developing and exerting a greater influence on energetics. Yet, it is doubtful that the full significance of advection is demonstrated in these examples owing to the restrictive ventilation regime. Certainly, very small or negative

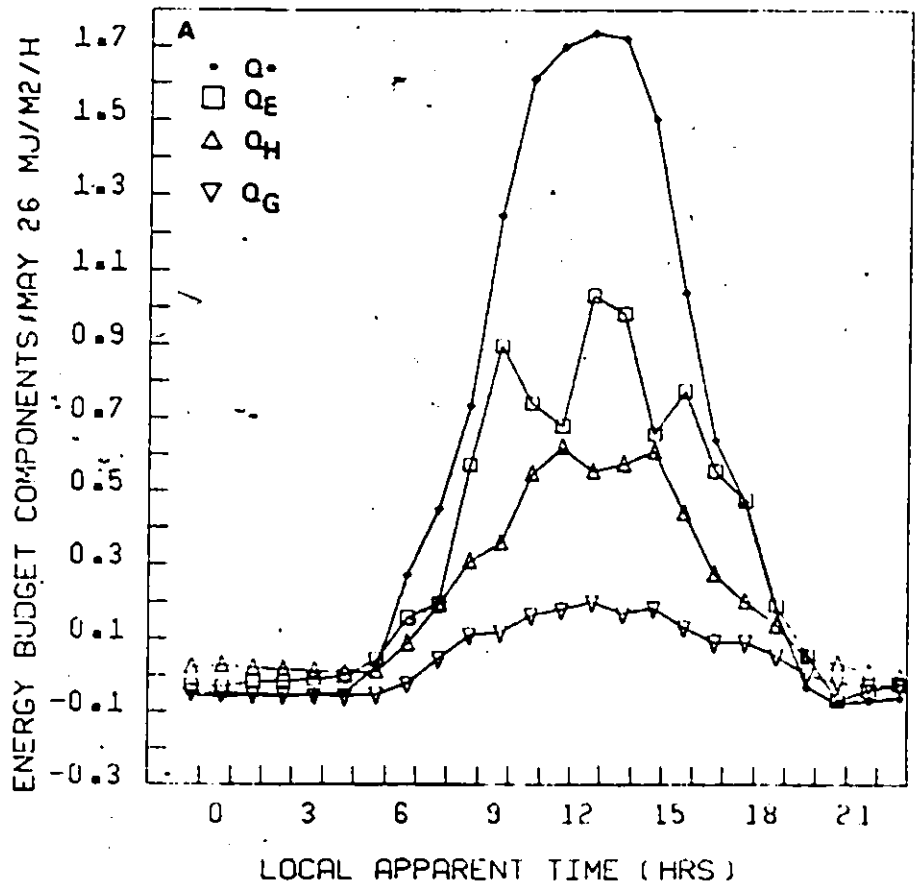

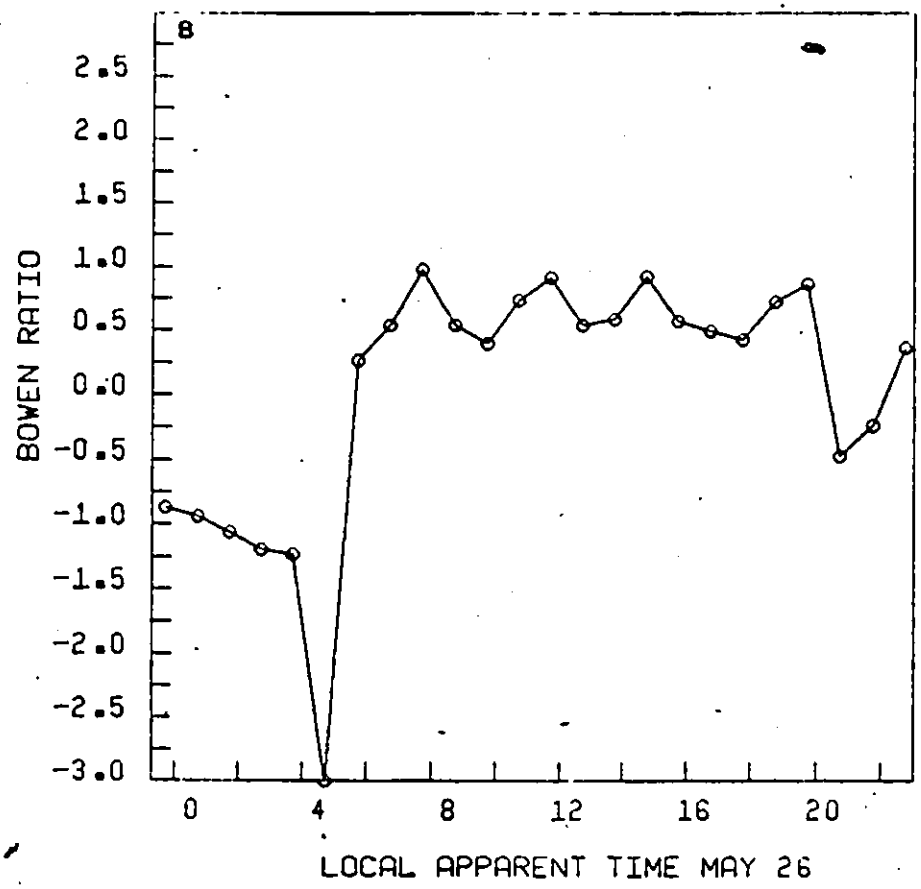

Figure 4.12. a. Energy budget components for May 26.
Figure 4.12. b. Variation in Bowen ratio for May 26.

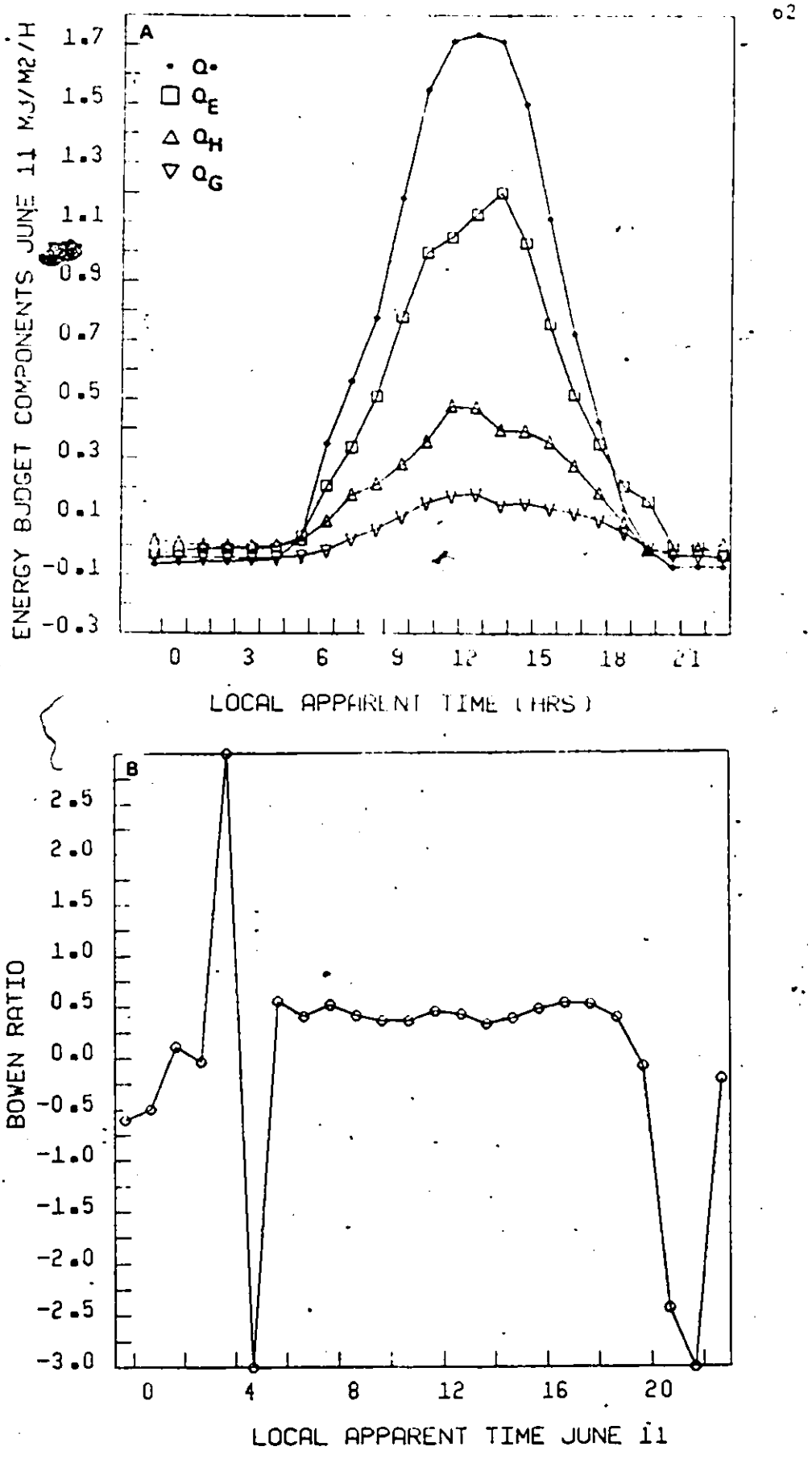

Figure 4.13. a. Energy budget components for June 11.
Figure 4.13. b. Variation in Bowen ratio for June 11.

Bowen ratios are not approached in these cases during the daytime.

One interesting outcome of the energy budget results is presented in Figures 4.14 and 4.15 . Model estimates of the latent heat flux are added to the sensible heat flux. The sum should equal net available energy. It is apparent that although the smallest and largest values compare well there appears to be a bias towards overestimating $Q_H + Q_E$ for intermediate values. A plausible explanation for this stems from the underestimation of net available energy. Net radiation was measured directly but as mentioned earlier, generally underestimates true net radiation due to shading effects. Another factor may involve the horizontal divergence of net radiation. As the crop increases in height, the sides of the crop around the perimeter of the greenhouse present a large area for radiation receipt. An upward-viewing pyradiometer is unable to account for the incident flux on vertical surfaces. At noon, when the sun is near the zenith this is of little consequence. Similarly, near dusk the entire growing surface is shaded by the opaque north wall. In mid afternoon or morning, the maximum effect would be expected. A comparison of the June 11 and June 24 results indicate that the greater errors occur when the crop is taller. This problem may be accentuated in winter. Conversely, the error may be insignificant in large commercial greenhouses where the perimeter of the crop, as a proportion of the total growing area, is smaller.

4.6 THE GLAZING U-FACTOR

The values derived for the glazing U-factor were determined from

$$U_G = \left[Q_{H*} - \frac{A_w}{A_s} U_w \Delta T\right] \frac{A_s}{A_G} \Delta T^{-1}, \qquad (MJm^{-2}h^{-1}C^{-1}) \qquad (4.1)$$

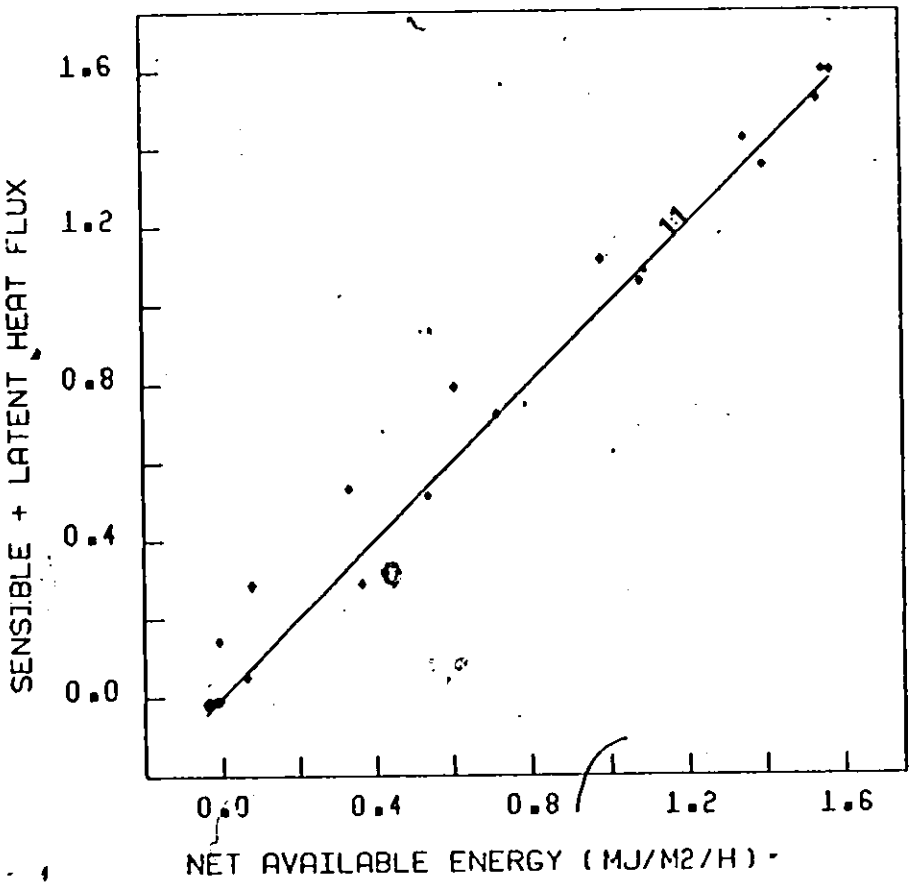

Figure 4.14. Comparison of $Q_H + Q_E$ and $Q^* - Q_G$ for June 11.

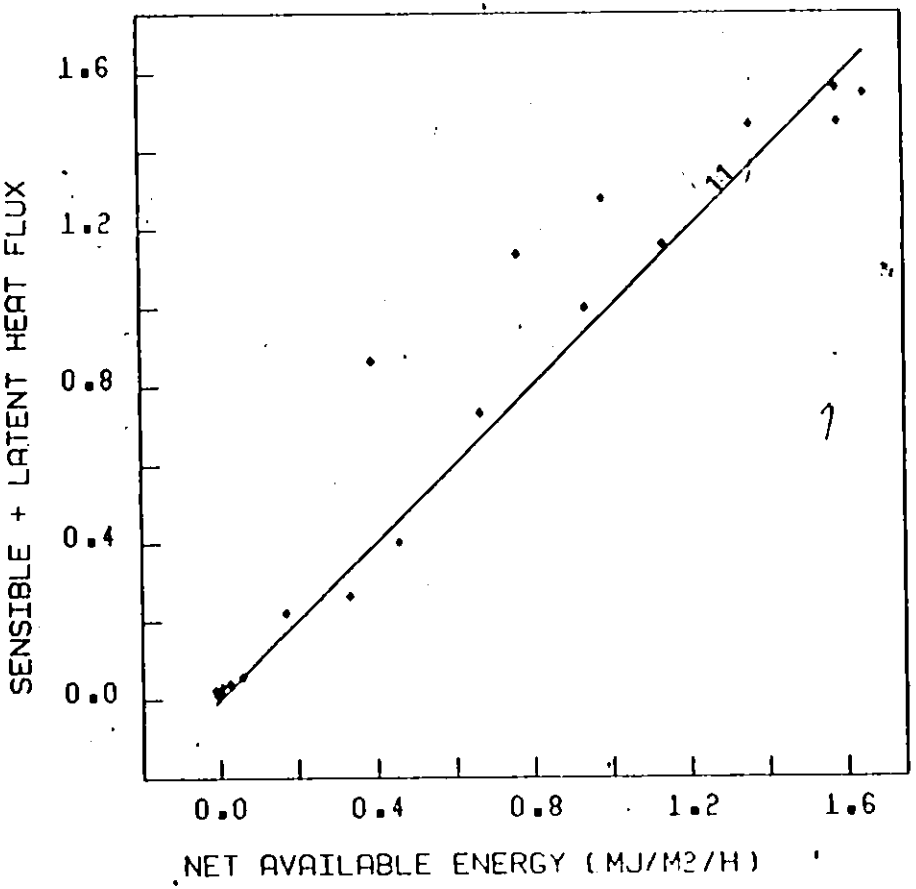

Figure 4.15. Comparison of $Q_H + Q_E$ and $Q^* - Q_G$ for June 24.

where U_w is the wall U-factor, A_w A_s A_G are the areas of wall, ground surface and glazing respectively (m^2), ΔT is the inside-outside temperature difference. A value for U_w of 0.001759 $MJm^{2}h^{-1}C^{-1}$ was determined from tables of Mazria (1979) ($\simeq$ 0.086 BTU $ft^{-2}h^{-1}F^{-1}$).

The values for the glazing U-factor varied from a minimum of 0.0103 to a maximum of 0.0133 $MJm^{-2}h^{-1}C^{-1}$ ($\simeq$ 0.50-0.65 BTU $ft^{-2}h^{-1}F^{-1}$). The smaller of these values is only 70% of that most commonly reported in the literature for double glazings (0.0143 $MJm^{-2}h^{-1}C^{-1}$). The larger of the two values occurred on a single day when average windspeed exceeded 5 ms^{-1} (11.3 m.p.h.).

One explanation for this discrepancy with published results may involve a sampling error of inside air temperature. The dry bulb temperature of the upper psychrometer was used in the evaluation of ΔT. It was chosen because it was located only 0.5 m from the inner polyethelene surface. Nevertheless, due to its location near the ridge of the greenhouse where warm air tends to accumulate, particularly if recirculation is poor, ΔT may have been too large, thereby reducing the derived value for U. However, three common practices in estimating U-factors tend to bias derived values for U towards overestimation. First, inside temperature is commonly recorded centrally in the greenhouse near screen height. This is not particularly effective in estimating air temperature near the glazing. Second, studies are usually conducted in the heating season when latent heat transfer at the glazing is at a maximum. Third, soil heat flux is rarely subtracted from furnace or boiler output. Model sensitivity to assumptions regarding glazing U-factors is presented in Chapter Five.

4.7 VENTILATION RESISTANCE

Figure 4.16 illustrates the change in the derived values for the ventilation resistance from May 26 to June 24. The results appear to correspond to the anticipated growth of the crop. Unfortunately, there is no independent assessment of r_v other than that the derived value for May 27 appeared to provide satisfactory results for May 26. Although, it should be noted that May 26 residuals showed the greatest variability of all days analysed. The ability of r_v to indicate crop growth in periods as short as two days (eg. May 27 to May 29) would seem to be fortuitous considering the uncertainties in the model discussed thus far. Of course, the data presented are for the period of most rapid plant growth and extrapolation of the relationship would be unwarranted. Nevertheless, it appears that variations in r_v related to dry matter production or leaf area index would warrant further study.

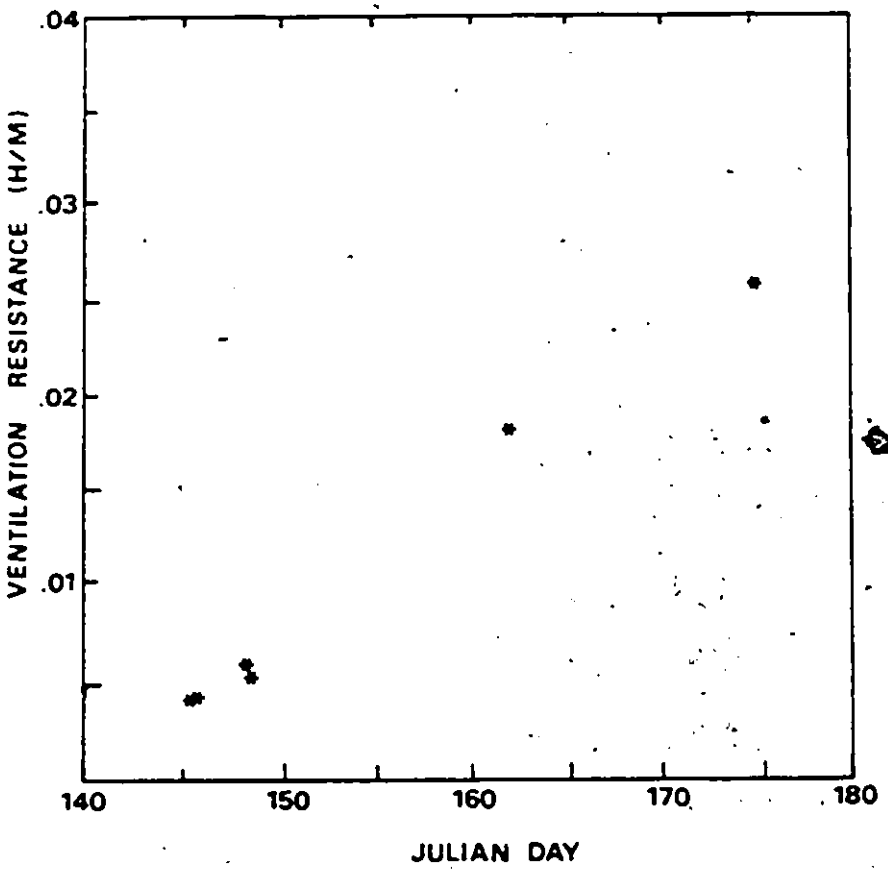

Figure 4.16. Variation in ventilation resistance over measurement period.

CHAPTER FIVE

MODEL SENSITIVITY

The ability of the greenhouse combination model to predict evapotranspiration depends on the proper parameterization of several terms and measurement accuracy. Similarly, these two types of potential error determine whether measured evapotranspiration is a true representation of reality. Because (2.3) was used to determine actual evapotranspiration, model estimates and measured values are not independent of each other. For example, errors in the assumption of ventilation rate and temperature manifest themselves in both measured and model results, though not necessarily to the same degree or even of the same sign. Gravimetric or lysimetric measures of evapotranspiration do provide independent measures of Q_E but were not a part of the measurement program.

The ability of the combination model to approximate "true" evapotranspiration as defined by (2.3) has already been illustrated by the plot of residuals for three measurement periods. The effect of systematic error in three assumptions and three measurements will be illustrated through the plot of residuals for a single day May 26. This day was chosen because the advection term underwent extreme variation. Also, since the residual plot for May 26 was the poorest of all the days analysed, it could be determined if systematic errors were responsible for this result.

Figure 5.1 a shows the effect of a $\pm$ 20%, $\pm$ 10% and 0% change in ventilation rate leaving all other assumptions and measurements

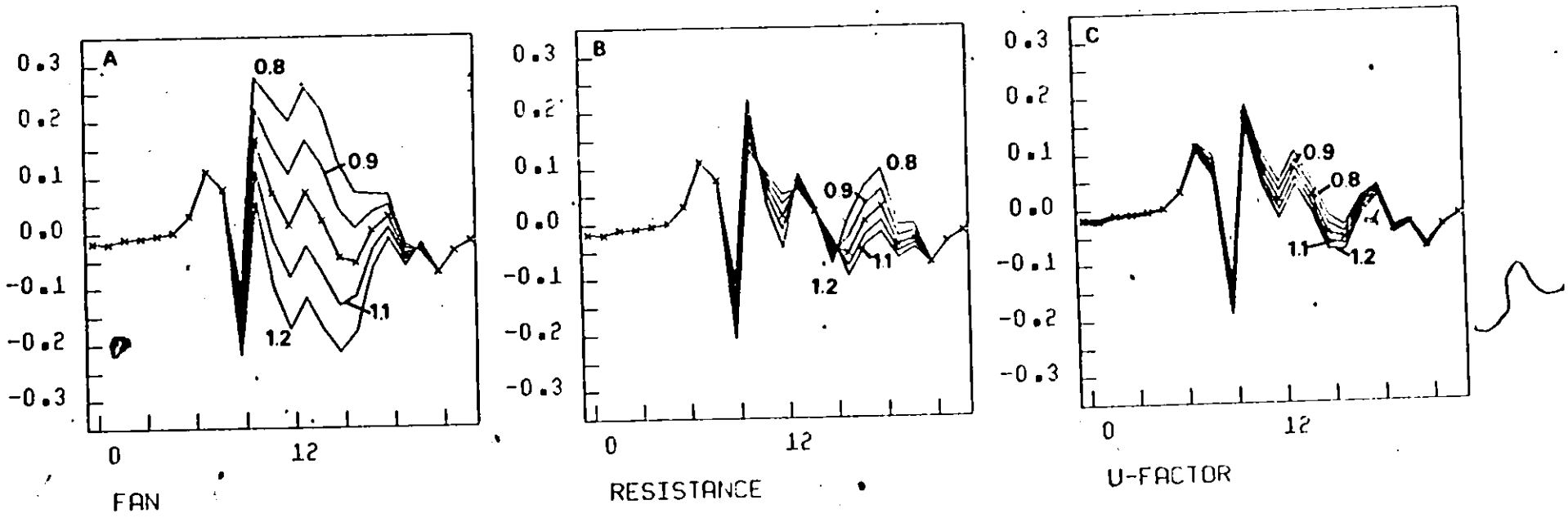

Figure 5.1. Model sensitivity to variations in, a. ventilation rate, b. ventilation resistance, c. glazing U-factor for May 26.

unchanged. Changes in ventilation rate have a greater impact on measured Q_E than the advection term of the model. Departures are greatest at midday when Δe is largest and zero when the fan is off.

Figure 5.1 b shows the effect of similar percentage changes in ventilation resistance on model agreement. The result indicates that errors in estimating r_v are not as important because the ventilation resistance appears only in the model formulations. What is different in this case is that changes in r_v magnify both the positive and negative changes in the advection term, unlike ventilation rate where positive errors cause model underestimations at all times.

Figure 5.1 c shows how errors in the U-factor affect model agreement. Errors are greatest when the inside-outside temperature difference is the largest but because of the relatively small magnitude of Q_{H*} in relation to advection and equilibrium terms, fairly large errors can be tolerated.

Figure 5.2 a demonstrates how $\pm$ 20%, $\pm$ 10% and 0% errors in net radiation affect model agreement. All differences here are a result of changes in the equilibrium term of the model. Mocel agreement is much more dependent on accurate radiation measurement than any of the errors discussed so far. It highlights the importance shading effects may have on model agreement and limitations posed by using solar radiation as a surrogate for net radiation if Q* is not measured.

Figures 5.2 b, c indicate the effect of a $\pm$ 4%, $\pm$ 2% and 0% error in dry-bulb and wet-bulb temperature measurements. The effects are pronounced and compare with 20% errors in radiation measurement. While the fan is off temperature measurement error has little effect on measured Q_E because the rate of change in T and T_w are used to calculate the

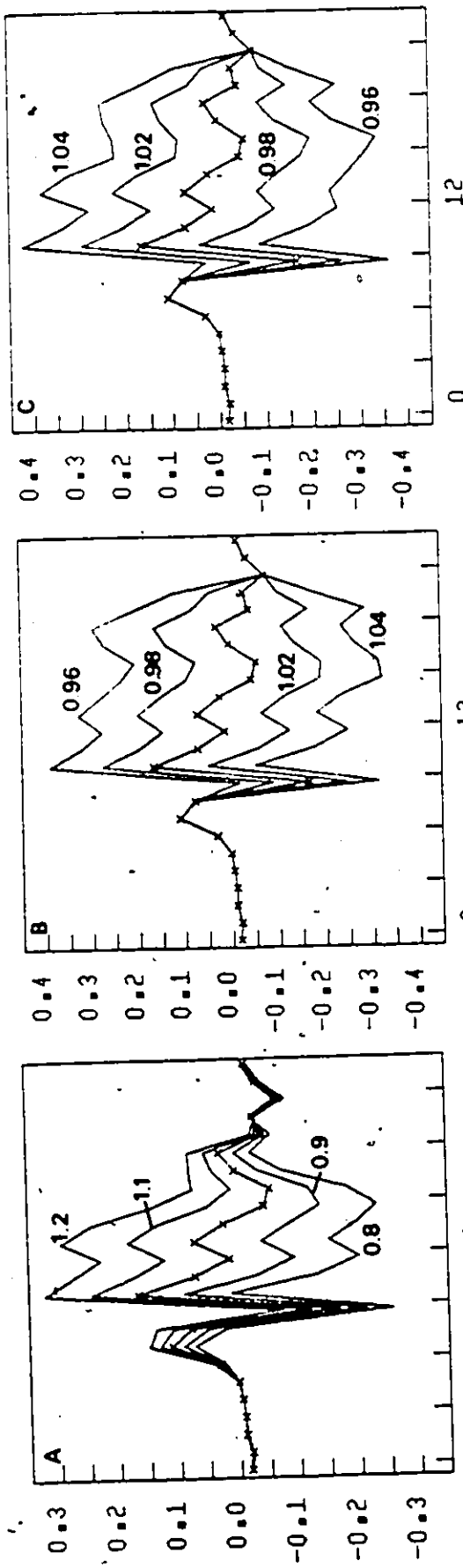

Figure 5.2. Model sensitivity to variations in, a. net radiation, b. dry-bulb temperature, c. wet-bulb temperature for May 26.

latent heat flux. When the exhaust fan is on, errors in T and T_w manifest themselves in the advection term as well. Particularly when ΔD is small, very slight errors in T or T_w can reverse the sign of the advection term causing poor model agreement. Errors in T_w are seen to have a greater effect than similar errors in T. This results from the method of calculating vapour pressure using (2.17) and (2.18). The accurate measurement of temperature is the most important requirement for the successful application of the combination model.

CHAPTER SIX

THE COMBINATION MODEL AS A DESIGN TOOL

The combination model provides a useful framework to examine the environmental control that greenhouse structure and management exercise on the micro-climate. The equilibrium term of the model is dependent on the available energy at the surface. Both the net radiation and ground heat flux are terms which the greenhouse designer can control. Solar transmission by various greenhouse structures and glazing materials has been a traditional focus of research. Hourly transmissions range mostly between 46% and 137%. The longwave radiation transmittance of commonly used glazings ranges between 0.0 and 0.9. The enhancement of ground heat storage by increasing thermal mass has been the focus of recent research aimed at maximizing the solar heating fraction of the total heating load. Limited experimentation indicates that this fraction can reach 100%.

Glazing heat loss can be controlled by choice of greenhouse structure and glazing. Unfortunately, optimum solar transmission characteristics do not correspond to optimum heat retention characteristics. Hence, glazings have been designed to optimize the former while moveable curtains or panels have been used to provide the latter.

The advection term of the model describes the impact of importing energy from the outside environment. The largest effect of greenhouse design is through ventilation rate. Changes in the ventilation resistances resulting from different fan speed are within the control of the designer,

subject to economic constraints. Changes in the ventilation resistance resulting from crop growth, however, are less well known. As the data analyzed in this study suggest, with a fixed ventilation rate, the ventilation resistance increases dramatically during the early stages of canopy development. However, the limited data set is not representative of a fully developed canopy nor typical of monocultures raised in commercial greenhouses. Row orientation and pruning practice may also influence the ventilation resistance. Nevertheless, traditional cropping strategies may exhibit 'typical' ventilation resistances which will facilitate the design of ventilation systems.

The advection term also demonstrates the influence of ambient air temperature and humidity on the latent heat flux. Geographical and temporal variations in wet-bulb and dry-bulb air temperatures clearly precludes a single ventilation rate from being appropriate in all environments. However, the greenhouse designer may also manipulate the incoming air temperature and humidity by use of evaporative pad cooling systems. By drawing the intake air through a wall comprising a water-soaked porous pad the dry-bulb temperature is lowered to within 1.5 C of the outside wet bulb temperature. The impact of this practice on the greenhouse microclimate will be discussed later. It is pointed out, however, that a constant intake wet bulb depression simplifies the parameterization of advection.

The fact that the three terms of the combination model can be manipulated by greenhouse design suggests that a unique combination will define an optimum environment. Defining an optimum environment poses several questions. In commercial greenhouses, maximum crop profitability has traditionally been used as a measure of the design's success. This

approach suffers from both management and market influences. The environmental conditions necessary for optimum plant productivity are no more straight forward. Although this area of research is beyond the scope of this thesis, it is of note that the last several years has seen significant redefinition of optimum light intensities, particularly in elevated carbon-dioxide atmospheres in greenhouses, and in optimum root temperature environments (Simpkins et al., 1979).

Not only would the optimum vary between crops but the optimum for crop growth does not necessarily coincide with optimum solar heating or water application if this resource were scarce. The optimum for solar heating in particular would be of interest in domestic greenhouses where energy saving is valued above plant production.

For the purpose of this discussion "potential evapotranspiration" will be used as a benchmark condition. It will be defined as the condition where 100% of the net available energy is utilized in evapotranspiration. From (2.1) this corresponds to

$$Q_E = Q^* - Q_G \quad . \qquad (6.1)$$

This condition is of particular significance. It implies that sensible heating of the air is absent. Hence, conditions under which (6.1) apply are the coolest possible without the aid of artificial refrigeration. All of the radiant energy absorbed by the crop is dissipated by the latent heat flux.

No energy remains to warm the crop above air temperature. Hence, sensible heating is suppressed. This condition is beneficial to plant dry matter production. Dry matter production is positively correlated

with evapotranspiration (Monteith, 1975). There are two principle reasons for this. First, high leaf temperatures enhance respiration. Since respiration is a process which consumes carbohydrates produced by photosynthesis, net photosynthesis and dry matter production are adversely affected when leaves become too hot (Thiessen, 1976; Oke, 1978). Second, transpiration is the primary transport mechanism for soil nutrient movement into plants. The cessation of transpiration severely restricts root solute uptake (Crafts, 1961). Thus cooler leaf temperatures and high transpiration rates correspond to optimal plant growth all other factors being constant.

The condition of zero sensible heating corresponds to a Bowen ratio of zero. Several workers have found that evapotranspiration equalled or exceeded net available energy. This measurement program indicated that Q_E never exceeded 70% of $Q^* - Q_G$. Thus a Bowen ratio of zero delimits those results reported in the literature for greenhouses from those positive values for β commonly reported in open non-advective landscapes and in this measurement program. A zero Bowen ratio also corresponds to the poorest conditions for collection and storage of solar energy from the sensible heat of the air. This does not represent the absence of solar collection altogether because of the energy collected as Q_G. However, it does point out a basic incompatibility between optimal plant growth and sensible heat collection.

6.1 METHOD OF ANALYSIS

The greenhouse combination model is given by

$$Q_E = \frac{s}{s+\gamma}(Q^*-Q_G) + \frac{\rho C_p}{r_v}(D_i-D_e) \sim \frac{s}{s+\gamma} Q_{H^*} + \frac{\gamma}{s+\gamma} Q_{E^*} \qquad (6.2)$$

When potential evapotranspiration exists, sensible heat flux is zero which implies that the exhaust air temperature equals the inlet and outside air temperature. Glazing sensible heat flux and condensation flux are both zero. Thus (6.2) can be rewritten as

$$Q^* - Q_G = \frac{S}{S+\gamma}(Q^*-Q_G) + \frac{\rho C_p}{r_v}\left[(T_i-T_{wi}) - (T_i-T_{we})\right] , \qquad (6.3)$$

and

$$T_{we} = T_{wi} + \frac{\gamma}{S+\gamma}\frac{r_v}{\rho C_p}(Q^*-Q_G) . \qquad (6.4)$$

Equation (6.4) indicates that for fixed values of net available energy, ventilation resistance and exterior wet-bulb temperature at screen level, there is a unique value for exhaust wet-bulb temperature such that the advective term of the combination model is sufficiently large for potential conditions to exist. The upper limit to T_{we} is $T_{we} = T_e = T_i$, corresponding to saturated exhaust air. The lower limit for T_{we} is $T_{we} = T_{wi}$, corresponding to the absence of advection, which implies that the intake and exhaust relative humidities are equal.

If the derived value of T_{we} lies between these two limits, then potential conditions are possible if water supply does not restrict evapotranspiration. If the derived value lies outside the two limits, then potential conditions (and a zero Bowen ratio) are not possible.

Hourly solar radiation and dry and wet bulb temperature data were collected for the meteorological station at Woodbridge Ontario, near Toronto, approximately 60 km east of the measurement site at Greensville. Hourly average monthly solar radiation fluxes were reduced from clear

sky data for the years 1968 to 1978. Clear sky data for the months of June and September were analysed corresponding to the time of greatest solar intensity and the end of the ventilation season respectively.

6.2 RESULTS

The solar transmission for the Brace greenhouse was determined from data collected from the measurement program of 1978. During this time very little data was collected for totally overcast sky conditions because these were almost always accompanied by vigorous thunderstorm activity which made data collection inappropriate. Thus, the solar transmission data for all of the measurement program illustrated in Figure 6.1 are for clear sky conditions. The inside and outside radiation regimes were related by regressions, $K\downarrow_i = 0.009 + 0.254\ K\downarrow_o + 0.138\ K\downarrow_o^2$ (MJ m^{-2} h^{-1}, $r = 0.97$) and this relation was used to derive inside hourly radiation values from the Woodbridge data. Differential roof and wall transmission is represented by the inflection point near 2.0 MJ m^{-2} h^{-1}.

The determination of net radiation inside the greenhouse was less straightforward. As discussed earlier the regression of inside net radiation upon inside solar radiation, while having high correlation coefficients, had varying slopes throughout the measurement program for individual days. A physical explanation for this involves the variation in the upward emitted surface longwave radiation flux. After several uninterrupted clear days the soil would continually warm. The increase in soil temperature and particularly the increase in soil surface temperature increased the emitted longwave flux thereby decreasing net radiation Q*. Conversely, on a clear day which followed several rainy days, the soil block was cooler thereby moderating surface temperature. As a result the upward longwave flux was smaller and Q* was larger. One would expect similar seasonal or diurnal trends in net radiation as a result

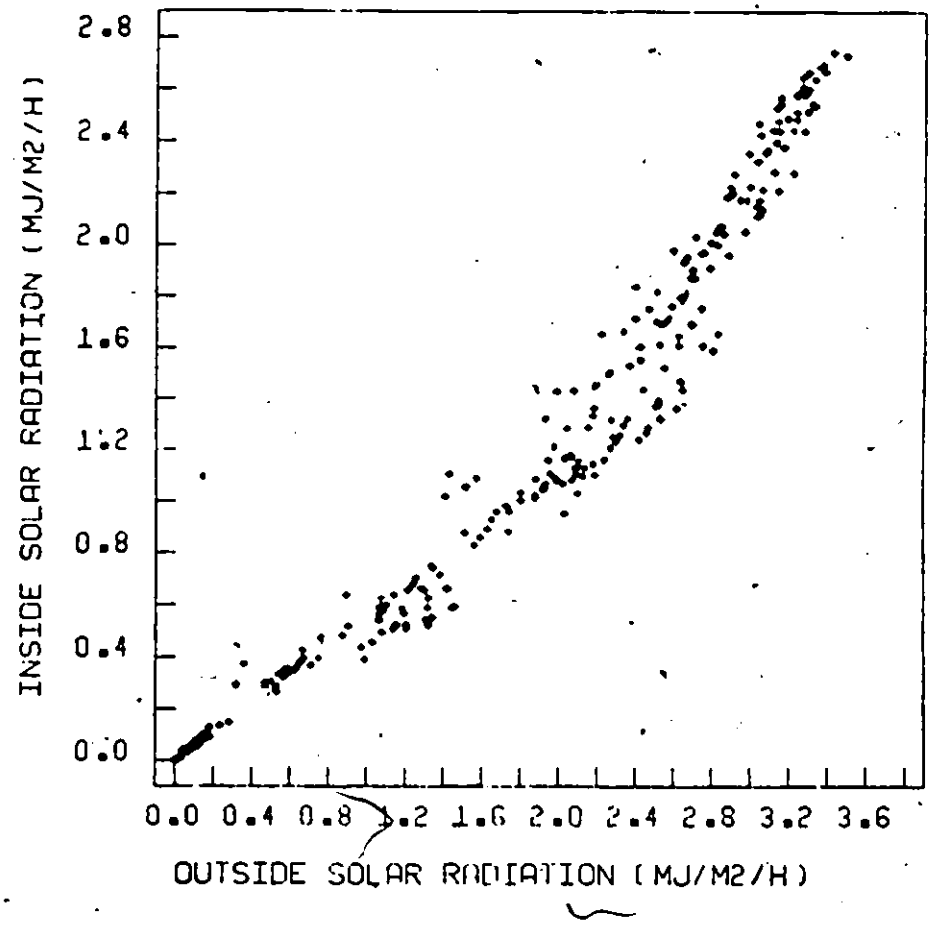

Figure 6.1. Relationship between measured hourly totals of solar radiation outside and inside Brace greenhouse.

of soil warming as well.

Evidently, the soil heat flux Q_G followed a similar pattern as well. After the soil block had cooled following several rainy days, on a subsequent clear day a large vertical temperature gradient promoted a large soil heat flux. After the soil block had warmed following successive clear days, the vertical temperature gradient and/or soil thermal conductivity had decreased sufficiently to inhibit soil heat flux. Maximal soil heating thus, coincided with maximal net radiation and vice versa. This implied that variations in $Q^* - Q_G$ net available energy, would tend to be conservative with respect to either alone. Figure 6.2 shows the regression of net available energy and inside solar radiation for all data measured in 1978, (slope = 0.61 r = 0.94). The relationship is very satisfactory despite the inclusion of rafter effects but more importantly, the regressions for individual days showed slopes varying between 0.59 and 0.63 with similarly high statistical correlations. This indicated that net available energy could be estimated from outside solar radiation for cloudless days and since net available energy was required for (6.4), the necessity to estimate Q^* and Q_G independently, was eliminated.

Figure 6.3a shows the derived values of T_{we} (dotted line) for Toronto. The upper solid line is the exhaust and therefore intake dry-bulb temperature and the lower line the intake wet-bulb temperature. The assumed value for the ventilation resistance is 0.03 hm^{-1} corresponding to largest value measured in the 1978 measurement program corresponding to an underdeveloped crop canopy.

The results indicate that potential conditions can not exist in the Brace greenhouse in this locale for most of the day because the exhaust wet bulb temperature would have to exceed the exhaust dry bulb temperature,

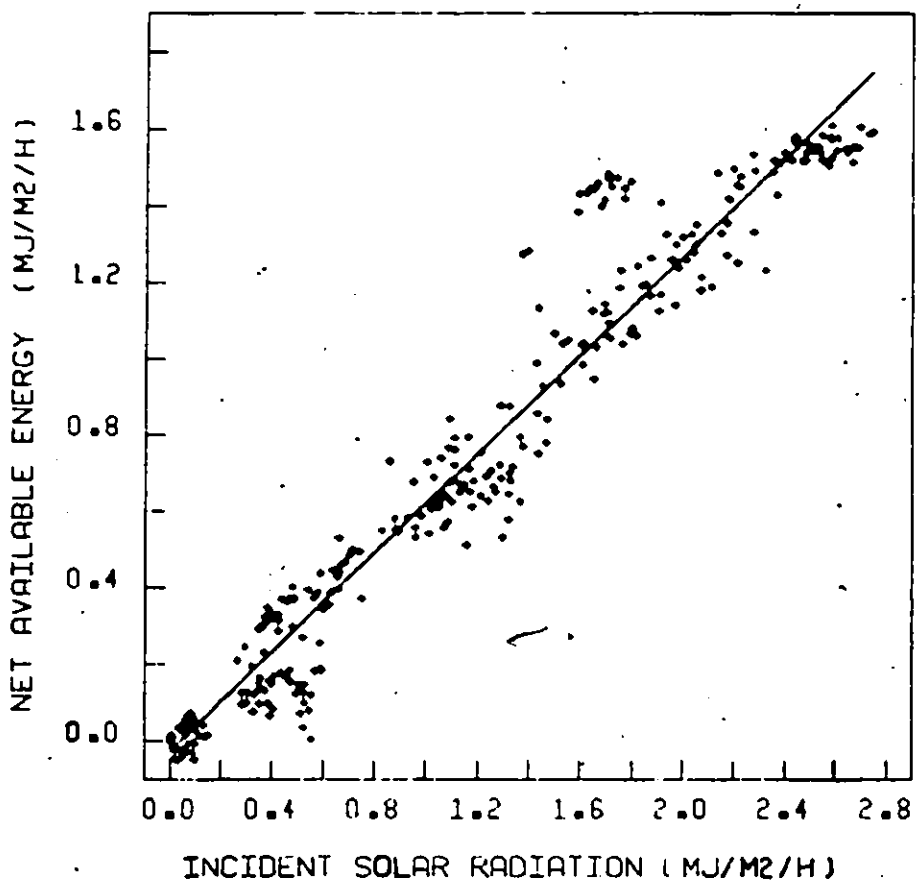

Figure 6.2. Relationship between inside solar radiation and net available energy inside Brace greenhouse.

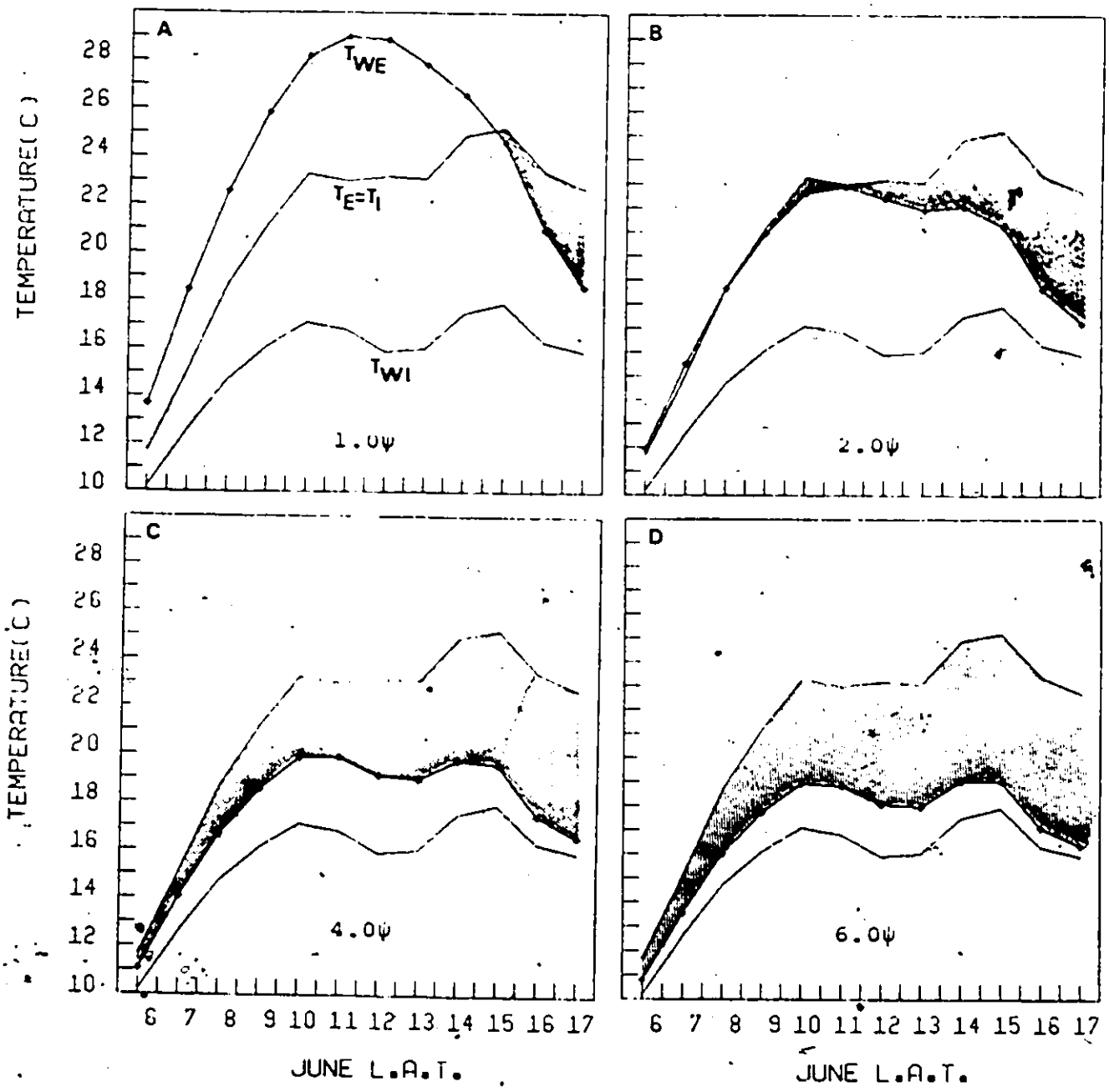

Figure 6.3. The effect of changing ventilation rate on exhaust wet-bulb temperature in Brace greenhouse in June.

which is an impossibility. These results corroborate the 1978 experimental findings which indicated positive sensible heat fluxes at all times and thus conditions under which zero or negative Bowen ratios could not occur. It was postulated that the low ventilation capacity of the experimental greenhouse was responsible for inhibiting advection. Figures 6.3 b, c and d indicate the effects of increasing the ventilation rate by a factor of 2, 4 and 6. The stippled area indicates the potential for negative Bowen ratios under these ventilation regimes. Since the dotted line T_{we} represents the derived value for the boundary condition of (6.1) then an exhaust wet bulb temperature in excess of this indicates greater evapotranspiration than can be accounted for by net available energy. Hence, negative sensible heating and thus negative Bowen ratios would prevail if actual T_{we} fell into this zone. As the ventilation rate and thus advection become more pronounced, the likelihood for this to occur increases. Ventilation rates two to three times greater than those used in the experimental program are likely to be more typical of those used in commercial greenhouses. Ventilation rates six times as great may not be commonplace, although it is not unreasonable that an open-sided greenhouse may permit such air exchange during windy conditions. An interesting feature of Figure 6.3d is that almost any exhaust wet bulb temperature between T_e and T_{wi} in Toronto would be sufficient to promote potential evapotranspiration with this air exchange rate. It would seem reasonable to assume therefore that the experimental findings of the authors cited earlier were plausible for a given set of environmental conditions.

As (6.2) and (6.4) indicate, advection is not solely determined by the ventilation rate. The humidity of the intake air influences advection.

Furthermore, the derived exhaust wet bulb temperature is also influenced by the radiation load or net available energy. The daily trend of T_{we} illustrates this. In Figure 6.3b for example, zero Bowen ratios are possible in early morning only if the exhaust air is completely saturated. This is because the intake wet bulb depression is quite small. As the relative humidity of the intake air decreases towards mid-day exhaust humidities below saturation will sustain potential evapotranspiration. This occurs despite the increase in net available energy towards noon. As net available energy begins to decrease after noon, derived values of T_{we} decrease abruptly even though intake wet bulb depressions are relatively constant. This results from the increase of the advective term in relation to the equilibrium term, as is indicated in (6.4). When the radiation load decreases it becomes easier for advected energy to augment equilibrium evapotranspiration to potential conditions.

Figure 6.4a, b, c, d shows a similar pattern for Toronto in September. In September however, it is more likely that potential conditions will exist. Despite the slightly smaller intake wet bulb depressions, the radiation load at the equinox is sufficiently small to be dominated by advection. Again, potential conditions are seen to be only unlikely in the case of the ventilation regime used in the experimental greenhouse.

It is apparent now that for a given outside set of solar radiation and temperature conditions there is a range of ventilation rates which could satisfy potential conditions. The minimum ventilation rate is one which occurs when the exhaust greenhouse air is saturated. This corresponds to $T_{we} = T_e = T_i$. From equation (6.4)

$$r_v = \frac{(T_i - T_{wi})\,\rho C_p}{\frac{\gamma}{s+\gamma}(Q^* - Q_G)} \qquad (6.5)$$

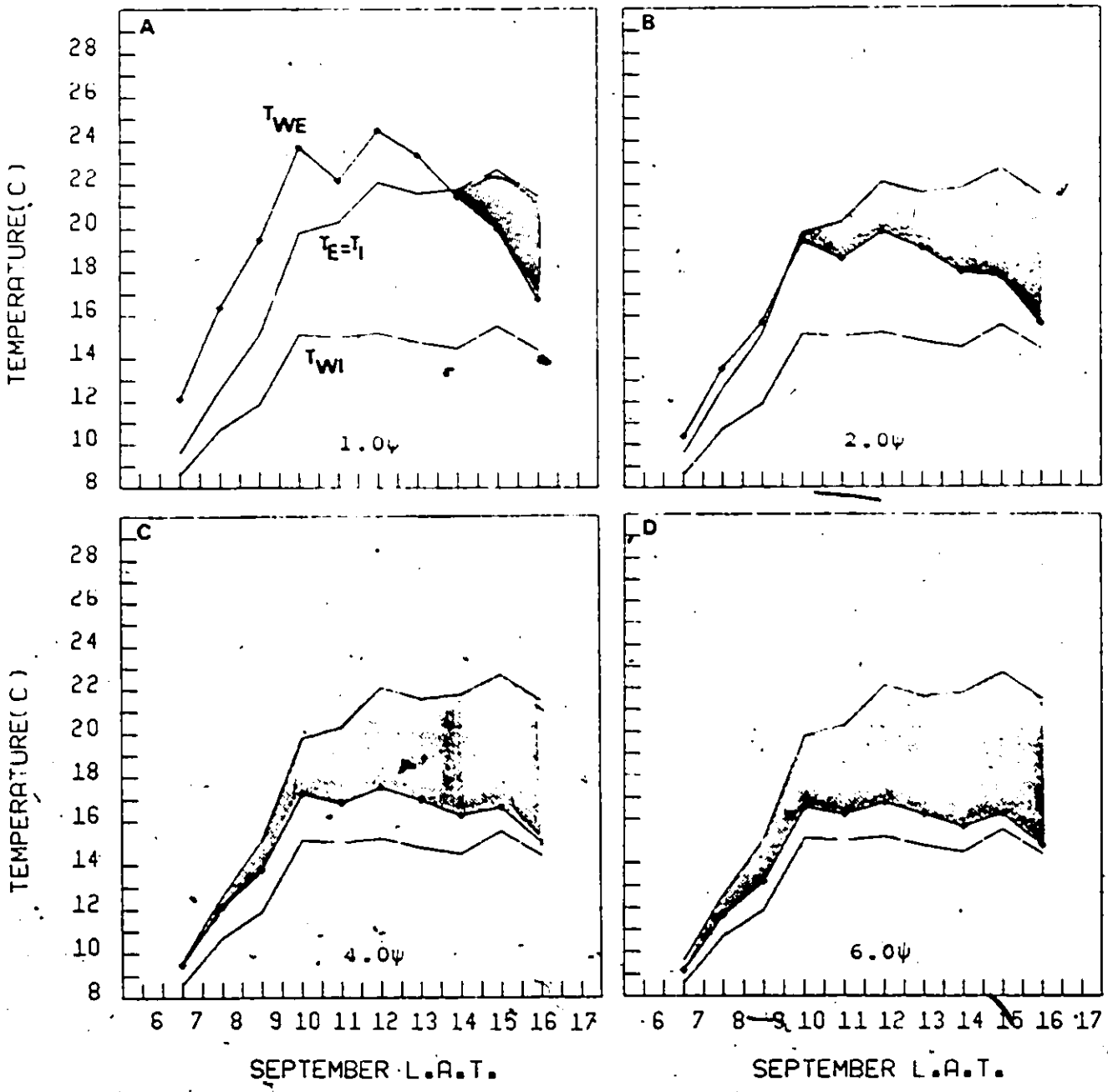

Figure 6.4. The effect of changing ventilation rate on exhaust wet-bulb temperature in Brace greenhouse in September.

The daily trend of maximum allowable ventilation resistance (minimum ventilation rate) for June and September for Toronto is shown in Figures 6.5 and 6.6 . Although traditional greenhouse fan operation has been in the on/off mode, more recently staged thermostats and controllers have permitted a multiplicity of ventilation rates in commercial greenhouses. If a controller were constructed which measured outside wet bulb depression and inside net available energy or if the latter were estimated from known radiation transmission functions of outside solar radiation, then real-time control of ventilation rates would be possible. The major obstacle to this at this time is lack of knowledge of crop effects on the ventilation resistance. It should be noted that ventilation resistances derived from (6.5) are the maximum allowable and that lower resistances should constitute a design objective.

As Figures 6.5 and 6.6 suggest, the maximum allowable ventilation resistance to achieve potential evapotranspiration is dependent on the radiation load. Since both the short and longwave radiation fluxes inside and soil heat flux are influenced by greenhouse design, the choice of structure including glazing type is as critical a design decision as ventilation rate. Figure 6.7a, b, c, d indicates how $\pm$ 20% and - 50% change in net available energy inside influence the Brace experimental greenhouse in September for Toronto. Twenty per cent changes in net radiation are well within those reported in the literature for solar radiation. Differences between longwave fluxes between polyethylene and glasshouses may be expected to vary by a similar magnitude although very little experimental evidence has been collected in this area to date. Variations in condensation and dirt accumulation alone have been shown to affect radiation transmission in excess of 20%. Generally, however,

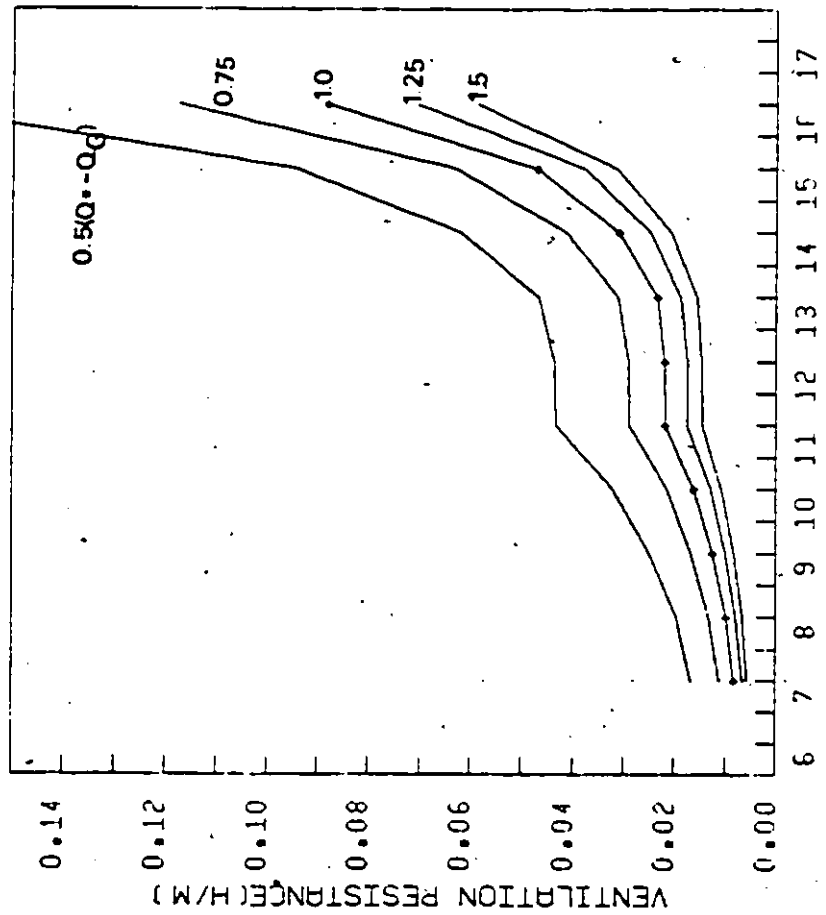

Figure 6.6. The hourly trend of maximum ventilation resistance for September.

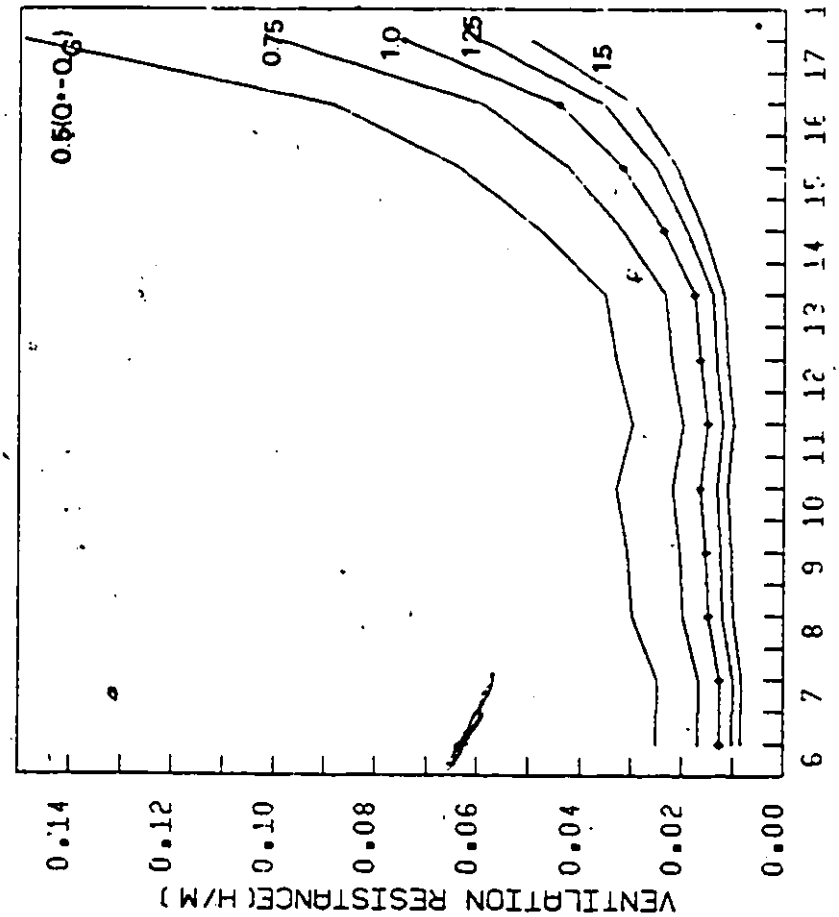

Figure 6.5. The hourly trend of maximum ventilation resistance for June.

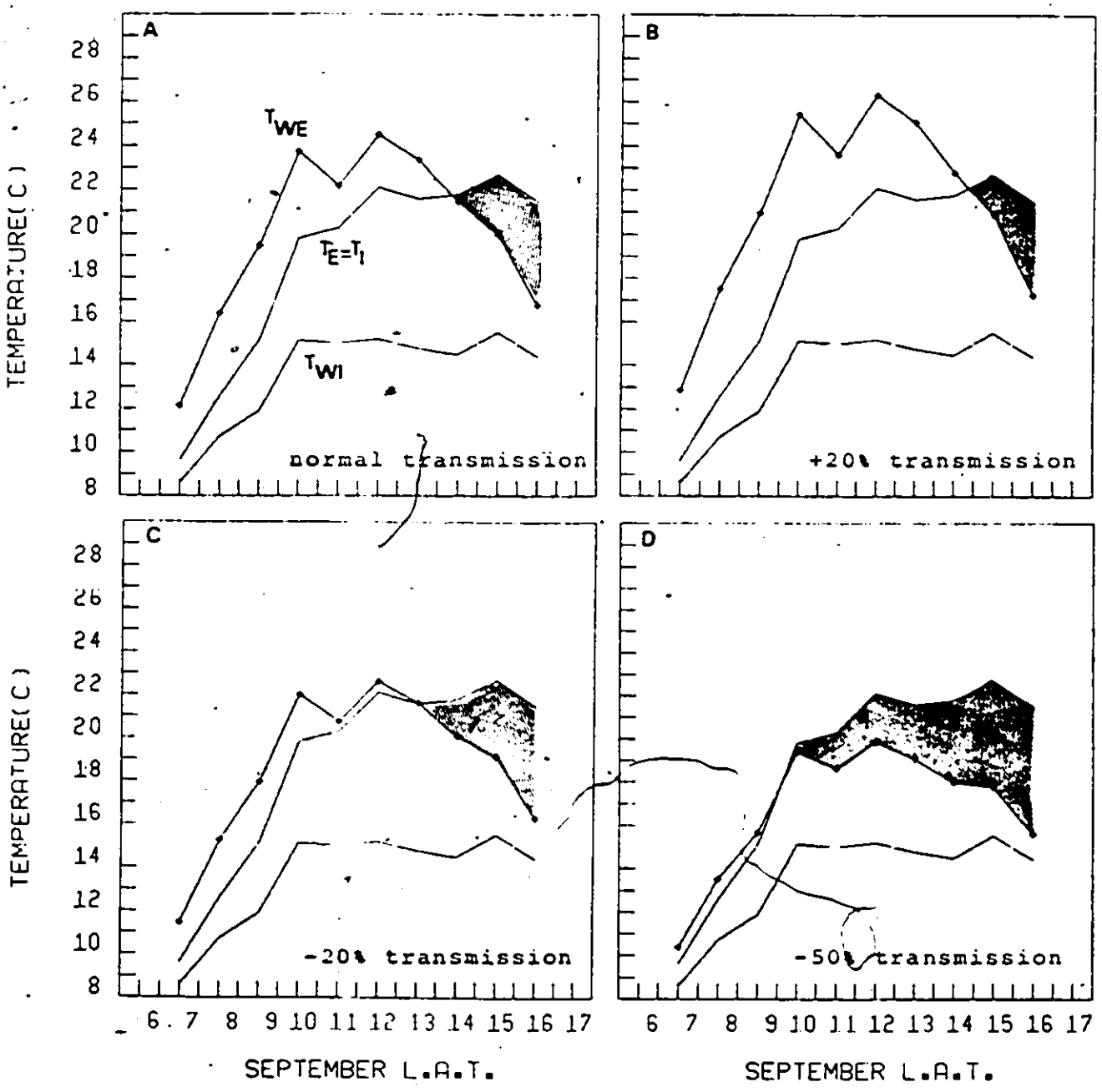

Figure 6.7. The effect of changing net available energy on exhaust wet-bulb temperature in Brace greenhouse in September.

the focus of greenhouse design has been to maximize solar receipt thereby allowing light saturation levels which maximize photosynthesis and dry matter production. It is not clear that reducing the radiation load to enable potential evapotranspiration would outweigh the negative aspect of lower light intensities.

An important consideration in this regard results from the findings of Chiapele and Damagnez (1977) and Van Bavel (1979) who have studied the effects of glazing greenhouses with spectral bandpass filters. The glazing permits the transmission of photosynthetically active radiation, necessary for plant photosynthesis but absorbs or reflects the ultraviolet and near infrared wavelengths. The filter has been shown to reduce net radiation by as much as 50%. Figure 6.7d indicates the pattern of exhaust wet bulb temperature with a 50% reduction in net available energy. Comparison with Figure 6.4 indicates that the likelihood of potential conditions are similar to those for a twofold increase in ventilation rate. This type of greenhouse glazing is becoming commercially available so the added cost of this design remains unclear. It would of course be decreased by the reduction in required fan capacity and operating costs.

Figure 6.8 generalizes the relationship between maximum ventilation resistance, exhaust wet bulb temperature and outside solar radiation for the Toronto summer. For typically high noon hour solar radiation levels the ventilation resistance is relatively insensitive to temperature. For example, if the intake wet bulb temperature is 15 C and the intake dry bulb temperature is 27.5 C, then saturated exhaust air has a maximum allowable temperature of 27.5 C. This corresponds to a ventilation resistance of 0.03 hm^{-1} which is the resistance determined

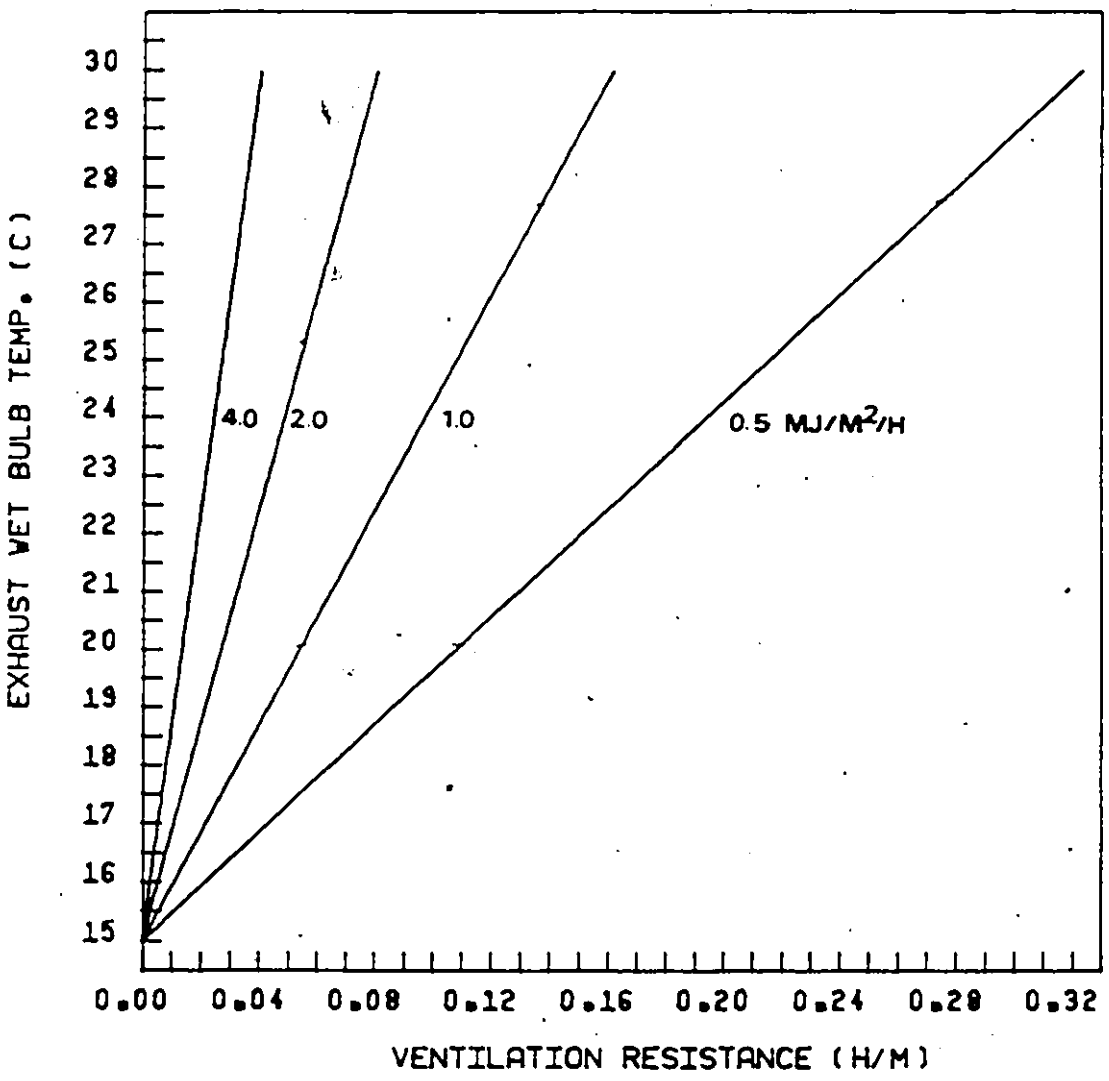

Figure 6.8. The relationship between exhaust wet-bulb temperature and ventilation resistance for varying outside solar radiation loads.

for the end of the 1978 experimental program. Since saturated exhaust air corresponds to the maximum allowable ventilation resistance (minimum fan rate), then a minimum intake wet bulb depression of (27.5 - 15.0 =) 12.5 C is required to enable potential evapotranspiration to proceed. An intake wet bulb depression of 5 C indicates that the saturated exhaust air would have a temperature of 20 C. This corresponds to a ventilation resistance of 0.013 hm^{-1} or an increase of ventilation rate of almost 230%. For an incident solar flux outside of 1.0 $MJm^{-2}h^{-1}$, the corresponding maximum allowable ventilation resistances would be 0.13 hm^{-1} and 0.055 hm^{-1} respectively ($\approx$ 230%). For lower radiation levels lower fan speeds and a smaller absolute change in fan speeds are necessary although the percentage change remains relatively unaltered.

Figure 6.9 is similar to Figure 6.8 but expresses the relationship between ventilation resistance and intake relative humidity. For low radiation loads fairly high relative humidities can be tolerated. For example, for the lowest radiation curve, intake relative humidities as high as 90% will still permit potential evapotranspiration with ventilation resistances corresponding to those in the measurement program (0.03 hm^{-1}). However, under typically high noon hour loads the intake air cannot exceed 30% R.H. if potential conditions are to prevail.

This has interesting implications for the design of evaporative pad cooling systems. As Monteith (1981) demonstrates, it is erroneous to assume that cooling the intake air by saturating it reduces surface temperature. The opposite is, in fact, the case. This is because the surface in question is composed of leaves which have their own evaporative cooling system comprising the stomata. As saturated air enters the greenhouse, it is unable to accept any more moisture unless its

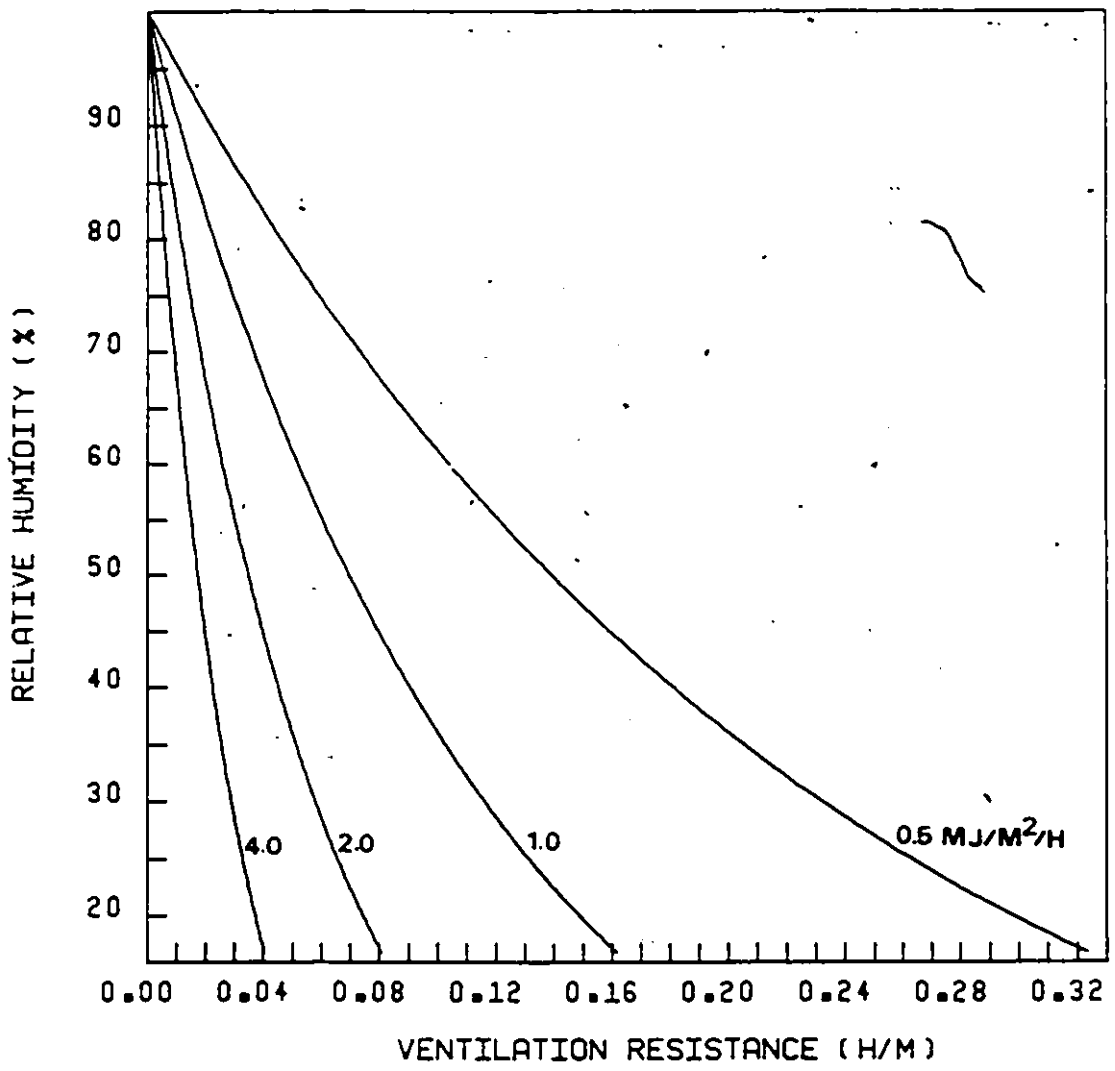

Figure 6.9. The relationship between intake relative humidity and ventilation resistance for varying outside solar radiation loads.

temperature is increased. Upon encountering leaves, it creates a situation where the vapour pressure gradient between stomata and air is zero or negligible. Thus transpiration ceases. At the same time however, the leaves are accumulating radiant energy and increase in temperature. This creates a large leaf to air temperature gradient and sensible heating of the air ensues. Evaporative pad "cooling" systems cause leaf warming. Leaf warming allows plants to dispel accumulated energy through sensible heating. However, the presence of sensible heating violates the design requirement for potential evapotranspiration or zero Bowen ratios. As Figure 6.9 illustrates, for saturated intake air the ventilation resistance must be zero and hence the ventilation rate infinity to achieve potential conditions. In practice, commercial evaporative pad systems may only decrease dry bulb temperature to within 1 or 2 C of the outside wet bulb temperature. Even at relative humidities of 95% however, ventilators must have a rate of approximately 10^3 $m^3m^{-2}h^{-1}$ to achieve resistances as low as 10^{-3} hm^{-1}. The difficulty in supplying such a ventilation rate is compounded by the aerodynamic resistance of the pad itself which reduces fan efficiency.

Since zero Bowen ratios are clearly impossible with evaporative pads it is interesting to postulate what effects the pads do indeed have on the greenhouse microclimate and the plant.

Since the leaves are increasing in temperature and warming the air, the humidity will fall below saturation and the air will be able to accept more moisture. As well, the vapour pressure of the leaf will increase. This will promote a positive vapour pressure gradient and permit the leaf to transpire to some extent.

Examination of the advection term of the combination model indicates that the maximum amount of transpiration that can take place would saturate the exhaust air. This corresponds to an exhaust wet bulb depression of zero. Since the intake wet bulb depression is also zero, this would correspond to the absence of advection. If we consider for the moment the situation where average inside temperature equals outside temperature, then the glazing heat transfer terms are inoperative. Hence, evapotranspiration will proceed at the equilibrium rate. If the exhaust air was less than saturated, then the advection term becomes negative and evapotranspiration is sub-equilibrium. As well, the reduction in transpiration that would correspond to a positive wet bulb depression implies a coincident increase in sensible heating. Thus, the inside air temperature would increase and the glazing heat loss would also reduce evapotranspiration to sub-equilibrium levels.

If the greenhouse were initially designed for potential conditions, then saturated exhaust air would correspond to the condition where all net available energy was utilized in transpiration ($\beta = 0$). The installation of the evaporative pad causes sub-optimal evapotranspiration even when the exhaust air is saturated. The increase in leaf temperature and decrease in nutrient uptake associated with suppressed evapotranspiration would not improve plant productivity.

Finally, the evaporative pad would serve a useful function in highly advective environments. In a desert situation for example, where the intake wet bulb depression is very large and the radiation load very high both the equilibrium and advection terms may promote an evaporative flux which the plant or soil moisture regime is unable to supply. When stomatal closure ensues both nutrient uptake is diminished and leaf

temperature increases. A case could be made therefore, to regulate the intake air humidity by diverting a portion of the influx through an evaporative pad system, thereby partially modifying the advective influence. As Figures 6.8 and 6.9 suggest, however, modifying the radiation load would have an equal if not greater impact on the evaporation rate.

CHAPTER SEVEN

CONCLUSIONS AND RECOMMENDATIONS

A physically based greenhouse evapotranspiration model has been developed and tested with data collected from an experimental greenhouse. The model accounts for four processes which affect evapotranspiration. These are radiant energy supply, advection, glazing sensible heat loss and condensate accumulation on the glazing. The first three of these terms can be evaluated with meteorological measurements. The last term requires measurements of the amount of condensate on the glazing. Condensate accumulation was only assessed qualitatively in this study and was omitted in the analysis. Comparison of hourly model estimates with measured evapotranspiration showed very good agreement when the first three terms alone were used. The principle reason for good agreement was the small magnitude of the condensate term in summer. Nocturnal air temperatures were typically only 1-2 C below dew point temperature which are not conducive to large latent heat fluxes at the glazing.

The division of the evaporative flux into three components provides insight into the mechanisms responsible and their relative importance. Because the data analysed correspond to clear sky conditions, it is relatively easy to discern that short term fluctuations in evaporation are caused by variations in advection. This accounts in part, for the inability of empirical models, based on in situ measurement of radiation alone, to adequately represent latent heating. Nevertheless, the analysis indicates that radiation dominates evaporation on a daily

basis. Since this is too long a time interval for useful estimates of irrigation requirements and for many solar heating applications, empirical models do not provide adequate resolution for the prediction of the latent heat flux. The relative importance of radiation is greatest during the noon hour period and diminishes during early morning and late afternoon. In general, the relative role of advection is greatest in late afternoon when relative humidities outside are still relatively low and irradiances are low. Relative roles nocturnally are less clear because the magnitude of the fluxes are sufficiently small to be cominated by instrumental and sampling errors.

There is no single, distinctive greenhouse environment. The role of advection in the evaporative flux is not limited only to short term fluctuations in evaporation but may be a significant or dominant component of total evaporation on a daily basis. The advective influence on evaporation is maximum when moisture supply is ample inside the greenhouse, the outside relative humidity is low and ventilation rates are large. The latter is dependent on greenhouse design but the former two depend on location, season, weather and greenhouse management.

The interrelationships between outside and inside environments as formalized by the model are largely within the control of the greenhouse designer. The Bowen ratio can be manipulated to maintain a wide range of desired environments. By altering fan speed, radiation transmission and incoming relative humidity, the greenhouse is capable of providing optimum environments for plant growth. The same three variables can be altered to enhance sensible heating of the air for solar heating purposes. Conversely, by leaving the design criteria unchanged

the crop will be subjected to varying demands in terms of sensible and latent heating throughout the day and season. Although a convenient assumption, this study shows that a constant Bowen ratio should not be assumed over a seasonal or diurnal period.

In keeping with the empirical findings of several authors evaporation can equal or exceed net available energy at the crop surface. The process wherein evaporation consumes all radiant energy at the expense of sensible heating is beneficial to plants by lowering leaf temperature and maximizing nutrient uptake. Conversely, the condition of zero Bowen ratios deters the collection and storage of sensible heat for later use as a means of reducing heating costs. Because a zero Bowen ratio also corresponds to large rates of water usage, it may not constitute an appropriate design objective in environments where water conservation is important. The evaporation mechanisms delineated by the model allow the designer to create the microclimate required for a particular application, with the inherent tradeoffs in not satisfying all applications simultaneously. In particular, maximal crop productivity in commercial greenhouses is not compatible with the collection and storage of sensible heat of exhaust air. As a corollary to this, it is important to examine methods of extracting and storing the latent energy in the exhaust air as this is the principle if not exclusive process by which radiant energy in greenhouse environments is dissipated.

Since overheating is the principle problem in greenhouses in the summertime, the combination model was utilized to outline design criteria which would circumvent this problem. By manipulating ventilation resistance and radiative transfer through the glazing, the greenhouse manager can maintain interior greenhouse temperatures at or near ambient

temperatures. This requires an ample moisture supply and maintaining a water demand on the crop which does not exceed its vascular transport capabilities. Empirical evidence from several greenhouses and from open advective landscapes indicates that this is possible.

The practice of saturating intake air with evaporative pad cooling systems is shown to inhibit evapotranspiration and associated nutrient uptake. Locations with high humidity analogous to the evaporative pads would similarly, prevent optimal evapotranspiration rates from being attained.

A relation is presented which permits the real-time maintenance of optimal evapotranspiration. The monitoring of inside net available energy and outside wet-bulb depression allows for an adjustment of fan speed that will maintain desired conditions. Unfortunately, the suitability of this approach is not merely dependent on the volume of air passing through the greenhouse but the efficiency with which the air can withdraw sensible and latent heat from the surface. The data analysed suggest that it becomes progressively more difficult for air at a given exchange rate, to accomplish this during the early stages of plant development. The resistance offered by the plant canopy over its life cycle and for different crops and planting strategies should constitute a primary focus in future studies.

The present data indicate that the requirement for direct measurement of net radiation may be relaxed because net available energy represented a near constant proportion of inside solar radiation. If the solar transmission characteristics of a particular design were known, then the design requirements to obtain optimal evapotranspiration could be determined from routine meteorological observations of solar radiation

and wet-bulb depression.

With ventilators off, the combination model indicates that evapotranspiration is easily determined from the equilibrium term when the greenhouse is the same temperature as outside. Of course, these conditions rarely occur because fans are usually turned off when it's cold outside. Hence the two glazing terms may be significant at these times. Although both sensible and latent heat fluxes at the glazing constitute energy losses, they have opposite effects on evapotranspiration. The former reduces evapotranspiration to sub-equilibrium levels. The latter enhances evapotranspiration whereby the glazing becomes a water vapour sink for a closed hydrologic cycle within the structure itself.

Glazing heat transfer has been analysed extensively. Most research has implicitly assumed that heat loss is in sensible form. It is likely for this reason that glazing heat loss coefficients derived in this analysis were somewhat smaller than those commonly reported. Most of the latter were derived for the heating season when glazing condensation is a maximum. The latent heat flux at the glazing is difficult to parameterize and this difficulty was compounded by the small magnitude of the flux. However, it is important to distinguish between these two modes of heat loss. While double or triple glazings will benefit greenhouse energy conservation by reducing both modes of heat loss, transpiration is adversely affected by eliminating condensation. It is recommended that their respective roles be distinguished in future studies.

APPENDIX ONE

SENSIBLE HEAT FLUX MEASUREMENT

The energy budget of uniform surfaces has traditionally been assessed by measuring a vertical property gradient and ascribing a diffusivity or resistivity between two or more measurement heights. For example, the surface sensible heat flux is evaluated by measuring air temperature at two heights above the crop surface and determining the eddy diffusivity K_H between these two measurement heights. Thus

$$Q_H = \rho Cp \, K_H \, \frac{\Delta T}{\Delta z} \quad . \qquad \text{(A.1.1)}$$

In order for the two temperature measurements to be representative of the surface requires the assumption that any change in air temperature is in fact a response to changes in the sensible heat flux below. This one dimensional approach is appropriate in the presence of buoyant convection because the vertical transport of sensible heat from the underlying surface represents the sole source of energy for air warming. This ignores radiative divergence within the air mass which is negligible during the daytime.

Equation (A.1.1) has been successfully applied in many instances in the presence of mechanical convection. However, this requires a special set of conditions. Clearly, when the wind is blowing the air temperatures being sampled by the sensors are not determined by sensible heat flux from the underlying surface but rather of some surface upwind. Nevertheless, if the surface upwind was identical to the study surface it is of little

consequence that measured air temperature did not originate from directly below because its energetics are identical to the upwind location. When the measurements are made over an infinite homogeneous plane the measurements are said to lie within the "fully adjusted boundary layer".

The successful measurement of the sensible heat flux using (A.1.1) generally requires an evaluation of whether the upwind surface is sufficiently "infinite" to satisfy its assumptions. An understanding of the "leading edge" effects of the upwind boundary of the study surface ensures in the majority of instances that sensors are suitably located for energy budget analysis of this type.

Several crop surfaces of interest however, do not satisfy these requirements and necessitate a different method of analysis. Irrigated fields fall into this category because quite often the fully adjusted boundary layer is not sufficiently deep for multi-level sensors to lie within this zone.

Dyer and Crawford (1965) demonstrated such an approach for estimating the surface sensible heat flux over a heavily irrigated field. The approach is based on a box model (Figure A.1.) and is given by

$$Q_{Ho} - Q_{Hh} = \rho C_p \int_0^h u \frac{\partial T}{\partial x} dz \qquad (A.1.2)$$

where Q_{Ho} and Q_{Hh} are the sensible heat fluxes of the surfaces and at height h at the top of the box respectively and u is horizontal wind speed. This steady state two dimensional model assumes uniformity in the cross wind component y. Thus measurements required include the vertical

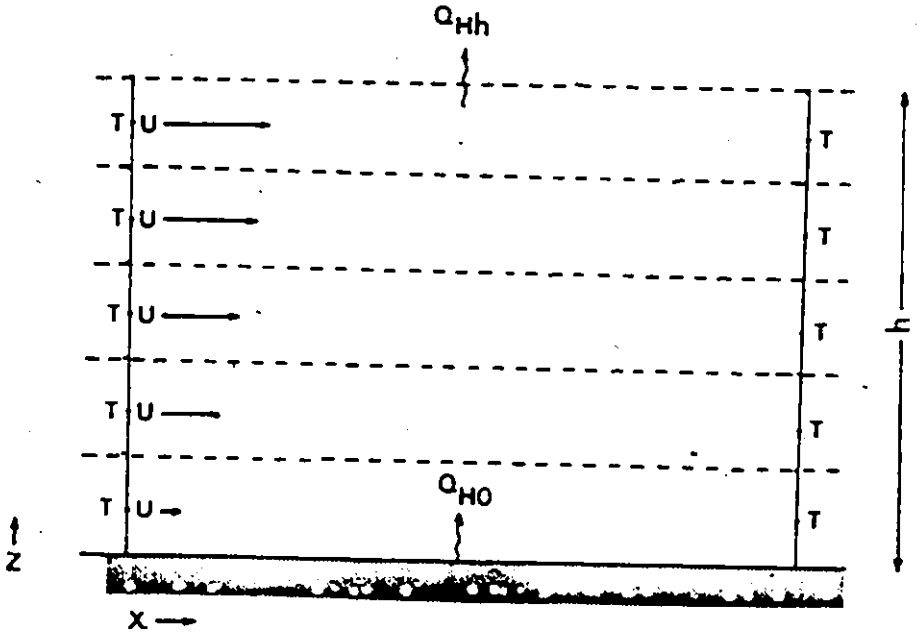

Figure A.1. Components of the Dyer and Crawford model.

distribution of temperature and windspeed at the upwind and downwind boundaries of the box. The drawback of (A.1.2) is that although it describes the energy traversing the four sides of the box it cannot account for that leaving the top of the box. Hence the evaluation of Q_{Ho} is limited to those instances when Q_{Hh} is zero. Fortunately, in the case of irrigated fields Q_{Hh} may be zero because quite often a temperature inversion occurs at some height above the surface. The reason for the occurrence of inversions in advective environments is described in detail in Chapter Two. Of importance here is the fact that a zero or negligible vertical temperature gradient at inversion height h implies that (A.1.2) can be employed to evaluate the surface sensible heat flux because Q_{Hh} is zero.

By covering the irrigated plot with glazing the use of (A.1.2) can be extended to conditions where temperature inversions are absent. By placing a cap on the top of the box the convective exchange at height h in the Dyer and Crawford model is replaced by a hybrid conductive/convective exchange through the greenhouse roof. The sensible heat flux through the top of the box is more easily parameterized even though it may not in fact be zero. This is because the conductivity of commonly used glazings is constant over the range of temperatures normally encountered. If the inner and outer glazing temperatures are measured directly then

$$Q_{Hh} = k\frac{\Delta T}{l} \qquad \text{(A.1.3)}$$

where k is the thermal conductivity of the glass and l is glazing thickness. If inside air temperature and screen temperature are used then

$$Q_{Hh} = U\ (T_{in} - T_{out})\ , \qquad (A.1.4)$$

where $U = \frac{1}{1/hci + 1/k + 1/hco}$ $(Wm^{-2}\ C^{-1})$ and hco and hci are the outside and inside convective exchange coefficients.

In mechanically ventilated greenhouses hci is relatively constant and only variations in hco affect the determination of U. With double or triple glazings variations in hco have progressively less impact on the heat transfer through the glazing and the glazing heat transfer coefficient is more easily determined.

The greenhouse box model is unique because we are dealing with an eight sided box. The base or growing surface is the heat source. The sum of heat loss from all other sides balances the surface sensible heat flux thus

$$A_s Q_H = \rho Cp\ \psi\ (T_e - T_i) + A_g U (T_{in} - T_{out}) \qquad (A.1.5)$$

where A_s and A_g are the areas of the surface and glazing respectively, U is the glazing heat loss coefficient or U-factor and ψ is the ventilation rate. The three dimensional conductive heat loss from the four sides and top of the box are lumped in the second term of (A.1.5). The assumption is made that the greenhouse air is well mixed and that the temperature and wind regime about the greenhouse is uniform. The first term of (A.1.5) is analagous to the right hand side of (A.1.2) and represents the two extra "sides" of the greenhouse comprising the intake and exhaust fans. The increase in temperature of the exhaust air T_e over intake air T_i results from surface warming. The assumption is made that the volume exchange of air is well mixed and hence the integration of

air temperature over height is unnecessary. The exhaust air is necessarily cooler than it might be were the greenhouse glazings a perfect insulator. Hence, glazing heat loss is added to ventilation heat loss to derive a value for the surface sensible heat flux. A similar expression to (A.1.5) is used for the latent heat flux and forms the basis of the greenhouse combination model derived in Chapter Two.

APPENDIX TWO

LIST OF SYMBOLS

α_g	glazing albedo
α_s	surface albedo
β	Bowen ratio
γ	psychrometric constant
Δ	finite difference
ε_g	glazing emissivity
ε_s	surface emissivity
θ	angle (degrees)
λ	latent heat of vaporization of water
μm	micrometers
ρ	air density; longwave reflectance
σ	Stefan-Boltzman constant
τ_g	glazing longwave transmission
ψ	ventilation rate
A	area
C	heat capacity
C_p	specific heat
D_i	intake wet-bulb depression
D_e	exhaust wet-bulb depression
E	evaporation rate
$K\downarrow$	incoming solar radiation
$K\uparrow$	reflected solar radiation
K^*	net solar radiation
K_H	eddy diffusivity for sensible heat
K_W	eddy diffusivity for water vapour
L	length
$L\downarrow$	incoming longwave radiation
$L\uparrow$	emitted longwave radiation
L^*	net longwave radiation
P	atmospheric pressure

$Q\downarrow$	incoming allwave radiation
$Q\uparrow$	upward allwave radiation
Q^*	net radiation
Q_H	surface sensible heat flux
Q_L	surface latent heat flux
Q_G	soil heat flux
Q_P	photosynthetic flux
Q_{H*}	glazing sensible heat flux
Q_{L*}	glazing condensation flux
S	slope saturation vapour pressure-temperature curve
T_i	intake dry-bulb temperature
T_e	exhaust dry-bulb temperature
$\overline{T}_{in}$	average inside temperature
$\overline{T}_{out}$	average outside temperature
T_{wi}	intake wet-bulb temperature
T_{we}	exhaust wet-bulb temperature
U	glazing heat transfer coefficient
V	air volume
W	width
a_g	glazing solar absorptivity
e_i	intake vapour pressure
e_e	exhaust vapour pressure
e_g	glazing vapour pressure
e_s	saturation vapour pressure
h	height
l	glazing thickness
r	radius
t	time
u	horizontal wind speed

REFERENCES

Balcomb, J.D., J.C. Hedstrom, R.D. McFarland, 1977: Simulation analysis of passive solar heated buildings - preliminary results. Solar Energy, Vol. 19, 277-282.

Besant, R.W., R.S. Dumont, 1979: Comparison of 100 per cent solar heated residences using active solar collection systems. Solar Energy, Vol. 22, 451-453.

Businger, J.A., 1963: The glasshouse (greenhouse) climate. In Physics of the Plant Environment. Ed. W.R. Van Wijk. Amsterdam: North-Holland Publishing Co.

Chiapale, J.P., J. Damagnez, P. Denis, 1977: Modification of a greenhouse environment through the use of a collecting fluid. Proc. Int. Symp. Controlled Env. Agr. Tucson, 122-138.

Crafts, A.S., 1961: Translocation in Plants. New York: Holt, Rinehart and Winston.

Davies, J.A., C.D. Allen, 1973: Equilibrium, potential and actual evaporation from cropped surfaces in southern Ontario. J. Appl. Meteor., 12, 649-657.

Dilley, A.C., 1968: On the computer calculation of vapour pressure and specific humidity gradients from psychrometric data. J. Appl. Meteor., 7, 717-719.

Dyer, A.J., T.V. Crawford, 1965: Observations of the modification of the microclimate at a leading edge. Quart. J. Royal Meteor. Soc., 91, 345-348.

Dyer, A.J., 1967: The turbulent transport of heat and water vapour in an unstable atmosphere. Quart. J. Royal Meteor. Soc., 93, 501-508.

Froelich, D.P., L.D. Albright, N.R. Scott, 1979: Steady periodic analysis of a glasshouse thermal environment. Trans. A.S.A.E., 22(2), 387-399.

Hanan, J.J., 1967: Water requirements of carnations, general effect of substrate and air movement. Colorado Flower Growers Assoc. Bull., 207, 2-4.

Kimball, B.A., 1973: Simulation of the energy balance of a greenhouse. Agric. Meteor., 11, 243-260.

Latimer, J.R., 1970: Investigation of solar radiation instruments at the national radiation center of the Canadian Meteorological Service. International Solar Energy Conference, Melbourne, Australia, March, 3(1), 1-6.

Lawand, T.A., R. Alward, B. Saulnier, E. Brunet, 1975: The development and testing of an environmentally designed greenhouse for colder regions. Solar Energy, 17, 307-312.

Linacre, E.T., J.H. Palmer, E.S. Trickett, 1964: Heat and moisture transfer from trimmed glasshouse crops. Agric. Meteor., 1(3), 165-183.

Lourence, F.J., W.O. Pruitt, 1969: A psychrometric system for micro-meteorology profile determination. J. Appl. Meteor., 8, 492-498.

Mastalerz, J.W., 1977: The Greenhouse Environment, John Wiley and Sons, Inc.

Mazria, E., 1979: The Passive Solar Energy Book, Emmaus, Pa: Rodale Press.

Mihara, Y., M. Hayashi, 1979: Studies on the insulation of greenhouses (I). Overall heat transfer coefficient of greenhouses with single and double covering using several material curtains. J. Agr. Meteor., 35(1), 13-19.

Monteith, J.L., 1965: Evaporation and environment. The State and Movement of Water in Living Organisms, ed. G.F. Fogg, New York: Academic Press.

Monteith, J.L., 1975: Vegetation and the Atmosphere, New York: Academic Press.

Monteith, J.L., 1981: Evaporation and surface temperature. Quart. J. Royal Meteor. Soc., 107, 1-27.

Morriss, L.G., F.E. Neale, J.D. Prostlethwaite, 1957: The transpiration of glasshouse crops and its relationship to incoming solar radiation. J. Agr. Engin. Res., 2(2), 111-122.

Nakayama, K., S. Yamanaka, 1975: Evapotranspiration of a tomatoe crop in a plastic house. J. Agr. Meteor., 31(1), 17-22.

Nakayama, K., J. Hanyu, S. Yamanaka, K. Ozawa, K. Ogata, 1980: Soil moisture movement into the root zone in a plastic house. J. Agr. Meteor., 35(4), 215-220.

Oke, T.R., 1978: Boundary Layer Climates, London: Methuen and Co. Ltd.

Penman, H.L., 1948: Natural evaporation from open water, bare soil and grass. Proc. Royal Soc. London, A193, 129-145.

Priestley, C.H.B., R.J. Taylor, 1972: On the assessment of surface heat flux and evaporation using large scale parameters. Mon. Weather Rev., 100, 81-92.

Rouse, W.R., R.B. Stewart, 1972: A simple model for determining evaporation for high lattitude upland sites. J. Appl. Meteor., 11, 1063-1070.

Simpkins, J.C., D.R. Mears, W.J. Roberts, H. Janes, 1979: Performance of the Rutgers solar heated greenhouse research units. Proc. 4th Ann. Con. Sol. Ener. Greenhouses, Piscataway, N.J., 118-127.

Stanhill, G., M. Fuchs, J. Bakker, S. Moreshet, 1973: The radiation balance of a greenhouse rose crop. Agr. Meteor., 11, 385-404.

Swinbank, W.C., A.J. Dyer, 1967: An experimental study in micrometeorology. Quart. J. Royal Meteor. Soc., 93, 494-500.

Szeicz, G., I.F. Long, 1969: Surface resistance of crop canopies. Water Resor. Res., 5, 622-633.

Takakura, T., K.A. Jordan, L.L. Boyd, 1971: Dynamic simulation of plant growth and environment in the greenhouse. Trans. A.S.A.E., 964-971.

Takami, S., Z. Uchijima, 1977: A model for the greenhouse environment as affected by the mass and energy exchange of a crop. J. Agr. Meteor., 33(3), 117-127.

Tan, C.S., T.A. Black, 1976: Factors affecting the canopy resistance of a Douglas Fir forest. Boundary Layer Meteor., 10, 475-488.

Tanner, C.B., M. Fuchs, 1968: Evaporation from unsaturated surfaces: a generalized combination model. J. Geophys. Res., 73, 1299-1304.

Tiessen, H., 1976: Greenhouse vegetable production in Ontario. Min. of Agr. and Food Bull., 526, 1-60.

Thom, A.S., 1972: Momentum, mass and heat exchange of vegetation. Quart. J. Royal Meteor. Soc., 98, 124-134.

van Bavel, C.M.H., E.J. Sadler, 1979: Experimental tests of a fluid roof concept. Proc. 4th Ann. Conf. Sol. Energy for Heating Greenhouses and Greenhouse-Residence Combinations, Piscataway, New Jersey, 128-136.

Walker, J.N., 1965: Predicting temperatures in ventilated greenhouses. Trans. A.S.A.E., 445-448.

Wray, W.O., J.D. Balcomb, 1979: Sensitivity of direct gain space heating performance to fundamental parameter variations. Solar Energy, Vol. 23, 421-425.